# Stratigraphy, chronology, styles and dynamics of late Quaternary eruptions from Taupo volcano, New Zealand†

By C. J. N. Wilson ‡

*Department of Earth Sciences, University of Cambridge, Downing Street, Cambridge CB2 3EQ, U.K.*

[Plates 1–4]

**Contents**



† This paper was produced by using the TEX typesetting system.

‡ Present address: Institute of Geological and Nuclear Sciences, Private Bag 2000, Taupo, New Zealand.

*Phil. Trans. R. Soc. Lond.* A (1993) **343**, 205–306

Taupo volcano is the southerly of two dormant caldera volcanoes in the rhyolite-dominated central portion of the Taupo Volcanic Zone in the North Island of New Zealand. Taupo has an average magma output rate of 0.2 $m^3$ $s^{-1}$ over the past 65 000 years, and is one of the most frequently active and productive rhyolite volcanoes known. The structure of the modern 'inverse' volcano was formed largely by caldera collapse associated with the voluminous 22 600 $^{14}C$ years BP Oruanui eruption, and has been little modified since except for collapse following the 1850 $^{14}C$ years BP eruption. The products of 28 eruptions (labelled $\Psi$, $\Omega$, A, ..., Z), all of which post-date the Oruanui eruption, are defined and described here. Twenty-seven of these eruptions are represented by pyroclastic deposits (of which three were accompanied by a mappable lava extrusion), and one eruption (Z) solely by evidence for a lava extrusion. The deposits of seven eruptions (B, C, E, S, V, X and Y) largely correspond to previously defined tephra formations (Karapiti, Poronui, Opepe, Waimihia, Whakaipo, Mapara and Taupo, respectively). The previously defined Motutere and Hinemaiaia Tephras are reinterpreted to represent the products of 12 eruptions (G to R), while the remaining eight deposits and one eruption are newly recognized. Eruption $\Psi$ occurred at *ca.* 17 200 $^{14}C$ or 20 500 calibrated years BP and eruption Z about 1740 calibrated years BP. Eruption volumes vary by more than three orders of magnitude between 0.01 and more than 44 $km^3$, and repose periods by more than two orders of magnitude from *ca.* 20 to 6000 years.

The eruption deposits reflect great variations in parameters such as volume, the dispersal characteristics of the fall deposits, the presence or absence of intra-eruptive time breaks, the formation of pyroclastic flows, the degree of magma–water interaction, the vesiculation state of the magma on fragmentation and the relative proportions of juvenile obsidian versus foreign lithologies in the lithic fractions. All but seven fall deposits are plinian in dispersal; two (Y1 and probably W) are sub-plinian, one (Y5) has been termed 'ultraplinian', while $\Psi$ and A are too poorly preserved for their dispersal to be assessed.

The lengths of repose periods in the post-Oruanui sequence range are not randomly distributed but show self-similar properties (fractal dimensionality); repose intervals ($r$, in years) of not more than 350 years follow $n = 53.5r^{-0.21}$, and those of not less than 350 years follow $n = 2096r^{-0.83}$, where $n$ is the number of eruptions. The shorter repose periods may reflect triggering processes, such as regional extension, affecting magma bodies during their viable lifetimes, while longer repose intervals (i.e. not less than 350 years) may reflect an episodicity of major rifting events or the production of magma bodies below the volcano. Bulk volumes ($v$, in $km^3$) of the eruption products also show self-similar properties (fractal dimensionality), with $n = 6.17v^{-0.46}$. However, there are then apparently random relationships between eruption volumes and the preceding or succeeding repose period such that prediction of the time and size of the next eruption is impossible. The post-Oruanui activity at Taupo represents 'noise' superimposed on the more uniform, longer term activity in the central Taupo Volcanic Zone,

where large (greater than 100 $km^3$) eruptions, such as the Oruanui, occur at more evenly spaced intervals of one per 40–60 000 years.

## 1. Introduction

### (*a*) *Taupo volcano*

Taupo volcano is one of the two dormant caldera volcanoes in the Taupo Volcanic Zone (TVZ) in the central North Island of New Zealand (figure 1). Taupo to the south and Okataina to the north form the extremities of a central rhyolite-dominated segment of the TVZ (Wilson *et al.* 1984) that has been a voluminous source of rhyolitic magmatism for the past *ca.* 1.6 Ma (Pringle *et al.* 1992). Eruption rates are roughly 0.2 $m^3\ s^{-1}$ (= 6.5 $km^3\ ka^{-1}$) at Taupo and 0.1 $m^3\ s^{-1}$ (= 3.5 $km^3\ ka^{-1}$) at Okataina over the past *ca.* 65 000 years (Wilson *et al.* 1984, modified here by revised volume (Taupo) and age data (Taupo, Okataina)), making these the two most productive individual rhyolite volcanoes in the world (cf. Crisp 1984). Taupo is the archetypal example of an 'inverse' volcano, where the proximal accumulation of ejecta has not compensated for subsidence associated with caldera collapse and regional tectonic extension (Walker 1984; figure 1).

#### (i) *Eruptive history*

Previous studies at Taupo have outlined its early history (before *ca.* 65 000 years BP) and a detailed picture of its late Quaternary and Holocene activity (Healy 1964; Vucetich & Pullar 1964, 1969, 1973; Vucetich & Howorth 1976*a*; Wilson *et al.* 1984, 1986; Froggatt & Lowe 1990). All the domes and pyroclastic deposits associated with Taupo volcano (and Maroa volcano, its immediate neighbour to the north) clearly post-date the voluminous Whakamaru-group ignimbrites dated at *ca.* 330 000 years BP (Wilson *et al.* 1986; Pringle *et al.* 1992). The activity from *ca.* 330 000 to 65 000 years BP is poorly understood, but it appears that the onset of the modern pyroclastic-dominated activity at Taupo commenced shortly after the Rotoiti event (64 000 years BP; Wilson *et al.* 1992) from Okataina volcano, contemporaneously with a marked decrease in the frequency and volume of lava-dominated eruptions at Maroa volcano. From *ca.* 64 000 to 27 000 years BP five explosive eruptions occurred (Vucetich & Howorth 1976*a*) from vents now concealed beneath Lake Taupo. At 22 600 $^{14}C$ years BP (Wilson *et al.* 1988), equivalent to *ca.* 26 500 calibrated years BP (Bard *et al.* 1990), the voluminous Oruanui eruption occurred (Vucetich & Howorth 1976*b*; Self 1983). My work in progress suggests bulk volumes of the Oruanui products are of the order 500 $km^3$ for the fall deposits, 300 $km^3$ of ignimbrite (Wilson 1991) and 500 $km^3$ of intracaldera fill, equivalent to more than 400 $km^3$ of magma. My work also suggests that much of the overall geometry of Lake Taupo was established at this time as the modern lake infills the caldera from this eruption, modified by the later smaller eruptions described in this paper. The Oruanui deposits were severely eroded during the following glacial maximum, and younger deposits rest on a palaeo-landscape with a topographic relief locally exceeding 200 m.

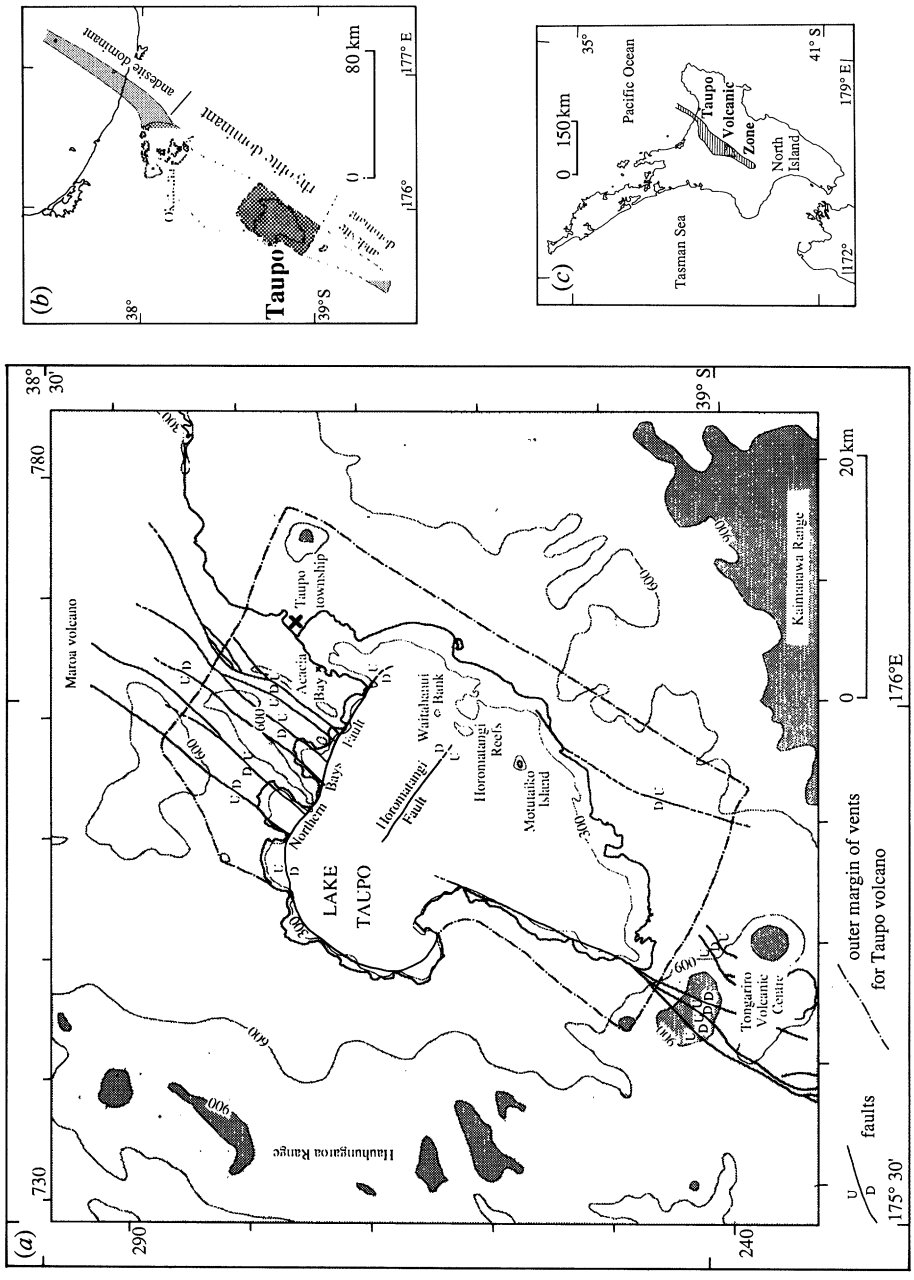


Figure 1. Location and index maps. (*a*) Topographic map of Taupo volcano, showing its inverse nature. Contours are at 300 m intervals. Major faults, and localities mentioned in the text are shown. In this and all other maps, the marginal ticks and numbers represent 10 km grid squares in the New Zealand metric map grid. From Wilson & Walker (1985). (*b*) Index map showing the position of Taupo and Okataina volcanoes within the central rhyolite-dominated Taupo Volcanic Zone (TVZ). The TVZ boundary is that defined in Wilson *et al.* (1984) as the envelope enclosing vents active after the Whakamaru-group ignimbrites, i.e. younger than 330 000 years. (*c*) Index map showing the position of the TVZ within the central North Island of New Zealand.

(ii) *Late Quaternary activity*

The post-Oruanui stratigraphy at Taupo has been studied in some detail (Baumgart 1954; Healy 1964; Vucetich & Pullar 1973; Froggatt & Lowe 1990) and a sequence of nine tephra formations established (table 1). In New Zealand tephrochronological studies, the term 'tephra formation' is used for rhyolitic deposits in the sense of '[containing] all the primary pyroclastic products of one eruptive episode, each separated by significant time intervals that are often marked by palaeosols' (Froggatt & Lowe 1990, p. 91). This mapping approach has been very successful, but has drawbacks when applied to interpreting the nature and frequency of eruptions in that only units demarcated by obvious palaeosols have been denoted as tephra formations. This leads to three problems.

1. The time breaks marked by obvious palaeosols in the Taupo Holocene sequence represent periods of at least 200 years. In contrast, during modern volcanic activity, breaks of more than a few months to years are usually considered long enough to separate eruptions (e.g. Wickman 1966). Eruption frequencies and recurrence intervals estimated using the assumption that each tephra formation represents one eruption (e.g. Froggatt 1982; Dibble *et al.* 1985) may thus be in error.

2. The time break represented by soil formation involves bioturbation, weathering and erosion of pyroclastic material. These processes may destroy thin deposits and thus lead to a biased estimate of the sizes of eruptions at a volcano.

3. Tephra formation isopachs are generally not based on preserved thicknesses of primary tephra but on the vertical distance between the underlying palaeosol (defining the base of the formation; Vucetich & Pullar 1964) and the top of the overlying palaeosol (Vucetich & Pullar 1964, 1973; Pullar & Birrell 1973). The incorporated palaeosol could include additions of loess or distal tephra from other sources, or represent a weathering interval during which material was lost. Thus tephra formation isopachs differ significantly from the isopachs needed to establish accurate estimates of eruptive volumes.

A detailed re-examination has thus been made of the eruption products from Taupo that overlie the 22 600 $^{14}$C years BP Oruanui deposits, in order to establish how many eruptions have occurred and what their timing, styles and volumes were. This has resulted in the discovery of numerous deposits of smaller eruptions within the previously mapped tephra formations. These findings imply that Taupo was more frequently active and with a wider range of eruption volumes than previously supposed.

The new stratigraphy is summarized in table 1, and the deposits described in ascending stratigraphic order below. Problems arise in matching the new stratigraphy with existing nomenclature, because several previously defined and named units (notably Motutere and Hinemaiaia) are re-interpreted as the products of multiple eruptions separated by time periods estimated to be of the order of tens to hundreds of years. Each eruption (and its deposits) is represented by a letter, $\Psi$, $\Omega$, A, ..., Z. Within each eruption deposit, numbers are used to designate portions or beds that can be widely correlated. The deposits are described this way because it is clear that many of them are too poorly exposed or areally restricted to form mappable tephra formations as has been done in the past. Appendix A summarizes all the type and reference localities for the deposits.

Table 1. *Summary of stratigraphic nomenclature, and adopted $^{14}C$ and calibrated ages for post-Oruanui pyroclastic deposits at Taupo volcano*

(Previously published names are those of Froggatt & Lowe (1990), except for subunits of the Taupo Tephra which are from Wilson & Walker (1985). For discussion of the adopted $^{14}C$ and calibrated ages, see the relevant text for each unit. Ages on the $^{14}C$ timescale are annoted thus: bold – numerous determinations on material carbonized by the eruption; normal – closely constrained by determinations on material immediately below or above the unit concerned; (bracketed) – constrained by bracketing determinations on material in palaeosols or peat above or below the unit; underlined – loosely constrained by ages on older and/or younger deposits. Asterisks denote ages that are newly presented and/or adopted in this paper; other values are after Froggatt & Lowe 1990.)

| previous published name | | nomenclature in this paper | adopted age (years BP) $^{14}C$ timescale | adopted age (years BP) calibrated timescale |
|---|---|---|---|---|
| | floated giant pumices | eruption Z | — | 1740 |
| | Taupo ignimbrite | Subunit Y7 | | |
| | early ignimbrite flow units | Subunit Y6 | | |
| | Taupo plinian pumice | Subunit Y5 | | |
| Taupo | Rotongaio ash | Subunit Y4 | **1850** | 1770 |
| Tephra | Hatepe ash | Subunit Y3 | | |
| | Hatepe plinian pumice | Subunit Y2 | | |
| | initial ash | Subunit Y1 | | |
| | Mapara Tephra | Unit X | **2150** | 2150 |
| | (not recorded) | Unit W | 2650* | 2750 |
| | Whakaipo Tephra | Unit V | **2700** | 2800 |
| | | Unit U | (2750)* | 2850 |
| | (not recorded) | Unit T | (3000)* | 3200 |
| Waimihia | Waimihia ignimbrite | Subunit S3 | | |
| Tephra | Waimihia plinian pumice | Subunits S1 and S2 | **3300** | 3550 |
| | | Unit R | 3950* | 4450 |
| | | Unit Q | 4050* | 4550 |
| | | Unit P | 4100* | 4750 |
| | | Unit O | 4150* | 4800 |
| | | Unit N | 4200* | 4850 |
| | Hinemaiaia | Unit M | (4500)* | 5250 |
| | Tephra | Unit L | 4550* | 5300 |
| | | Unit K | (4600)* | 5350 |
| | | Unit J | (4620)* | 5370 |
| | | Unit I | (5200)* | 5950 |
| | Motutere | Unit H | (5300)* | 6050 |
| | Tephra | Unit G | (5800)* | 6650 |
| | (not recorded) | Unit F | (6150)* | 7050 |
| | Opepe Tephra | Unit E | (9050) | 9950 |
| | (not recorded) | Unit D | 9780* | 11 380 |
| | Poronui Tephra | Unit C | (9800) | 11 400 |
| | Karapiti Tephra | Unit B | 10 100* | 11 800 |
| | (not recorded) | Unit A | (*ca.* 14 200)* | 17 000 |
| | (not recorded) | Unit Ω | (*ca.* 15 600)* | 18 800 |
| | (not recorded) | Unit Ψ | (*ca.* 17 200)* | 20 500 |
| | Oruanui Formation | | **22 600** | 26 500 |

### (*b*) *Chronology*

Froggatt & Lowe (1990) recently summarized $^{14}C$ ages relevant to the nine previously named tephra formations at Taupo. In addition, I have obtained a number of new ages on charcoal samples collected from the Taupo sequence (see Appendix B). (All $^{14}C$ ages discussed here are conventional, using the 5568 years half-life, with BP referring to AD 1950.) Froggatt & Lowe (1990) combined what they considered to be the most reliable ages for each formation and calculated a pooled mean, weighted by the standard deviation on each age determination (their table 1). However, the resulting figures are subject to appreciably larger errors than those given by Froggatt & Lowe, for two reasons. First, the method of combining age data pre-supposes that the ages represent measurements on the same event. This may be questioned when data are combined from peat or gyttja samples above or below a tephra, charcoal or other organic matter from palaeosols, and charcoal from within tephra units. Second, the errors given are only the 1 s.d. errors based on laboratory counting statistics for the individual age determinations. They take no account of errors due to sample spread (e.g. a finite thickness of peat is sampled to give a single age determination (Lowe 1986)), the presence of multiple events (e.g. the 'Hinemaiaia Tephra'; see § 2*h* below), differences between laboratories (e.g. pre-treatment techniques), or variations in age results from a uniform-age sample (e.g. ISG 1982; Scott *et al.* 1983).

In this paper, the available data have been re-examined and a value for the age of each unit on the conventional $^{14}C$ timescale adopted in the light of age data or interpolation between other dated horizons (cf. Nairn 1989). Values for each eruptive unit are given in table 1 and discussed in the relevant text. For the reasons given above, the resulting errors are difficult to calculate, but on any single $^{14}C$ age a 1 s.d. error of $\pm 2$–3% is considered to represent a realistic estimate of total error arising from field- and laboratory-induced uncertainties. In the older units, Ψ, Ω and A, a lack of $^{14}C$ data means the relevant ages are indicative only, and have 1 s.d. errors of realistically 5–10%.

A desirable aim also is to convert $^{14}C$ ages to calibrated, or calendar, years. However, further errors are introduced in conversion through counting errors on the calibration samples, as well as due to wiggles on the calibration curve which may thus yield a range of possible calibrated ages even for a hypothetically perfect, zero error $^{14}C$ age. Here two approaches are taken. First, for eruption E and younger events the adopted age on the $^{14}C$ timescale is matched on the relevant calibration curves in Pearson & Stuiver (1986), Pearson *et al.* (1986), Stuiver & Pearson (1986) and Becker *et al.* (1991). Where wiggles on the calibration curve gave a choice of intercepts (notably with eruptions K to R) a calibrated value was chosen by taking the highest probability intercept, and/or by interpolation between eruptions whose $^{14}C$ and calibrated ages were better constrained, and/or using field evidence (palaeosol development, etc.) for relative time breaks between eruptions. Second, for eruption D and older events the adopted ages on the $^{14}C$ timescale were converted to calibrated ages by using a third-order polynomial fitted to the $^{14}C$ against U/Th age data of Bard *et al.* (1990) (i.e. any wiggle variations seen in younger calibrations are neglected). These figures (table 1) represent an approximate, first-order attempt to provide a calibrated age chronology for Taupo. Note that on this basis, six of the tephras (Ψ, Ω, A, B (Karapiti), C (Poronui) and D) have late Pleistocene rather than Holocene ages,

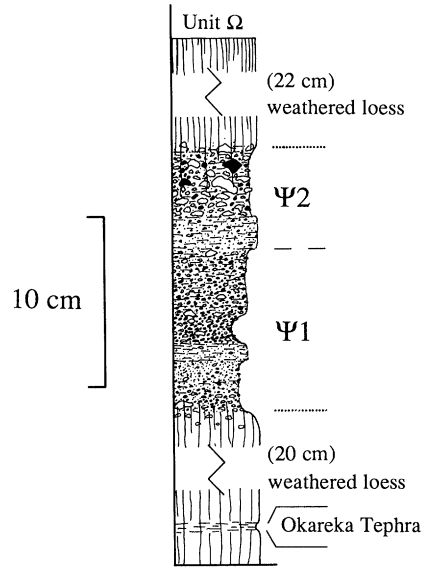


Figure 2. Stratigraphic column for the type section of Unit Ψ at 7704 2741 (Appendix A). In this and subsequent figures incorporating stratigraphic columns, the following conventions are used. The vertical extents of beds are to the scale indicated on each column. The horizontal extents of beds are not proportional to grainsize but represent the profile of the unit as it appears on the weathered surface of exposures, where beds containing or composed of very-fine ash protrude, while well-sorted (though coarser) lapilli to block beds erode more rapidly to form recesses. Within the limitations of scale, sizes of clasts are represented by symbols thus; lapilli to blocks are drawn in proportion to the vertical scale, coarse to medium ash (2–0.25 mm) material is shown by stippling, and fine ash (0.25–0.063 mm) and very fine ash (less than 0.063 mm) by dashes. Pumices and lithics are represented by open and closed symbols, respectively, palaeosols by irregular vertical lining, and erosion surfaces by wavy contacts.

taking the base of the Holocene to be at 10 970 calibrated years BP (Becker *et al.* 1991).

### (*c*) *Techniques and conventions*

(i) *Volumes*

Volumes are derived where possible from new isopach maps and using plots of ln(thickness) against $\sqrt{}$(isopach area) (Pyle 1989). An exponential decay of thicknesses away from vent has been assumed for deposits for which only limited data are available. For two eruptions (S (Waimihia) and Y (Taupo)) detailed calculations using a mass balance technique on the crystal content of 'dry' plinian fall deposits (Walker 1980, 1981*a*) have been used to imply that volumes derived by assuming exponential decay are underestimates by factors of 2–3 (see also §3*c*).

(ii) *Vent positions*

Only three deposits (D, F and W) can be related to subaerial vents whose positions are definable. All other vent sites are now submerged beneath Lake Taupo and their positions have to be estimated from isopach and isopleth maps. No examples of ballistic clasts have been found even for the most powerfully dispersed fall deposits, and so the vents are inferred to lie some kilometres beyond

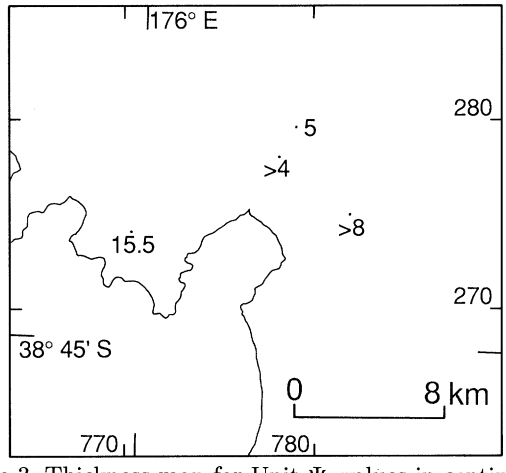


Figure 3. Thickness map for Unit Ψ, values in centimetres.

the most proximal exposures (Walker 1980, 1981*a*). In this paper a system based on the eruption column model of Carey & Sparks (1986, especially their fig. 16) is used whenever possible. First, the crosswind width of lithic isopleths is used to establish a column height estimate. Second, the downwind distance between adjacent isopleths is used to estimate the wind speed at which the isopleths would share a common source. The distance to that source, assumed to be along the dispersal axis indicated by isopleth and/or isopach data, is then indicated by the downwind distance indicated for the particular isopleth for the relevant column height. This approach is estimated to give positions to within *ca.* 3 km, the errors depending heavily on the quality of the isopach/isopleth data.

(iii) *Conventions and terminology*

Fall deposits are described as plinian or sub-plinian after Walker (1973) from their dispersal index ($I_d$), defined as the area covered by $0.01T_{max}$ or more of tephra, where $T_{max}$ is the maximum thickness (measured or inferred by extrapolation on a plot of ln(thickness) against $\sqrt{}$(isopach area)). Plinian deposits have $I_d \geq 500$ km$^2$. Maximum clast sizes, either pumice ($P_m$) or lithics ($L_m$), represent the average lengths of the longest axes of the five largest clasts found at each locality. Grid references for localities (eight digits) are to the nearest 100 m, and for vent sites (six digits) to the nearest kilometre, in the New Zealand metric map grid.

The terms 'dry' (or magmatic) and 'wet' (or phreatomagmatic) are applied respectively to explosive eruptions driven solely by the expansion of internal volatiles and those where some degree of interaction with external water has taken place (Houghton & Wilson 1989). Evidence for magma–water interaction includes the presence of water-flushed ashes whose thicknesses and/or abundances increase systematically towards vent (Walker 1981*b*) and of juvenile material which is poorly to moderately vesicular (Houghton & Wilson 1989). Other water flushed beds occur which do not show such features and these are interpreted as being due to conventional rain showers crossing the plume.

Dense, lithic clasts in the deposits are dominantly rhyolitic. The rhyolitic clasts are categorized as either juvenile (fresh and/or extremely abundant, grey to black

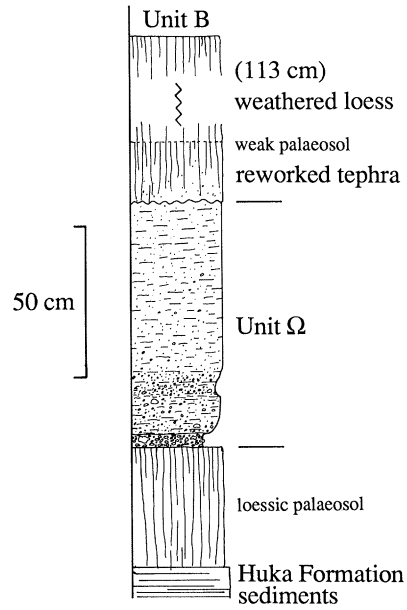


Figure 4. Stratigraphic column for the type section of Unit Ω at 7708 2741 (Appendix A).

dense pumice to obsidian) or foreign (hydrated/spherulitic obsidian, devitrified and/or hydrothermally altered). The dominance of one or other lithic categories is here interpreted as follows.

1. Juvenile lithics dominate: closed-vent activity, where poorly to non-vesicular magma reached to shallow levels in the vent, and that dome extrusion may have accompanied or followed explosive activity (Heiken & Wohletz 1987).

2. Foreign lithics (including non-rhyolitic lithologies) dominate: open-vent activity, where fragmentation occurs at some depth, and country-rocks forming the vent walls are eroded by the ejecta stream.

## 2. Tephra stratigraphy and descriptions

### (*a*) *Units Ψ, Ω and A*

These are three newly recognized fall deposits, found enclosed in loess overlying the Oruanui or older deposits and underlying the earliest of the previously recognized 'Holocene' eruptives. All three have been found together only at 7790 2796; elsewhere Units Ψ and Ω typically occur together. No direct age data are available, but their ages are constrained thus.

1. At four localities, Unit Ψ overlies loess containing a very fine grained distal rhyolitic tephra. This tephra has a ferromagnesian assemblage of hypersthene, hornblende and subordinate biotite, and is interpreted to be the Okareka Tephra from Okataina, approximately dated (from $^{14}$C ages of bracketing units) at *ca.* 18 000 $^{14}$C years BP (Nairn 1992).

2. At two localities, the palaeosol between Units A and B contains less than 1–2 cm thick traces of a very fine grained distal rhyolitic tephra which can be traced northwards to correlate with the 11 800 $^{14}$C years BP Waiohau Tephra from Okataina.

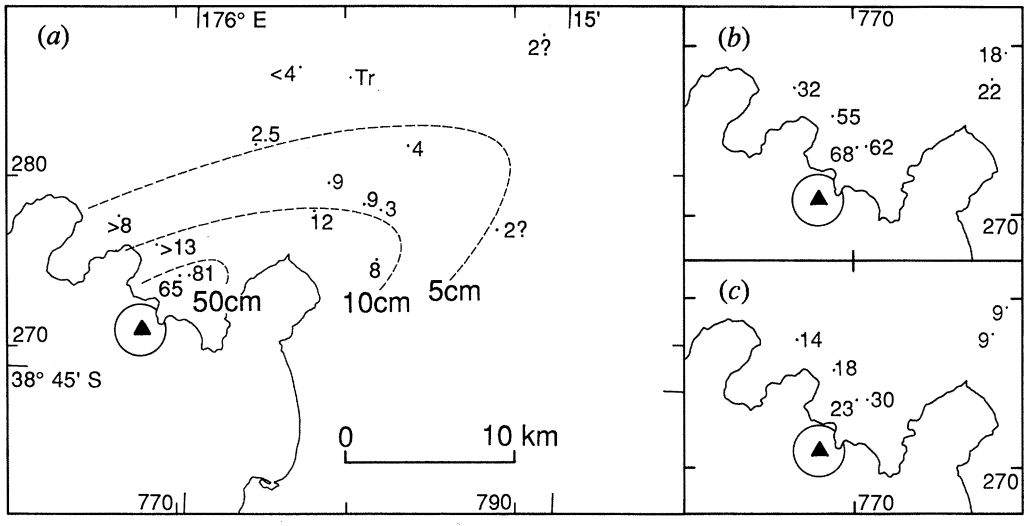


Figure 5. Isopach and maximum-clast size maps for Unit Ω. (*a*) Isopachs and thicknesses in centimetres. Here and in subsequent figures Tr = trace. (*b*) $P_m$ data (see § 1*c*(iii) for definition), values in millimetres. (*c*) $L_m$ data, values in millimetres. In this and subsequent maps, the filled triangle represents the inferred vent position, with a 3 km diameter circle to indicate the likely approximate 1 s.d. uncertainty in position (see § 1*c*(ii)).

3. At 7773 2864, Unit Ω is enclosed in the palaeosol below Puketarata Tephra from Maroa, approximately dated (from $^{14}C$ ages of bracketing units) at *ca.* 14 000 $^{14}C$ years BP (Froggatt & Lowe 1990).

By assuming uniform loess/soil accumulation rates at individual sites, and from measuring thicknesses of loess/soil between Units Ψ, Ω and A and any of the three 'foreign' tephras present, ages can be estimated ($^{14}C$ and calibrated (calendar) timescales, respectively):

Unit Ψ 17 200 and 20 500 years BP,

Unit Ω 15 600 and 18 800 years BP, and

Unit A 14 200 and 17 000 years BP.

These ages are very approximate only, due both to assumptions of uniform loess/soil accumulation rates and to uncertainties in the ages of the 'foreign' tephras, and 1 s.d. errors are realistically ±5–10%.

(i) *Unit Ψ*

A type locality is proposed at 7704 2741 where this unit is thickest (figure 2), and a reference locality at 7817 2750 where its post-Oruanui age is demonstrable. Unit Ψ consists of two fall subunits; Ψ1 is non- to normally graded, rich in foreign lithics and mostly well sorted. Matrix bearing (water flushed) material occurs only at the type locality and is thus tentatively inferred to represent local rain showers. Subunit Ψ2 is poorly sorted, with an ash matrix and abundant grey to black dense pumice to obsidian. Thickness data (figure 3) are inadequate to accurately constrain the volume or vent position, but in comparison to Unit Ω and younger deposits, a volume of (O) 0.05 $km^3$ is indicated. The eruption is inferred to have begun with dry, open-vent activity, then switched rapidly to wet activity which possibly accompanied lava extrusion.

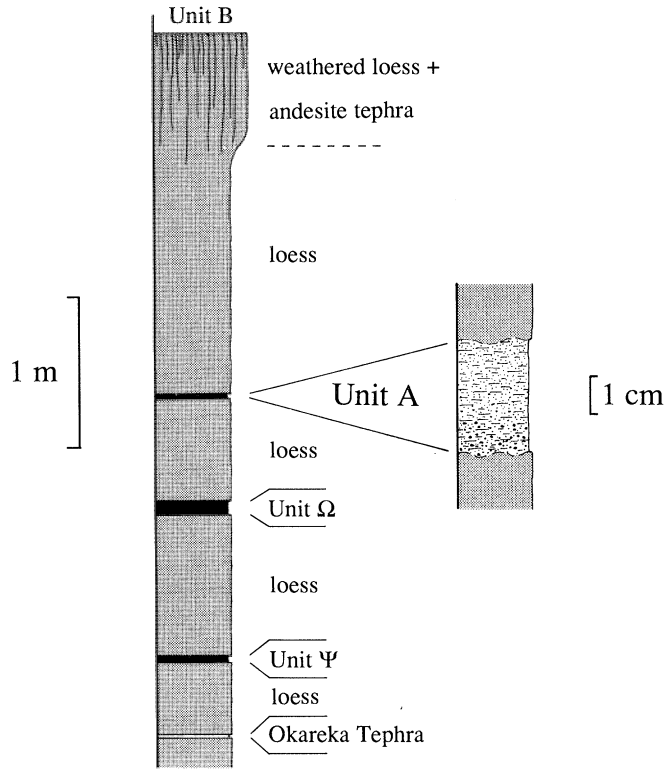


Figure 6. Stratigraphic columns for the type section of Unit A at 7798 2796 (Appendix A). The left-hand column shows the positions of Ψ, Ω, A and the Okareka Tephra (from Okataina) within the pre-B loess deposits, and detail of A is given on the right. Ornamentation for the loess is conventional.

(ii) *Unit Ω*

A type locality is proposed at 7708 2741 (figure 4). Typically Ω is a plinian fall deposit which consists of a thin (less than 5 cm) fines-poor bed of ash to lapilli overlain by greater thicknesses of poorly sorted, very-fine ash to lapilli material interpreted to have been water-flushed from the abundance of matrix, presence of vesicles, and similarity to Subunit Y3 (Hatepe ash; Walker 1981*b*). The limited thickness and grainsize data (figure 5) suggest a volume of *ca.* 0.1 $km^3$, and a source close to the northern shoreline of the modern Lake Taupo, at *ca.* 768 271. The eruption is interpreted to have started 'dry' but soon switched to 'wet' activity. Lithics are almost exclusively foreign, which suggests that the activity was open vent in style and not accompanied by dome formation.

Figure 7. Stratigraphic columns to show the nature of and lateral correlations in Unit B. Locality 2394 (Appendix A) is the designated type locality. The inset map in this and subsequent figures shows the localities with respect to the vent(s) active during the particular phase(s) (see text for details). In all columns, Unit B overlies the loessic palaeosol developed on the Oruanui ignimbrite or older deposits, and is overlain (after a period of weathering) by the andesitic Te Rato Lapilli. Grid references for localities are: 7602 2407 (2382); 7649 2462 (2391); 7740 2489 (2427); 7767 2533 (2425); 7796 2565 (2405); 7861 2639 (2401); 7837 2704 (2322); 7789 2729 (2394); 7771 2760 (1275); 7765 2786 (2472); 7737 2785 (2288); 7644 2809 (2478).

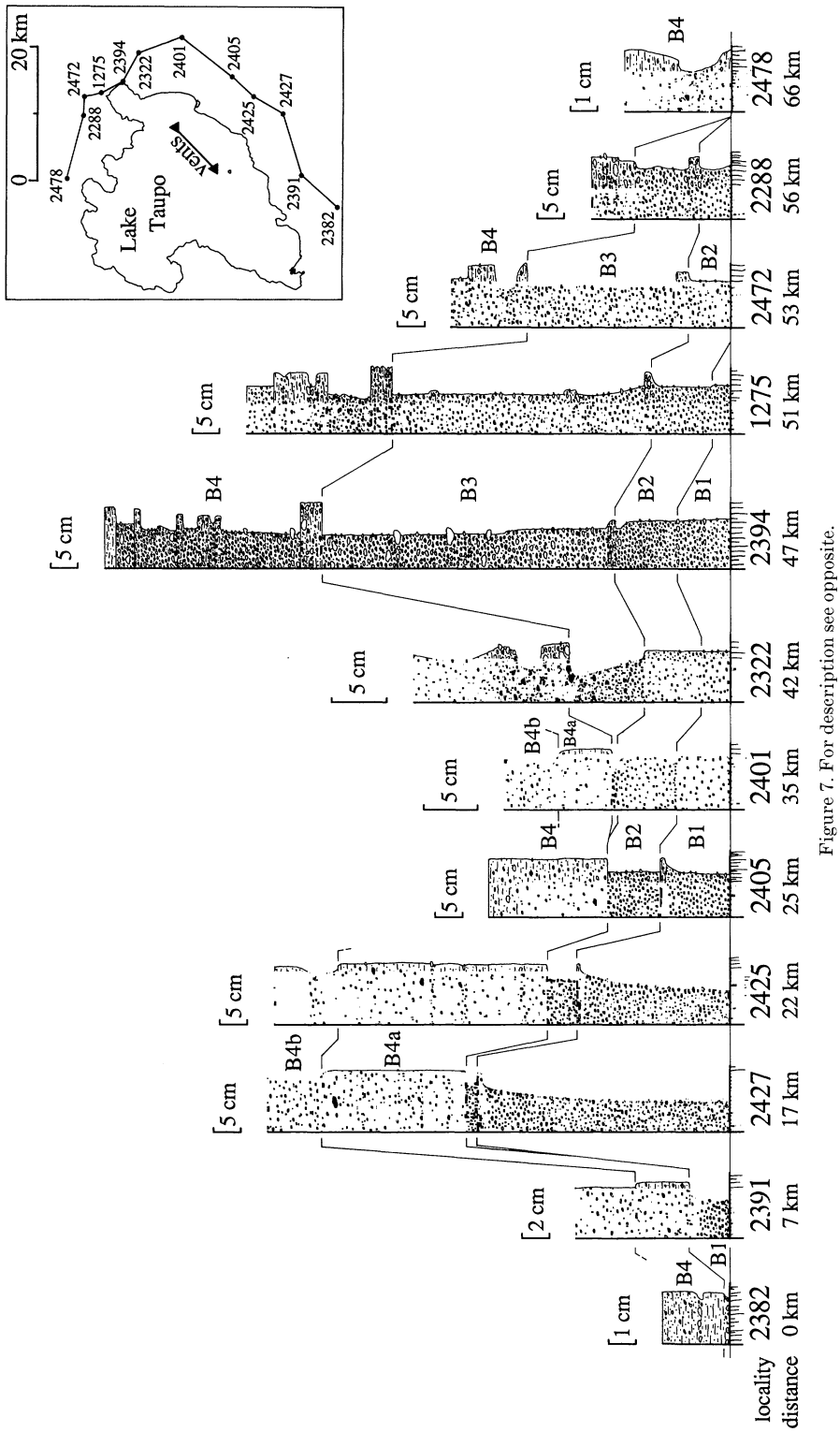


Figure 7. For description see opposite.

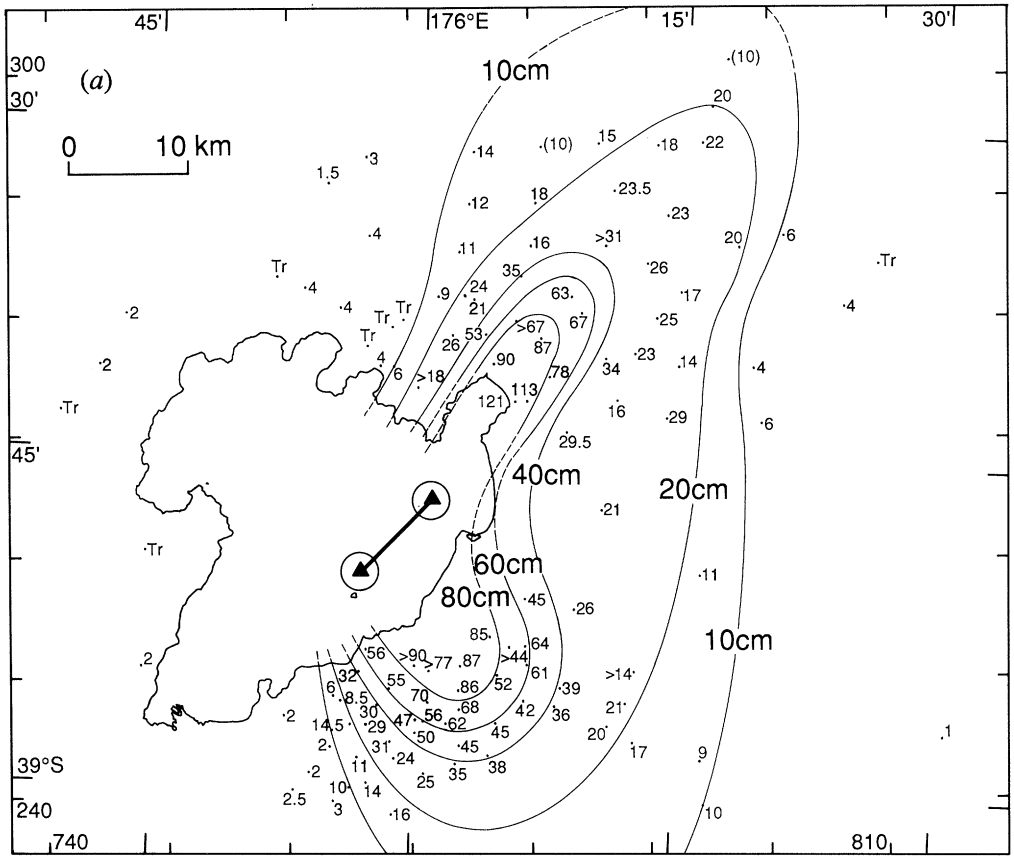


Figure 8. Isopach and isopleth maps for Unit B. (*a*) B total thickness; values and isopachs in centimetres. Here and in subsequent figures, A = absent, and bracketed values are where the deposit is heavily bioturbated; the thickness figure given is that estimated for pristine material on the basis of 10 cm (bioturbated) = 6 cm(pristine), as measured at several localities where both could be observed.

### (iii) *Unit A*

A type locality is proposed at 7790 2796 (figure 6) where A is a 3 cm thick fall deposit, which consists of poorly sorted, very-fine to medium ash with common dense pumiceous to obsidian clasts. The only other exposure is at 7747 2818. At 7790 2796, Unit A lies at roughly the expected stratigraphic level of Puketarata Tephra, but (i) its juvenile material is very sparsely porphyritic, and (ii) its ferromagnesian fraction is dominated by hypersthene, and biotite is absent.

In sharp contrast, the corresponding size fractions of Puketarata Tephra have noticeable contents of phenocrysts in the juvenile fragments, and an amphibole-rich, biotite-bearing ferromagnesian assemblage. The absence of biotite in Unit A also precludes correlation with any known Okataina tephra from this time period (Nairn 1981; Froggatt & Lowe 1990).

Eruption A is interpreted as a small phreatomagmatic event, possibly accompanying lava extrusion. Its volume is implicitly small from its limited thickness and preservation and is adopted as 0.01 km$^3$. No vent site can be identified.

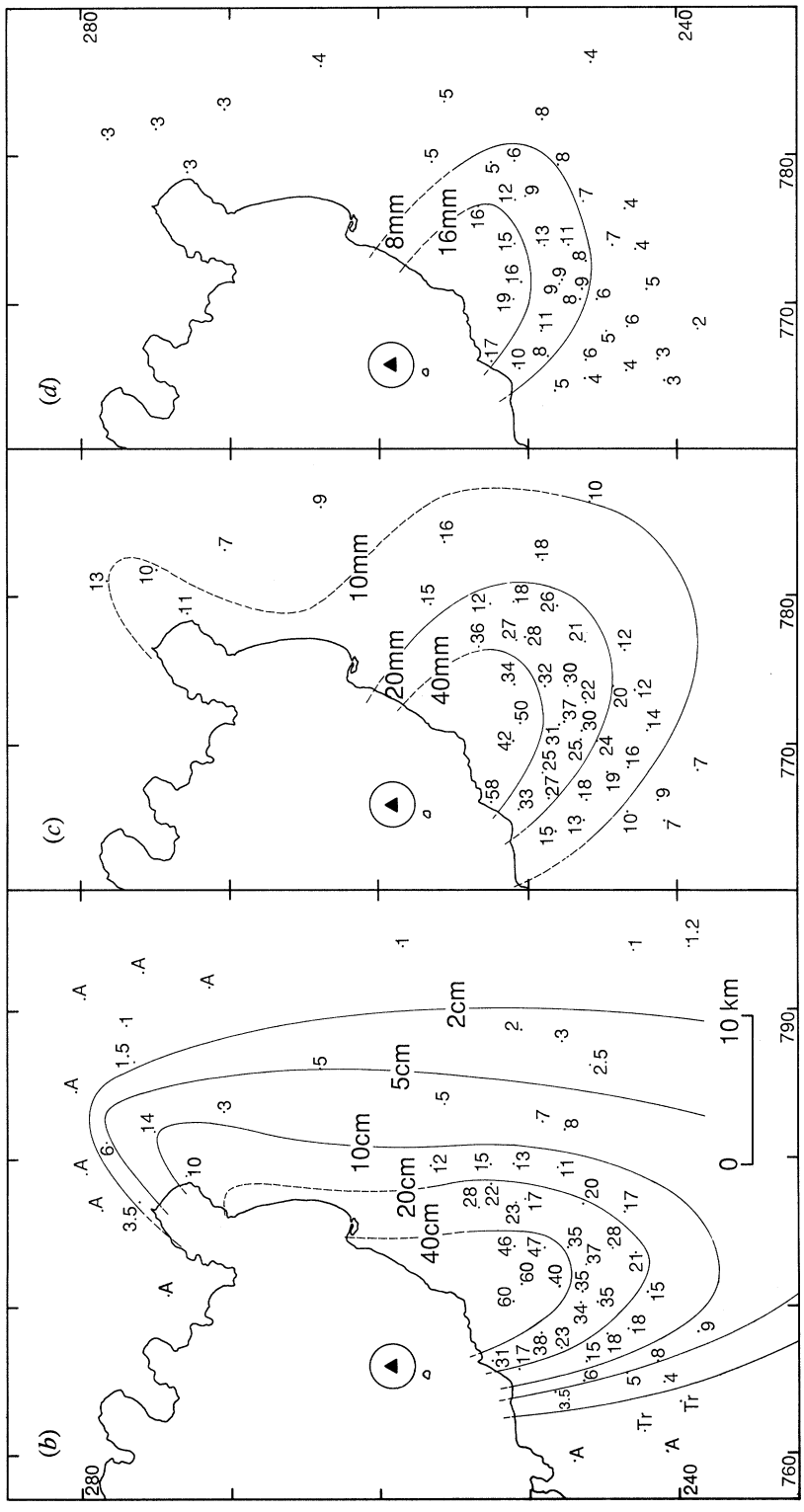


Figure 8. Isopach and isopleth maps for Unit B (*cont.*). (*b*) B1, thickness; values and isopachs in centimetres. (*c*) B1, $P_m$ data; values and isopleths in millimetres. (*d*) B1, $L_m$ data; values and isopleths in millimetres.

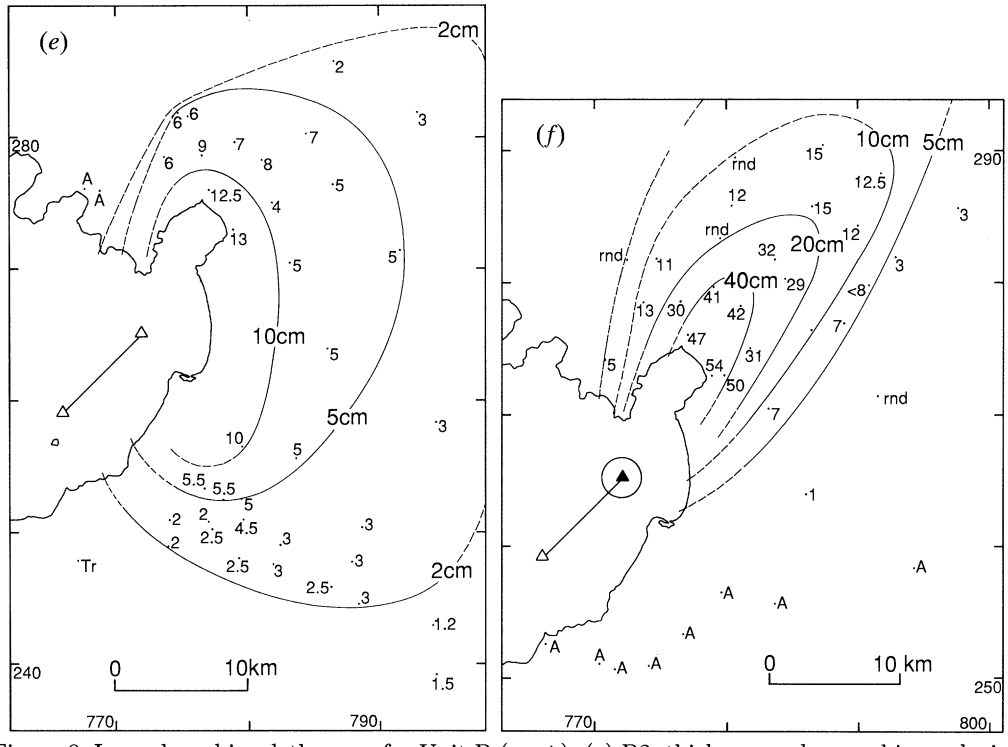


Figure 8. Isopach and isopleth maps for Unit B (*cont.*). (*e*) B2, thickness; values and isopachs in centimetres. The inferred vent(s) lie(s) between the two triangles (see text). (*f*) B3, thickness; values and isopachs in centimetres; rnd denotes B3 is present but its upper contact and thickness cannot be defined.

### (*b*) *Unit B (Karapiti Tephra)*

Unit B is the same deposit as that defined as Karapiti Tephra Formation by Vucetich & Pullar (1973), but excluding the overlying palaeosol. Evidence presented below implies that the dome at Acacia Bay and its associated pyroclastic deposits, included in a revised Karapiti Tephra Formation by Froggatt (1981*a*), belong to a separate, younger event (Unit D, below). An averaged $^{14}C$ age of 9820±80 years BP is presented by Froggatt & Lowe (1990), but the 10 year difference between this and their age for the Poronui Tephra (Unit C here) is incompatible with the extent of post-B bioturbation and soil formation. Two $^{14}C$ ages of 9910±130 (Froggatt 1981*a*) and 10 150±130 years BP (Appendix B) have been obtained from charcoal respectively in and immediately above Unit B, while Lowe & Hogg (1986) estimated an age of 10 100 years BP from peat accumulation rates. A $^{14}C$ age of 10 100 years BP is adopted here, equivalent to a calibrated age of 11 800 years BP.

Unit B is a markedly bilobate fall deposit (figures 7 and 8*a*). Where well exposed to the NE and SE of Lake Taupo it shows contrasting bedding and grainsize characteristics (figure 7). Sparse intervening exposures demonstrate that the two lobes belong to the one eruptive event and imply that they represent both sequential as well as apparently simultaneous deposits. Unit B is divided into four subunits, B1 to B4.

Subunit B1 is a plinian pumice fall deposit best developed SE of Lake Taupo,

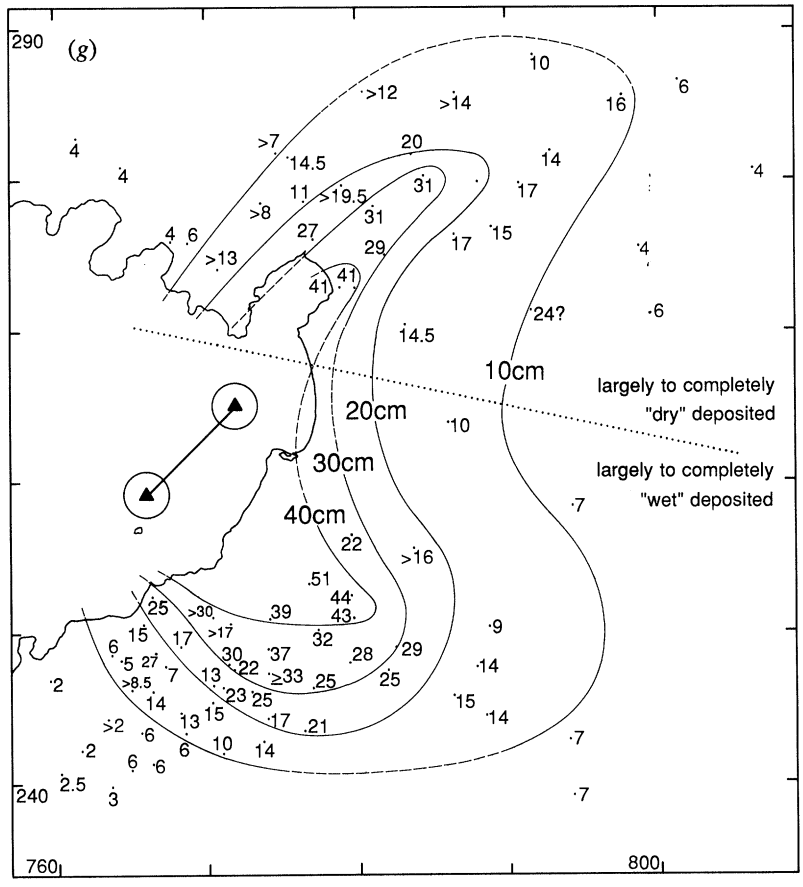


Figure 8. Isopach and isopleth maps for Unit B (*cont.*). (*g*) B4, thickness; values and isopachs in centimetres. See text for discussion of vent positions.

but with a minor lobe to the NE (figures 7 and 8*b*). Subunit B1 is non-bedded, often normally graded and generally well sorted. Lithics are very subordinate and are exclusively foreign. Isopach and isopleth data (figure 8*b–d*) yield a bulk volume of 0.23 km$^3$ and an estimated vent position at 766 259. At 7663 2524, 2 cm of fines-rich, poorly sorted fall material occurs at the base of B1, and is inferred to represent initial 'wet' activity, but this bed is not seen elsewhere. At many localities in the S part of its dispersal area, B1 grades up to a thin (less than 1 cm) bed rich in very-fine ash which weathers as a pronounced rib where overlain by B2. This capping bed is absent in the NE area where B2 overlies B1 with no grainsize break. These relationships and the isopach data (figure 8*b*) indicate that B1 was initially dispersed by a NW wind, but that the wind direction changed to SW during later stages to form the subordinate NE lobe. The very-fine-ash capping bed, where present, is interpreted as being generated by the settling out of fines during a local lull in deposition.

Subunit B2 is well sorted, non-bedded, and either non-graded or with a weak normal grading. It contains an unusually high proportion of lithics (sometimes greater than 50 modal %), giving it a speckled colour, which distinguishes it from

B1 in the NE area. Isopach data (figure 8*e*) suggest a source further NE than for B1 which, with the high content of lithics, is consistent with the vent propagating away from its position during B1 towards the inferred position for B3 (below). Isopach data yield a bulk volume of 0.1 $km^3$.

Subunit B3 is found only to the NE of Taupo (figures 7 and 8*f*). Stratigraphic correlations, especially the marked thinning from localities 2394 to 2322 and 2401 (figure 7), imply that B3 has an extremely narrow dispersal fan (figure 8*f*). Where B3 is thickest, the base of B4 is marked by a very poorly sorted, fines-rich band which weathers as a pronounced rib, but on the west and east fringes of the B3 dispersal fan this band is absent and B3 grades up with no demarcation into B4. B3 is poorly to non-bedded and inverse graded; its base is distinctly coarser than B2 and its top is comparable in grainsize to the base of B4. Isopach data (figure 8*f*) yield a volume of 0.15 $km^3$, and a vent position inferred at 772 265 because of the continuity between B3 and the NE lobe of B4 (see below). Lithic clasts are almost entirely foreign, mostly rhyolite lava, together with orange/brown hydrothermally altered material.

The remainder of B is included in Subunit B4 which totals 0.82 $km^3$. The nature, thickness and grainsize characteristics of B4 are very different in the two areas, NE and SE of Lake Taupo, respectively, where B4 is best developed.

In the SE area, where it is best preserved B4 can be divided into further subunits (B4a and B4b; figure 7). B4a is poorly to moderately bedded, very poorly sorted and has a vesicular matrix rich in very fine to fine ash. Lower parts of B4a are a buff to pale brown and contain a lithic population of both older lavas and obsidian, whereas upper parts are greyer, contain abundant grey moderately vesicular juvenile material and have an obsidian-dominated lithic population. B4a is interpreted to have been waterflushed, from its field characteristics and similarity to Subunit Y3 (Hatepe ash; Walker 1981*b*). B4b is pale grey, rich in poorly to moderately vesicular juvenile material, and has lithics dominated by obsidian, but is distinctly poorer in very fine ash than B4a.

In marked contrast, the NE lobe of Subunit B4 is a well bedded, normally graded deposit with well sorted, matrix-free material alternating with various numbers of thinner, matrix-bearing bands which weather as ribs on exposed surfaces (figure 7). Two features imply that the two lobes of B4 represent material erupted simultaneously.

1. Stratigraphic correlations imply that the prominent, matrix-rich basal band of B4 in the NE lobe is isochronous with the basal contact of B4a in the SE area. Both B4 lobes are voluminous and widespread enough that some distal relict of one or the other lobe would be expected to be preserved had the two lobes been erupted sequentially.

2. Lithic populations in both lobes show progressive changes from obsidian-subordinate (SE lobe) or obsidian-poor (NE lobe) in the basal parts of B4 to obsidian-dominated in the upper parts.

On the other hand, the different natures of the B4 lobes and their isopleth data are interpreted to suggest that at least two vents were active during B4 activity. For the NE lobe, the crosswind widths of isopleths indicate a peak column height of 24–27 km (method of Carey & Sparks 1986), and a vent sited at 772 265 (assumption of the same vent position as for phase B1 gave inconsistent results). For the SE lobe, the water-flushed nature of B4 and the isopleth shapes when compared (figure 8*g–i*)to those for B1 are interpreted to indicate the same vent

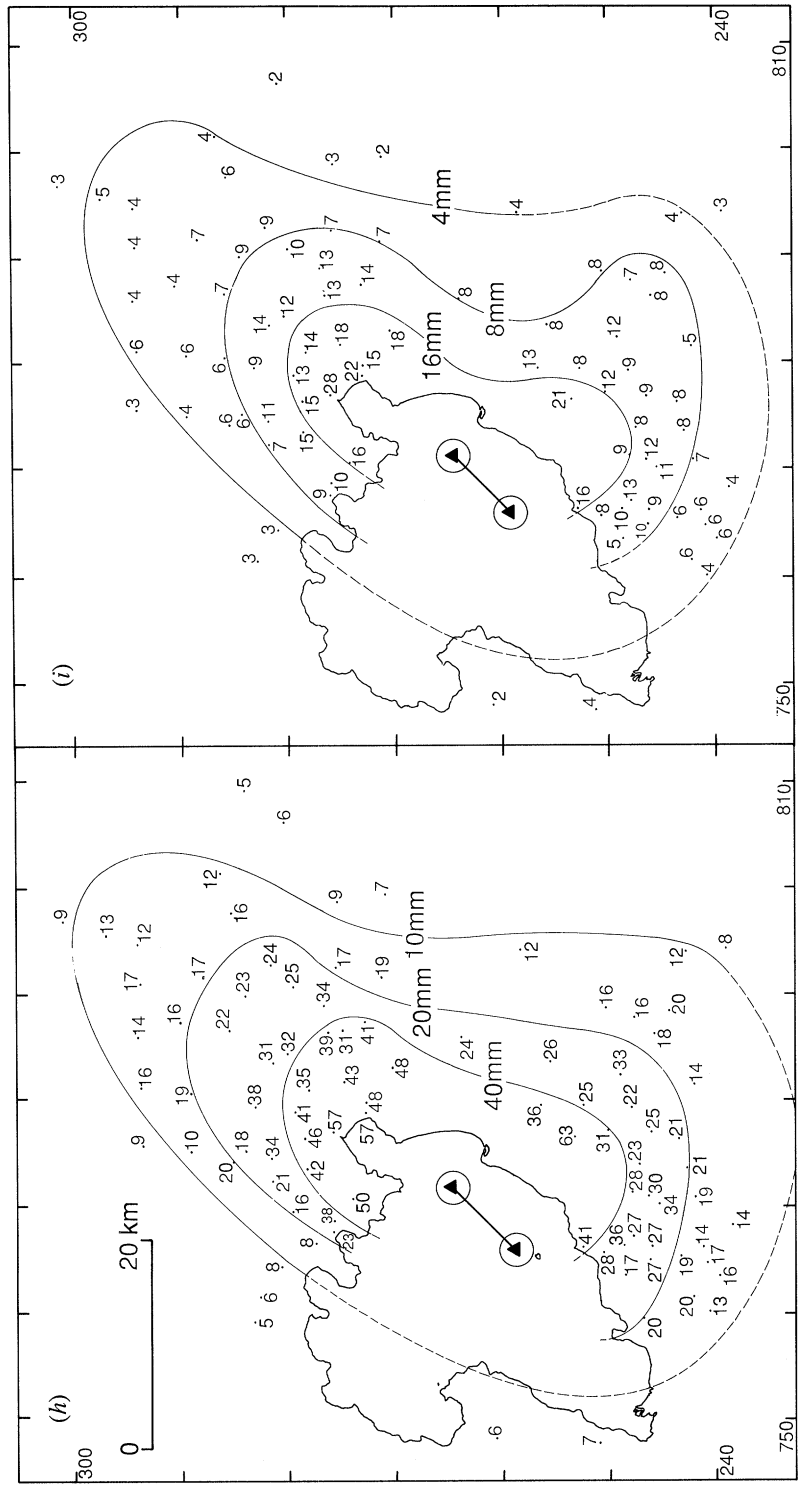


Figure 8. Isopach and isopleth maps for Unit B (*cont.*). (*h*) B4, $P_{m}$ data ; values and isopleths in millimetres. (*i*) B4, $L_{m}$ data ; values and isopleths in millimetres.

position as for B1. There is also the possibility of other activity having occurred from vents between these two sites (cf. B2, above).

Eruption B is interpreted to have resulted from dyke emplacement along a *ca.* 10 km long fissure. The first activity (B1) was largely 'dry', open-vent eruption from a vent at 766 259, initially with NW, then SW winds. Activity then migrated to the NE (B2) before breaking out in increasingly powerful open-vent activity from a vent at *ca.* 772 265 (B3). Activity continued at the B3 vent to generate the NE lobe of B4, while simultaneously resuming to the SW at the B1 vent (which had flooded with water while B2 and B3 were being erupted), to generate the SE lobe of B4. Both sets of activity began in open-vent style, but increasing amounts of poorly to non-vesicular juvenile material began to be erupted, particularly from the SW vent. The 'wet' eruption clouds from the SW vent were dispersed to the SE, whereas the 'drier' plume from the NE vent was dispersed NE along an axis identical to that for B3. The cause(s) of the differing B4 dispersal directions are not clear, but differential wind directions are the simplest explanation; NW in the troposphere (as implied by the water-flushed nature of the SE lobe) and SW in the stratosphere (as implied by column height estimates for the NE lobe). The eruption terminated with weakly explosive activity, possibly accompanying lava extrusion.

### (*c*) *Unit C (Poronui Tephra)*

The Poronui Tephra Formation was proposed by Vucetich & Pullar (1973) from a type locality at 7839 2535 to describe the pumice fall unit over their Karapiti Tephra Formation. Unit C here is broadly comparable, except that the upper parts of Vucetich & Pullar's Poronui Tephra Formation are here recognized to be a separate, younger deposit (Unit D, below). The adopted $^{14}C$ age of Unit C is 9800 years BP (from Froggatt & Lowe 1990), equivalent to a calibrated age of 11 400 years BP.

Unit C is a fall deposit which is divided into two subunits (figure 9). Subunit C1 is the coarser and thicker of the two, and can at most localities be further divided into three parts (C1a–C1c). C1a is the basal part of C1 which contains sparse to dominant amounts of a vesicular, fines-rich matrix, and is interpreted to have been water flushed. However, C1a shows irregular thickness variations (figure 10*c*) and is interpreted to have resulted from low-level (tropospheric) rain-flushing of fines accompanying deposition of coarse-ash to lapilli from a higher plume.

C1b is the thickest and coarsest part of Subunit C1. Mostly C1b is a fines-free, weakly to non-bedded pumice fall deposit, but in areas close to and E of vent matrix-bearing bands occur and are interpreted to reflect further low-level rain flushing. C1b is non- to weakly inverse-graded more than 20 cm thick, but strongly inversely graded in areas where it thins perpendicular to the dispersal axis. The visible lithic content of C1b increases up to its top contact and there is accompanied by minor quantities of faintly streaky pumices.

C1c is variable in appearance with azimuth around the vent (figure 9). Where thickest, it is distinguished from C1b by a pronounced reduction in grainsize, but this distinction fades towards the N and S perimeters of the dispersal fan. C1c is normally graded. It is non-bedded and well sorted to the E and N of Lake Taupo, but to the SE it is well bedded, with the beds defined by fluctuations in abundance of a vesicular, fines-rich matrix, and with a conspicuous ribbed appearance on weathered surfaces.

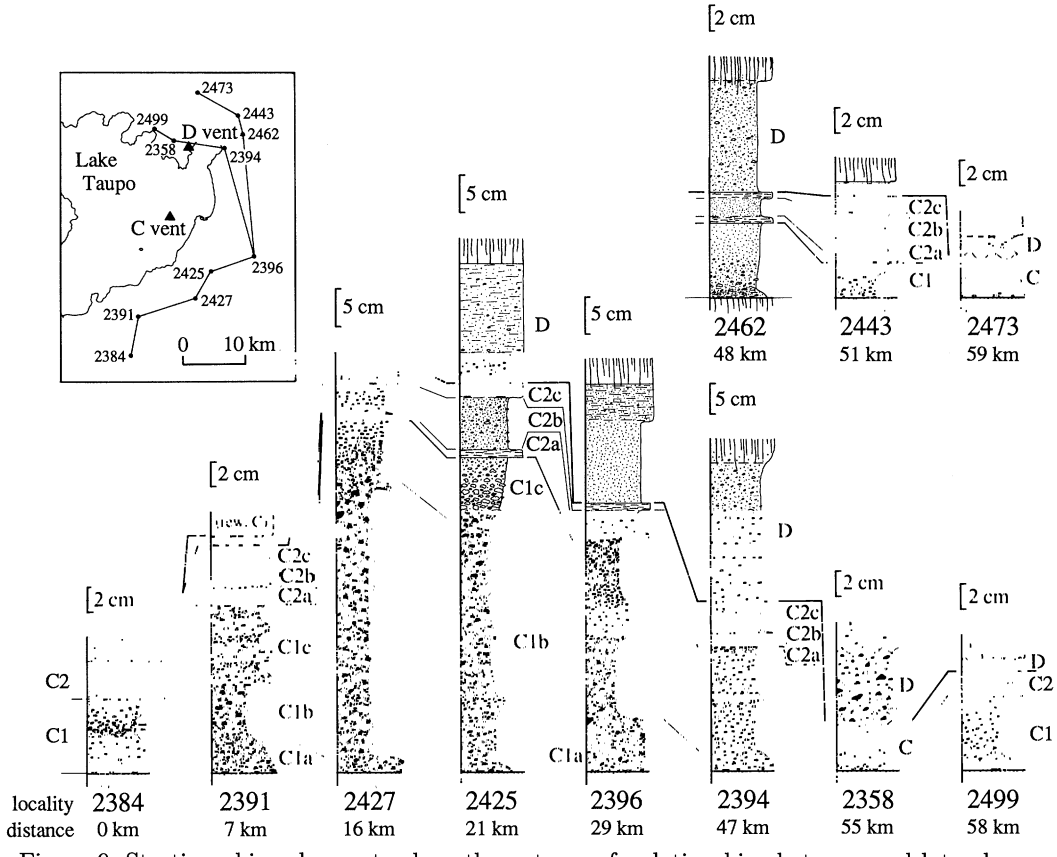


Figure 9. Stratigraphic columns to show the natures of, relationships between and lateral correlations in fall deposits of Units C and D. Localities 2425 and 2394 are the designated type localities for C and D (see figure 11, plate 1), respectively (Appendix A). In all columns, C rests on the palaeosol developed on the andesitic Te Rato Lapilli and/or B, and D is overlain by E. Grid references for localities are: 7636 2398 (2384); 7649 2462 (2391); 7740 2489 (2427); 7767 2533 (2425); 7837 2556 (2396); 7818 2750 (2462); 7811 2783 (2443); 7747 2818 (2473); 7789 2729 (2394); 7708 2741 (2358); 7677 2760 (2499).

Subunit C1 has an overall S dispersal, with a lesser E lobe (figure 10*b*) Isopach data yield a volume estimate of 0.55 km$^3$, while isopleth data (figure 10*h*, *i*) are used to infer a vent position at 770 262. Lithic clasts in C1 are mostly older lavas, with some hydrothermally altered varieties; obsidian is very subordinate.

Subunit C2 consists of a distinctive triplet of beds, with a well-sorted fine- to coarse-ash bed (C2b) between two beds dominated by very fine ash (C2a and C2c). The two fine beds show no systematic variations in thickness (figure 10*e*, *g*), and have a similar nature and inferred origin to the ash beds deposited during lulls and at the close of the AD 1912 Novarupta eruption (Fierstein & Hildreth 1992). C2b shows a general thinning away from Lake Taupo (figure 10*f*), consistent with a source at the C1 vent position. Unit C2b contains significant amounts of obsidian fragments, suggesting that it may have accompanied lava extrusion. Unit C2b has an estimated volume of 0.08 km$^3$, while isopachs for C2 as a whole (figure 10*d*) yield an estimate of 0.20 km$^3$ (i.e. to a first order, C2a and C2c have volumes of 0.06 km$^3$ each). The overall volume for Unit C is 0.75 km$^3$, which

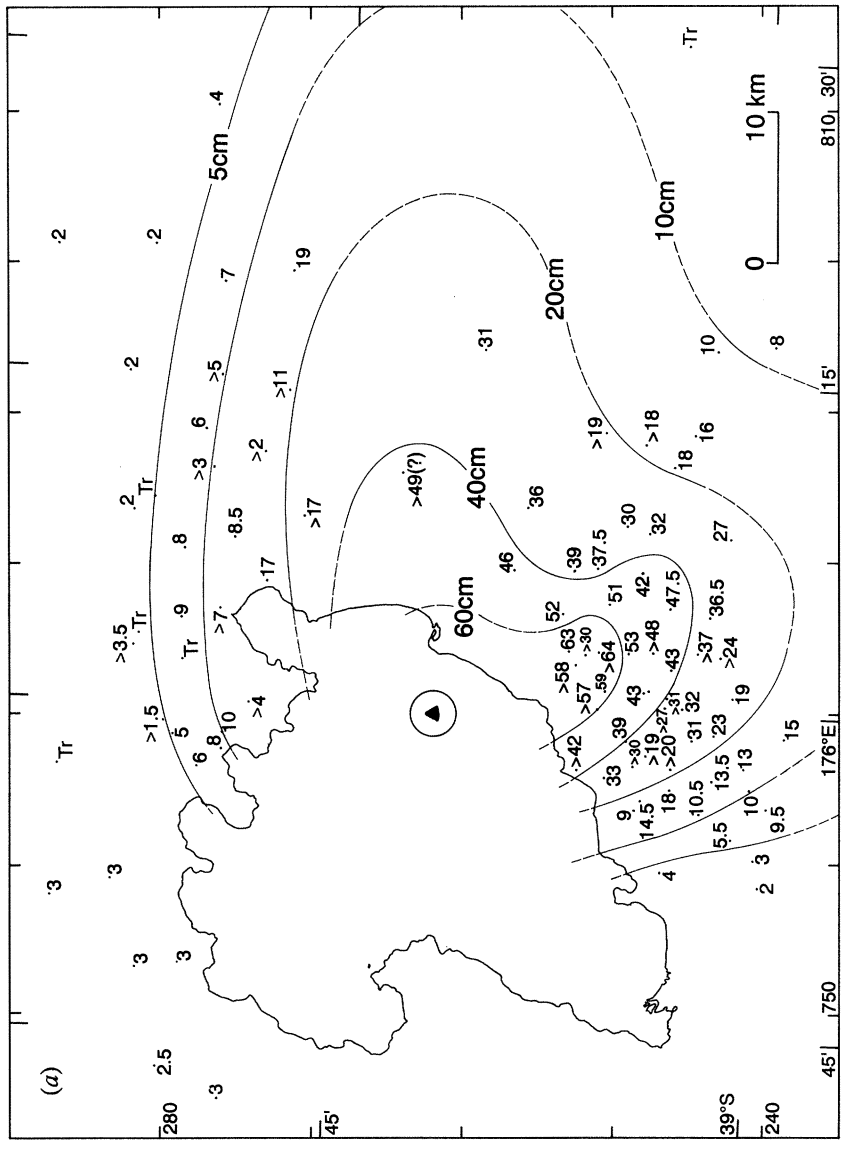


Figure 10. Isopach and isopleth maps for Unit C. (*a*) C total thickness; values and isopachs in centimetres.

includes a poorly preserved distal fringe of fine ash N and NW of Lake Taupo (figure 10*a*).

Unit C represents a plinian event similar in style to G and H. The overall inverse grading in C1a plus C1b implies an increasingly more powerful plume which peaked at *ca.* 28 km height from isopach data. The increase in lithic abundance up to the top of C1b suggests that this phase may have ended when wall slumping partially closed off the vent, sharply reducing the output rate and vigour of the column (thus the drop in grainsize into C1c). Subsequently the eruption continued to diminish in vigour; possibly water flooding the vent (cf. the bedded nature and presence of water-flushed beds in C1c) may have contributed to this decline. The eruption stopped during C2a for a period of hours to a few tens of hours (from

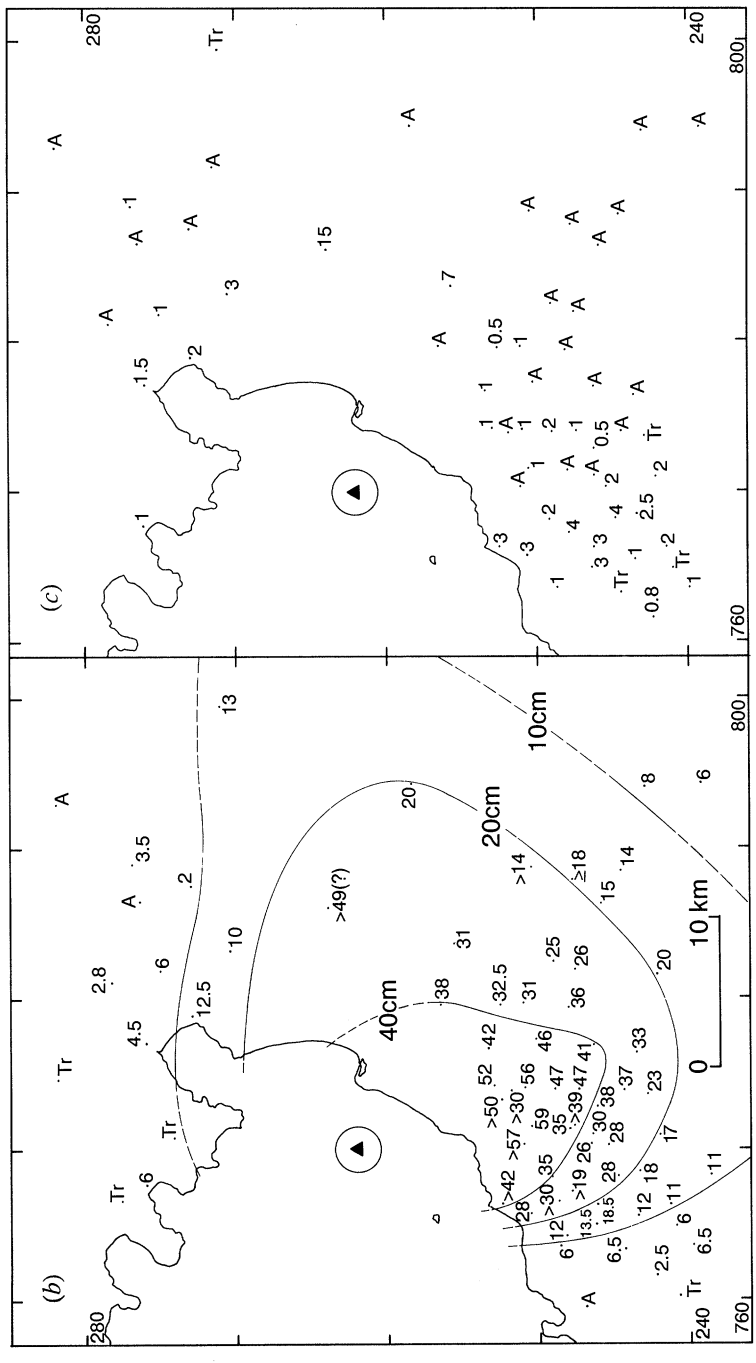


Figure 10. Isopach and isopleth maps for Unit C. (*cont.*). (*b*) C1, thickness; values and isopachs in centimetres. (*c*) C1a (basal water-flushed deposits in C1; see text), thickness; values in centimetres.

the lack of erosion, and by analogy with the Novarupta ashes), then resumed with weak explosive activity (C2b), possibly accompanying lava extrusion, before finally ceasing (C2c). Ash beds similar to C2a and C2c should have formed after every eruption at Taupo, but the Unit C examples are by far the best defined.

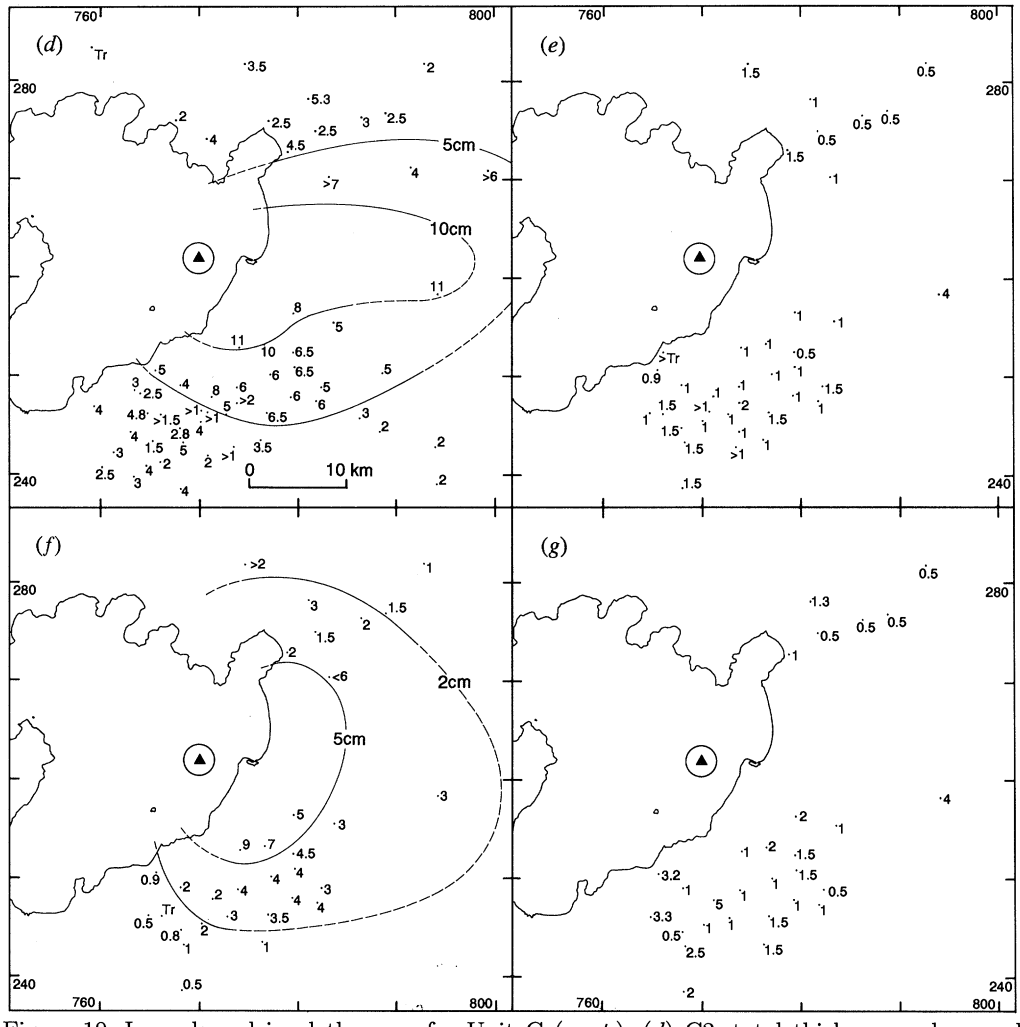


Figure 10. Isopach and isopleth maps for Unit C (*cont.*). (*d*) C2, total thickness; values and isopachs in centimetres. (*e*) C2a, thickness; values in centimetres. (*f*) C2b, thickness; values and isopachs in centimetres. (*g*) C2c, thickness; values in centimetres.

This is interpreted to reflect the rapid burial and preservation by Unit D and/or a subsequent andesitic fall deposit from Tongariro (Poutu Lapilli: Topping 1973).

### (*d*) *Unit D*

Unit D is defined here from a type locality at 7789 2729 where its relationship to Unit C is clearest (figure 11, plate 1). No age data are available on Unit D, but it is inferred to be separated from C by a time break of the order 20 years from two pieces of evidence seen at several localities:

1. Subunit C2 is locally disturbed and is stained brown by the incorporation of loess and the formation of a weathering horizon (e.g. at 7789 2729, figure 11).

2. Unit C is less continuous and more heavily bioturbated than Unit D (e.g. at 7890 2769).

This time break seems unlikely to be less than several years (from the staining

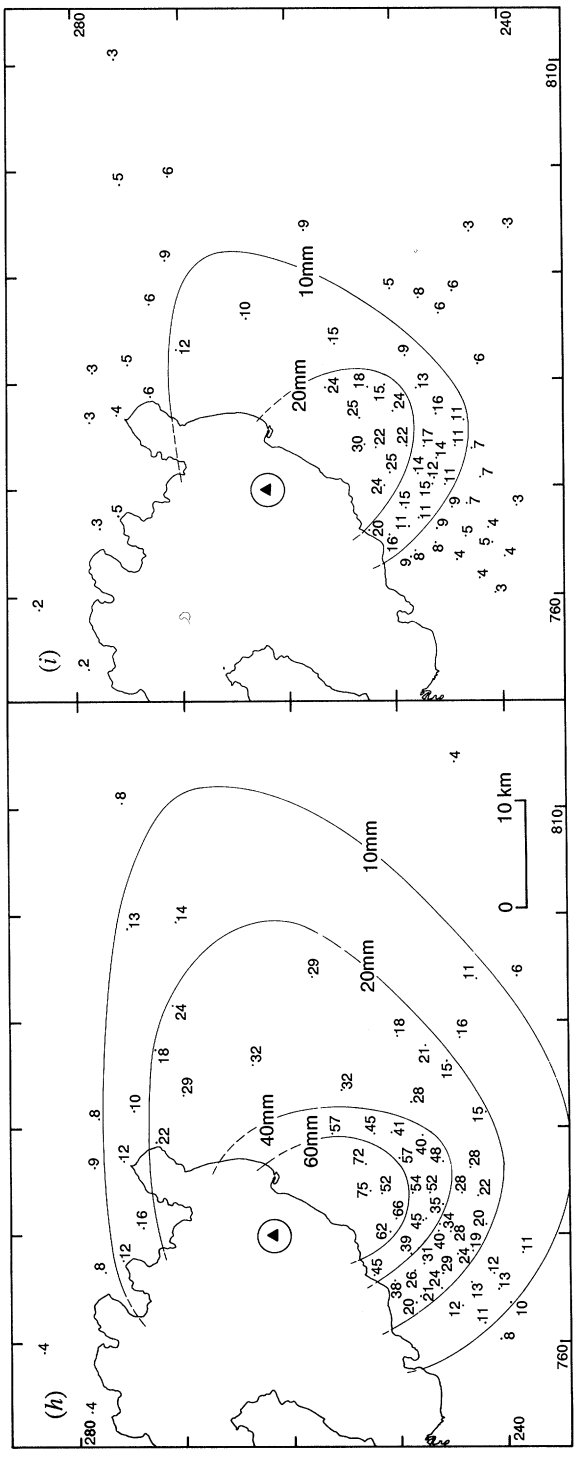


Figure 10. Isopach and isopleth maps for Unit C (*cont.*). (*h*) C1, $P_m$ data; values and isopleths in millimetres. (*i*) C1, $L_m$ data; values and isopleths in millimetres.

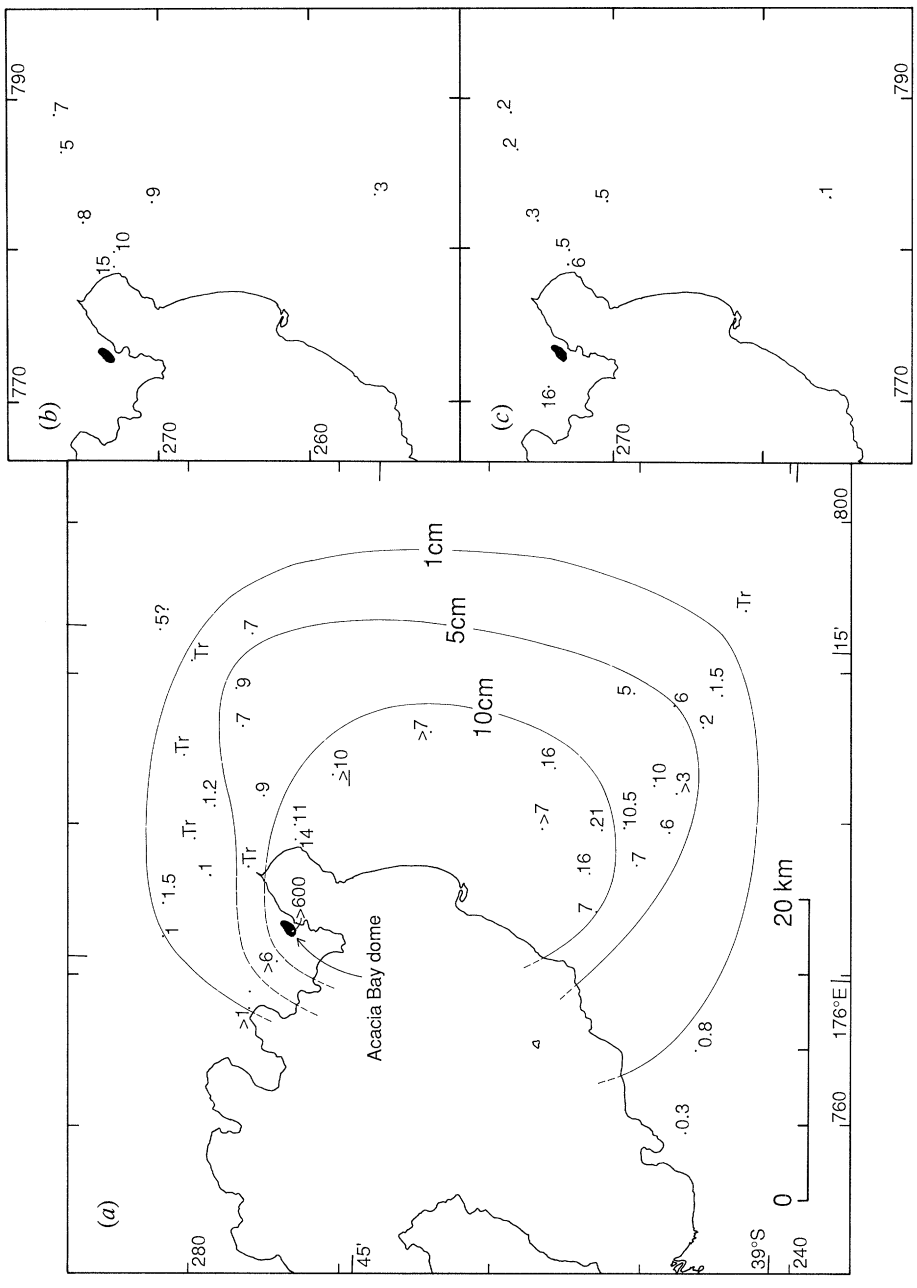


Figure 12. Isopach and maximum-clast size maps for Unit D. The area of the Acacia Bay dome (inferred source vent for D) is shown. (*a*) Isopachs and thicknesses in centimetres. (*b*) $P_{m}$ data, values in millimetres. (*c*) $L_{m}$ data, values in millimetres.

and bioturbation) or more than a few decades (from the preservation state of Unit C2, and visual comparisons with the degree of soil development on deposits of the 1886 AD Tarawera eruption). Adopted ages of Unit D are thus 9780 years BP ($^{14}$C timescale) or 11 380 years BP (calibrated timescale).

Unit D is a fall deposit which reaches a maximum thickness of 21 cm, and is dispersed mostly SE of vent (figure 12). D is generally moderately sorted, dominated by fine to coarse ash, and is interpreted to have been deposited dry.

However, at some localities (e.g. 7767 2533) the upper part of the unit is poorly sorted and rich in very fine ash, and is interpreted to have been rainflushed. The juvenile material is non- to moderately vesicular and angular in shape. Foreign lithics are extremely rare.

Unit D is interpreted to have been erupted from a vent now concealed beneath a $1.0 \times 0.5$ km$^2$ lava dome on land just NW of Acacia Bay township, for three reasons.

1. The coarsest Unit D material is found at 7708 2741, the closest locality to the dome where the base of D is exposed.

2. The dome-derived lava debris is overlain (e.g. at 7727 2730) by soil then by Unit E; Units C and D are absent and hence inferred to pre-date or be contemporaneous with the dome extrusion.

3. Unit D is relatively fine grained, contains lithics that are almost entirely obsidian, and is thus inferred to reflect weak explosions, possibly associated with a dome-building event. The Acacia Bay dome has previously been postulated as the vent site for all or part of the Karapiti Tephra (= Unit B) by Froggatt (1981*a*) and Froggatt & Lowe (1990), but isopach and isopleth data for Unit B (figure 8) preclude this.

The inferred proximal equivalents of Unit D deposits are poorly bedded pyroclastics with an exposed thickness of up to 6 m on the SE side of the Acacia Bay dome at 7729 2730. These have a grey matrix of very-fine to coarse ash, with subordinate lapilli to blocks (up to 40 cm) of juvenile material ranging from obsidian to moderately vesicular pumice. The blocks that are larger than 5 cm usually have pink haloes, interpreted as due to thermal oxidation of the matrix by hot blocks.

Unit D is interpreted to have resulted from weak explosive activity associated with the extrusion of gas-poor magma. The proximal deposits may represent a tuff ring into which the Acacia Bay dome was emplaced. Erupted volumes are estimated as 0.15 km$^3$ for the D fall, 0.003 km$^3$ for the proximal pyroclastics and 0.05 km$^3$ for the dome.

### (*e*) *Unit E (Opepe Tephra)*

The Opepe Tephra Formation was defined by Vucetich & Pullar (1973) from a type locality at 7798 2729. Unit E is used here in substantially the same sense, except that the thick post-E palaeosol (which encloses a new deposit, Unit F) is not included. They recognized two main subunits; a lower, bedded pumice fall deposit and an upper, coarser, more poorly bedded subunit, and this stratigraphy remains valid. However, in this paper Unit E is divided into four fall subunits, E1 which corresponds to the lower subunit of Vucetich & Pullar (1973), and E2 to E4 which correspond to most of their upper subunit. In addition, part of their upper subunit, here termed E5, is inferred to be a non-welded ignimbrite. The relationships between these units are shown in a series of sections (figure 13). Their type section at 7798 2729 is retained for E1, and a reference locality for E2–E4 proposed at 7943 2584 (figure 13). Froggatt & Lowe (1990) give an average $^{14}$C age of 9050±40 years BP, and this is adopted here, equivalent to a calibrated age of 9950 years BP.

Subunit E1 is a poorly bedded, mostly well-sorted fall deposit. The bedding is poorly to moderately defined by fluctuations in grainsize; finer bands are richer in lithic fragments, suggesting that throttling by vent-wall collapse may have

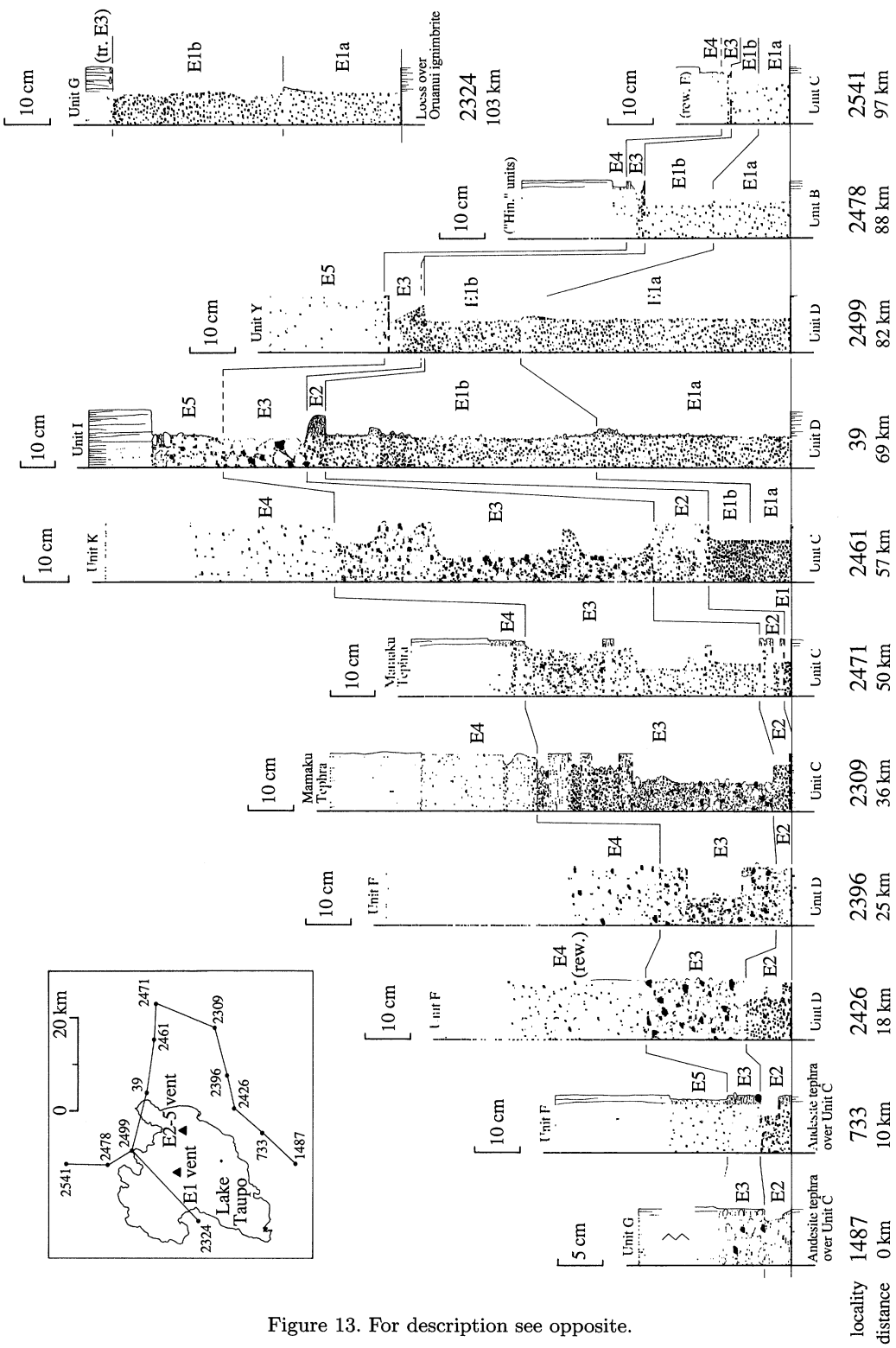


Figure 13. For description see opposite.

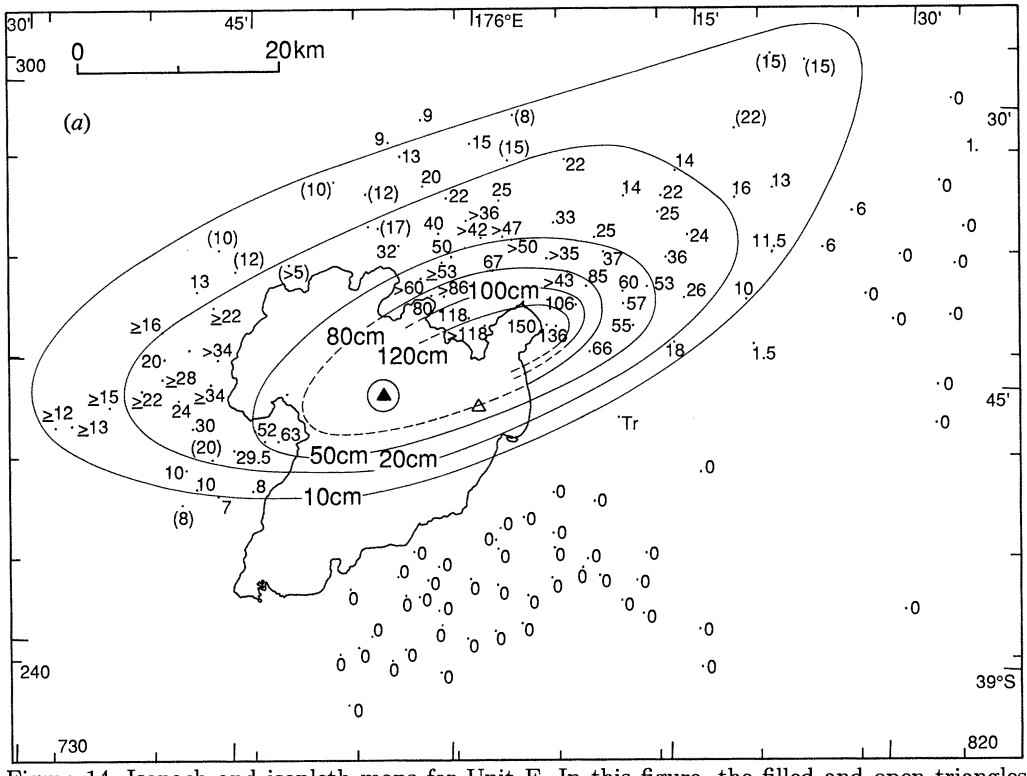


Figure 14. Isopach and isopleth maps for Unit E. In this figure, the filled and open triangles represent the active and inactive vent, respectively (see text for discussion). (*a*) E1, thickness; values and isopachs in centimetres. Bracketed values are estimated, as in figure 8*a*.

caused fluctuations in eruption column vigour. The top of the most obvious of these lithic-richer bands forms a distinctive marker plane over most of the E1 dispersal area and divides E1 into volumetrically subequal portions (E1a and E1b in figure 13). Lithic contents are often highest towards the top of E1b, suggesting vent-wall collapse may have caused the termination of this phase. Only rarely does any fine-ash matrix occur in E1 and then only in the topmost part of the unit (e.g. figure 13, locality 2461). The contact between E1 and E2 is defined by the base of a cohesive ultra-fine- to fine-ash band. The top of E1 is normally graded up to this band and E2 inversely graded above it. Isopach and isopleth data (figure 14*a*–*c*) imply a vent position for E1 further W than any others active since the Oruanui eruption. A best estimate for its position is at 763 266, consistent with the vent site being controlled by the Horomatangi Fault (Northey 1983, fig. 1). E1 is dispersed along a narrow zone both NE and SW of vent and isopach data yield a bulk volume of 1.0 km$^3$.

Figure 13. Stratigraphic columns to show the nature of and lateral correlations in fall deposits (E1–E4) and ignimbrite (E5) generated in eruption E. The type locality for the Opepe Tephra Formation designated by Vucetich & Pullar (1973) is locality 39, and this is retained for E. Locality 2309 is the reference locality for E2–E4. Grid references for localities are: 7649 2409 (1487); 7714 2479 (733); 7766 2540 (2426); 7837 2556 (2396); 7943 2584 (2309); 7995 2711 (2471); 7916 2714 (2461); 7798 2729 (39); 7677 2760 (2499); 7644 2809 (2478); 7645 2898 (2541) 7523 2615 (2324).

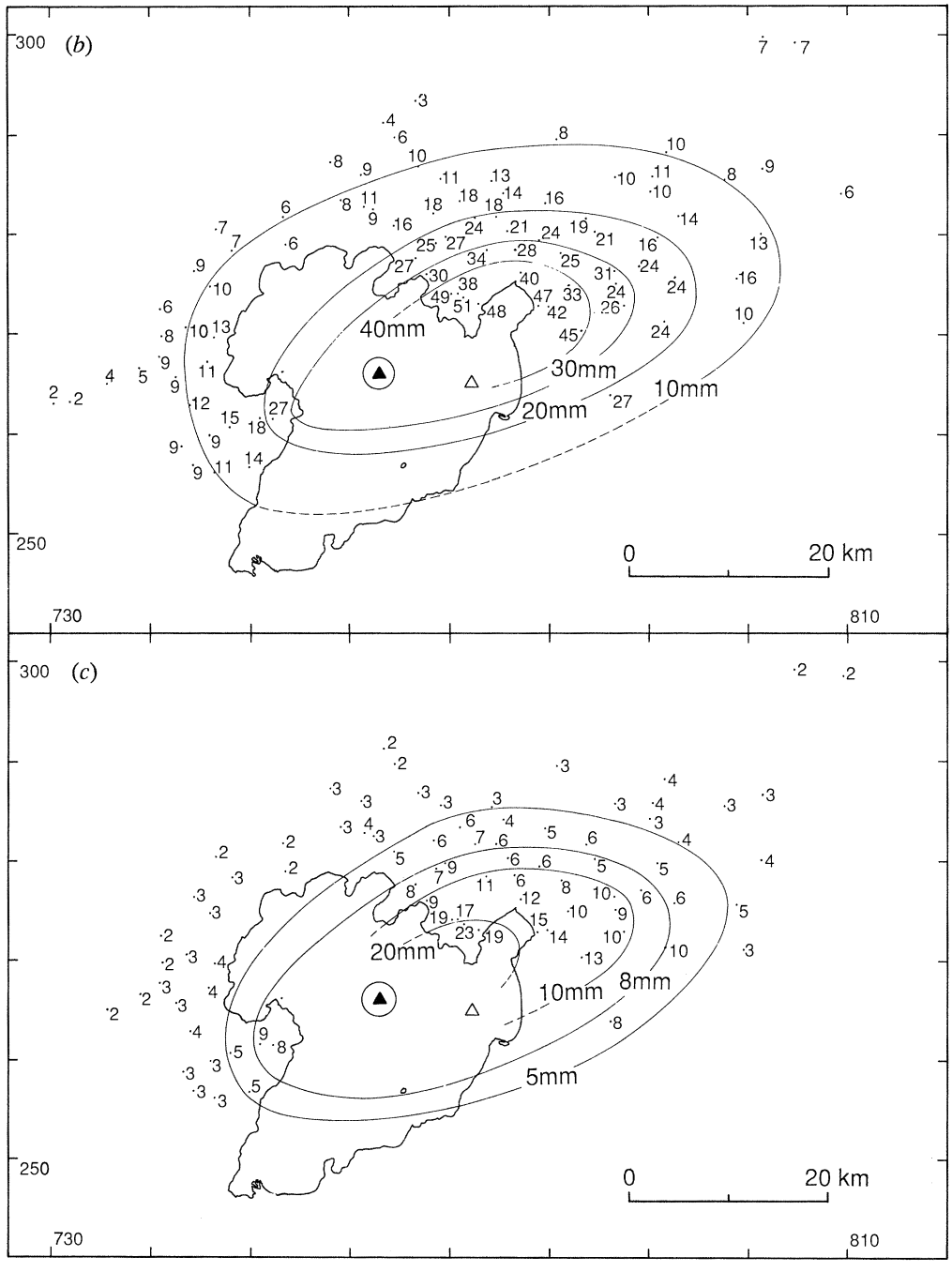


Figure 14. Isopach and isopleth maps for Unit E (cont.). (*b*) E1, $P_m$ data; values and isopleths in millimetres. (*c*) E1, $L_m$ data; values and isopleths in millimetres.

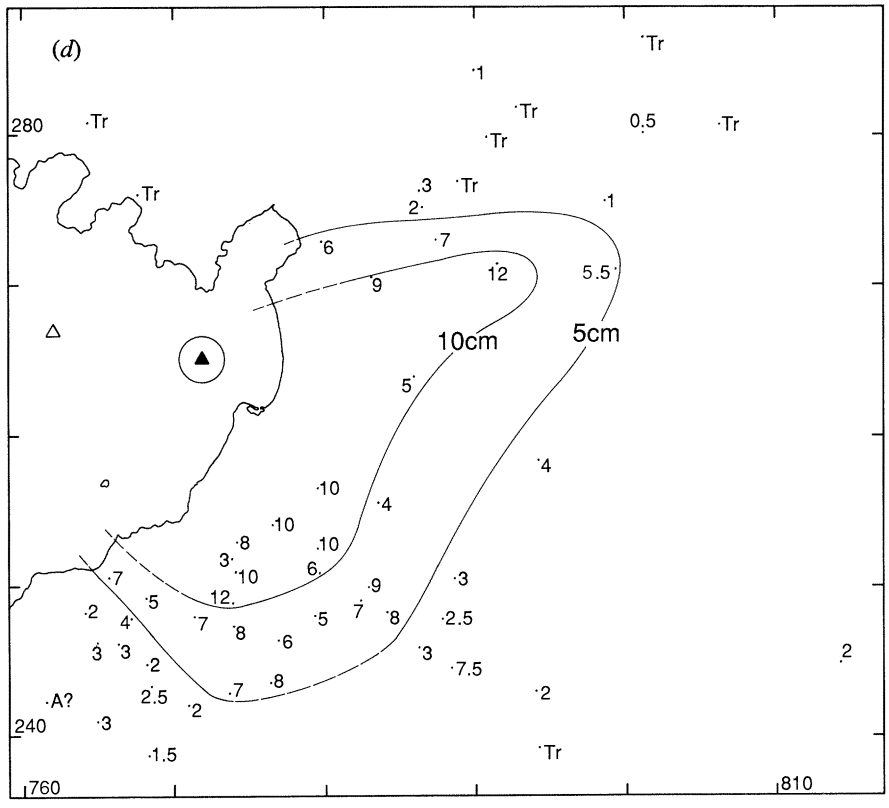


Figure 14. Isopach and isopleth maps for Unit E (*cont.*). (*d*) E2, thickness; values and isopachs in centimetres.

Subunit E2 is a thin, poorly to well-bedded, often poorly sorted fall deposit which is generally inverse graded and not more than 12 cm thick. The bedding is defined both by changes in maximum grainsize and the proportions of a cohesive ultra-fine-(clay grade) to fine-ash matrix. E2 dispersal (figure 14*d*) is markedly different from that of E1 and it is inferred to represent the first deposits from the vent position defined from E3 isopach/isopleth data. Isopach data yield a bulk volume of 0.15 $km^3$. The sharp contact and differing grainsize and dispersal characteristics of E2 versus E1 suggest that E2 activity started only at the very end of, or after E1 deposition.

E3 is a bedded fall deposit, which is coeval with or eroded by E5 ignimbrite in several localities close to Lake Taupo. Where thickest and/or best preserved (e.g. figure 13, localities 2461 and 2309) E3 is well bedded, generally poor in fines in its lower part and with several fines-rich beds in its upper part. E3 thins markedly N and S of its dispersal axis and contains variable amounts of fines, but remains distinctive because of its coarse grain size relative to E1 or E2. The consistent stratigraphy, aerodynamically equivalent sizes of pumices and lithics, and mantle-bedded nature indicate a fall origin for most of E3. However, in some proximal localities (e.g. 7798 2729) E3 has a sparse ash matrix, pumices are rounded, charcoal fragments occur, and the basal contact may be disturbed, suggesting an element of lateral movement, possibly by shearing under the E5 flow(s). E3 is the

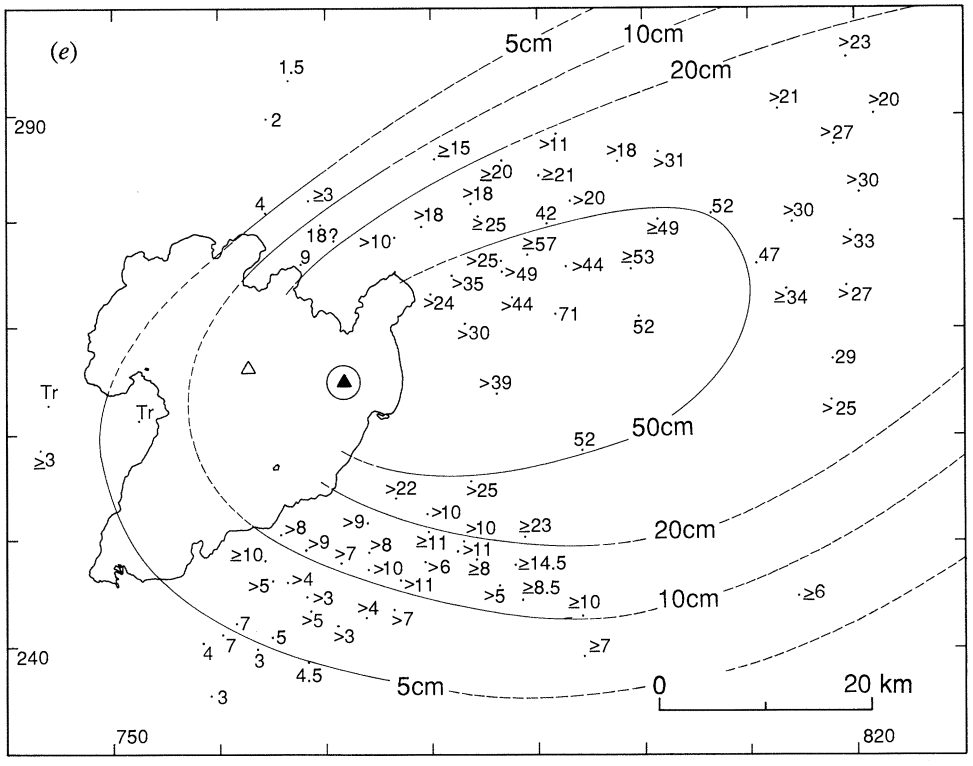


Figure 14. Isopach and isopleth maps for Unit E (*cont.*). (*e*) E3, thickness; values and isopachs in centimetres.

most voluminous (bulk volume of 1.95 $km^3$) and widely dispersed part of Unit E and represents a powerful 'dry' plinian event which became more episodic and 'wet'. Isopachs and isopleths (figure 14*e–g*) of E3 are incompatible with the vent position proposed for E1; a vent at 772 265 is proposed.

E4 is an enigmatic unit. Where seen unequivocally *in situ* (e.g. 7943 2584; figure 13, section 2309), it is a fall deposit, poorly bedded and very poorly sorted, dominated by very-fine ash to fine lapilli material, and resembling Subunit Y3 (Hatepe ash; Walker, 1981*b*). E4 is usually a pale yellow-brown colour, contrasting thus with the pink-brown colour of E2–E3. However, material of similar grainsize characteristics and colour to E4 also occurs as massive to bedded, vesicular deposits at many localities and is inferred to be E4 material which has undergone some syn- or post-eruption mass flowage. Unit E4 is too poorly preserved for an isopach map to be drawn, but overall isopachs for Units E2–E4 (figure 14*h*) yield a volume estimate of 3.6 $km^3$, implying a volume for E4 of 1.5 $km^3$.

E5 is used here for material in proximal areas (figure 14*i*) which is inferred to be ignimbrite. The distinction from remobilized E4 material is problematic, but evidence for a primary pyroclastic flow origin includes: an erosive base, massive appearance with no vesicularity in the matrix, and the presence of carbonized vegetation. The maximum thickness of E5 (100 cm) is at 7703 2741, and it reaches as far as *ca.* 20 km from the assumed source at the E2–E4 vent. The inferred ignimbrite occurs over *ca.* 650 $km^2$(figure 14*i*); assuming an average thickness of

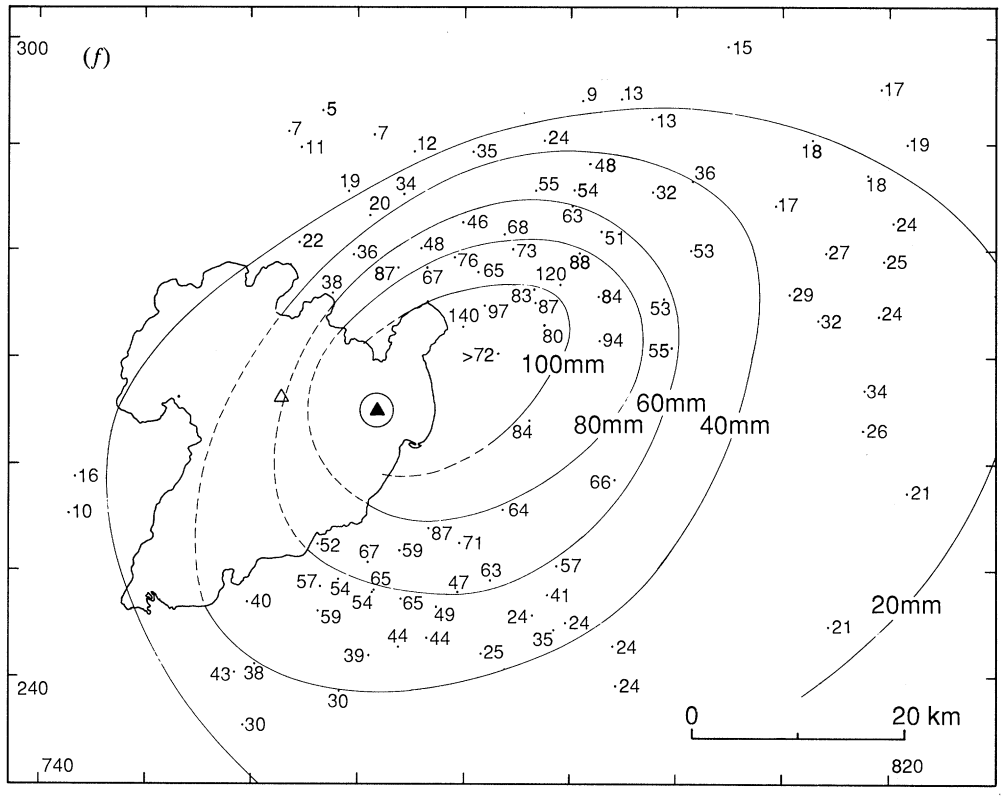


Figure 14. Isopach and isopleth maps for Unit E (*cont.*). (*f*) E3, $P_m$ data; values and isopleths in millimetres.

30 cm, its bulk volume is *ca.* 0.2 km$^3$. The relationships between E5 and secondary E4 mass-flow deposits around Lake Taupo require further work.

Unit E represents a complex eruption, whose interpretation is hampered by poor preservation of E2–E5. Isopach/isopleth evidence and the stratigraphic distinction drawn between E1 and E2–E4 imply that two vents were active in turn. The eruption began with dry activity from a W vent, and no signs of magma-water interaction are seen. The plume was sustained to a height of *ca.* 21 km, as estimated from isopleth data. Activity closed off there just before or simultaneously with activity beginning at an easterly vent *ca.* 9 km away. The bedding in E3 and isopleth data imply column heights reached 35–37 km on several occasions and were sustained for some time during earlier stages. A vesicular ash matrix in E2–E4 clearly indicates that wet deposition often occurred. A rough inverse relationship observed between the coarseness of beds and the amount of matrix in E2–E4 suggests that magma–water interaction occurred around the periphery of the eruption column, being most marked when the column was weakest. The resemblance between E4 and Y3 suggests that during E4 water penetrated the vent to thoroughly mix with the plume and cause water-flushed deposition of ash (cf. Walker 1981*b*). The widespread re-working of E4 could be explained by remobilization of the water-saturated ash, particularly as the ultra-fine-ash bearing beds in E3 would have acted then (as now) as impermeable horizons pre-

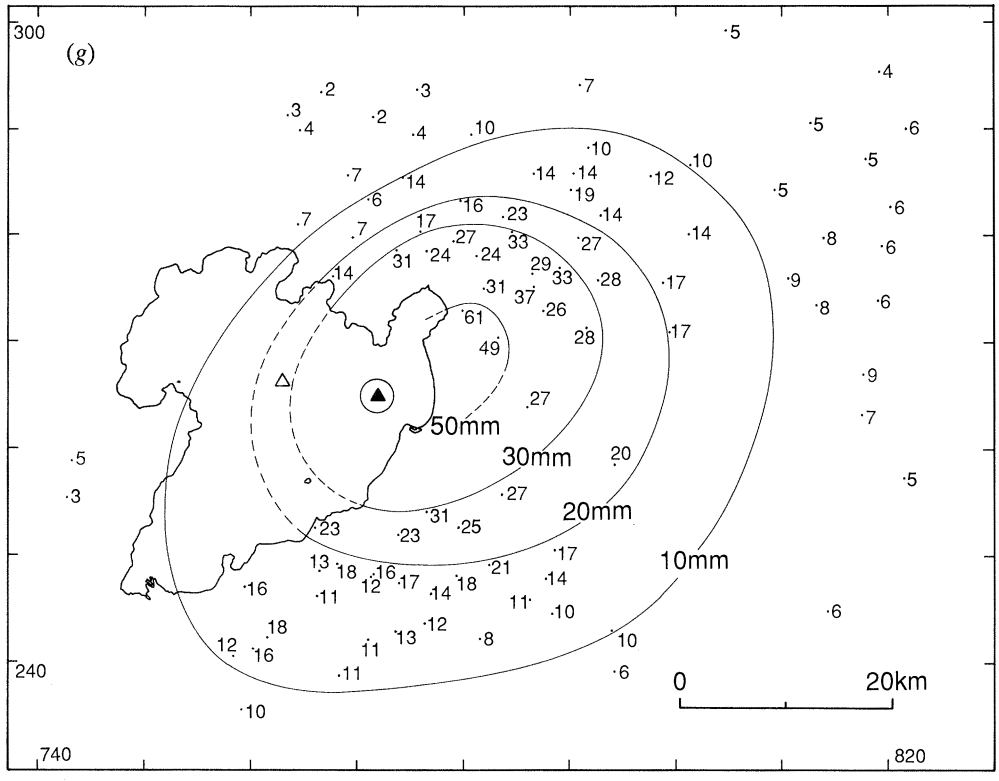


Figure 14. Isopach and isopleth maps for Unit E (*cont.*). (*g*) E3, $L_m$ data; values and isopleths in millimetres.

venting free drainage. The thin, widespread nature of the E5 ignimbrite suggests an energetic emplacement, probably by column collapse, but available data cannot constrain when this event occurred in the E3–E4 sequence. Lithic clasts in E are dominantly older lavas, often brown and hydrothermally altered. Obsidian is a subordinate component, but is nowhere abundant enough to suggest that dome extrusion accompanied or followed the eruption.

### (*f*) *Unit F*

Unit F is a fall deposit found in the top part of the post-E palaeosol, with a thin, locally carbonaceous palaeosol separating it from Unit G. A type locality for F is proposed at 7657 2506 (figure 15). Charcoal samples from the palaeosol between E and F at 7657 2506 and 7796 2565 yielded ages of 7450±140 and 6360±60 years BP, and from the palaeosol between F and G at 7742 2529 an age of 6050±70 years BP (Appendix B). Adopted ages for F are 6150 years BP ($^{14}$C timescale), or 7050 years BP (calibrated timescale).

Unit F is pale grey to brown, poorly bedded, poorly sorted and rich in very fine ash. It has a weak overall normal grading defined by a minor content of juvenile medium ash to fine lapilli. The juvenile fragments vary in density from moderately vesicular pumice to black obsidian; pumice clasts are generally rounded. Foreign lithics are rare.

Isopachs for F (figure 16) yield a bulk volume of 0.07 km$^3$ and show a bilobate

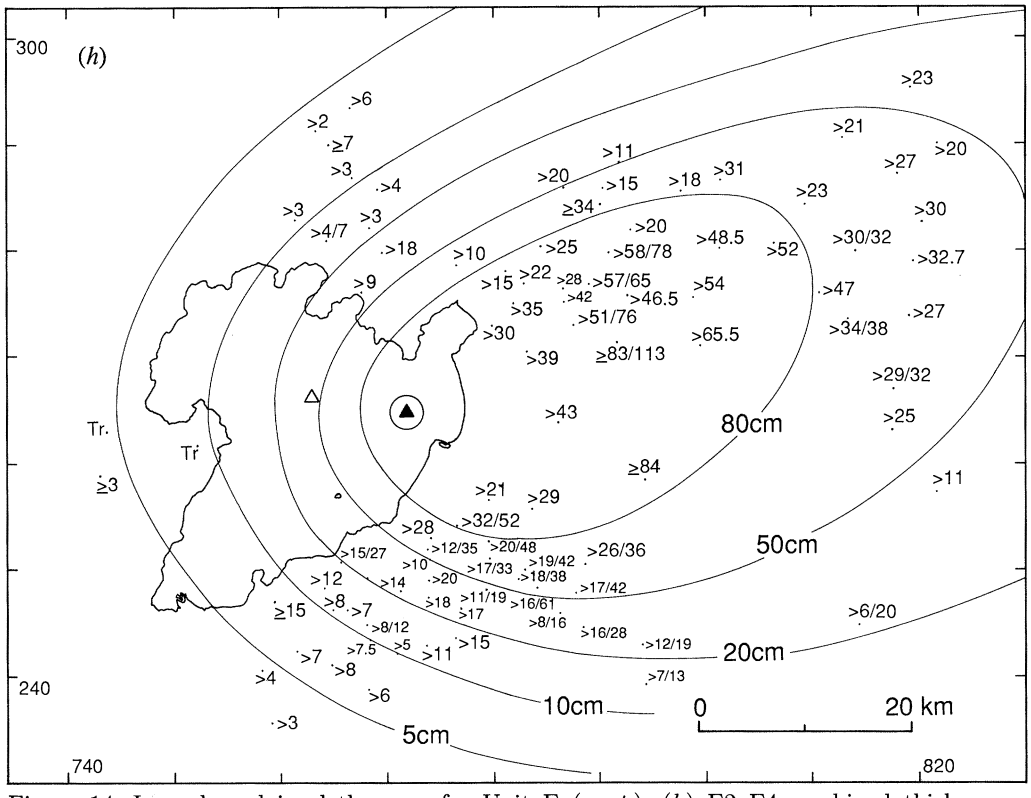


Figure 14. Isopach and isopleth maps for Unit E (*cont.*). (*h*) E2–E4 combined thicknesses; values and isopachs in centimetres. Where two data values are given, the first represents definite primary tephra and the second includes possible reworked material.

distribution consistent with this deposit being erupted from a vent site at 765 257, now occupied by the young rhyolite dome of Motutaiko Island. This dome was previously known to be older than 3300 and younger than 22 600 $^{14}$C years BP from the mantling stratigraphy (Froggatt 1981*b*), and was proposed as the vent site for the Poronui Tephra (= Unit C) by Froggatt (1981*b*). However, my new data strongly imply an alternative source for C to the north. The Motutaiko Island dome is thus inferred to have formed during eruption F; its volume is 0.05 km$^3$.

### (*g*) *Units G and H (Motutere Tephra)*

The nomenclature of the units here labelled Units G to R is complex. All these units were grouped as a single Hinemaiaia Tephra Formation by Vucetich & Pullar (1973), with a type locality at 7798 2729. Froggatt (1981*c*) divided this into a lower Motutere Tephra Formation and an upper, revised, Hinemaiaia Tephra Formation, with a type locality at 7742 2529. My data now suggest that the 'Motutere Tephra Formation' comprises two fall deposits (G and H), and that the 'Hinemaiaia Tephra Formation' represents at least 10 separate fall deposits (I to R).

A photograph of the 'Motutere Tephra Formation' at 7739 2518 is presented in figure 17*a*, plate 2. Froggatt (1981*c*, fig. 2) described this formation as consisting

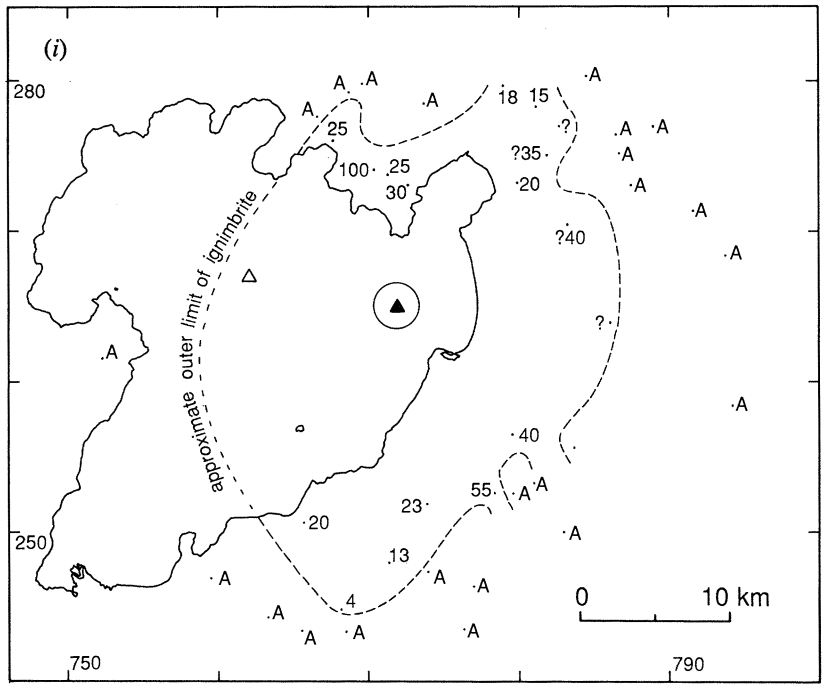


Figure 14. Isopach and isopleth maps for Unit E (*cont.*). (*i*) E5 (ignimbrite), thickness; values in centimetres.

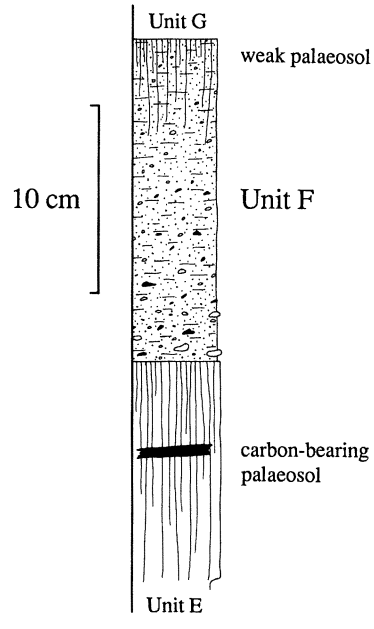


Figure 15. Stratigraphic column for the type section of Unit F at 7657 2506, showing the position of a $^{14}C$ sample (Appendices A and B, locality/sample 2413).

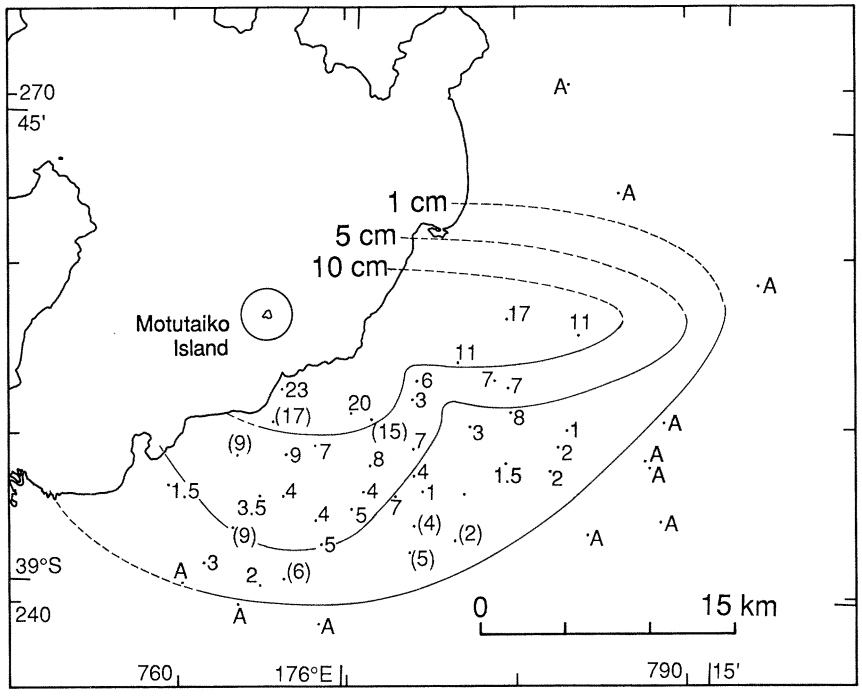


Figure 16. Isopach data for Unit F. Values in centimetres. Bracketed values are where the upper part of the unit is soilified and the deposit may be overthickened by bioturbation.

of two pumice lapilli beds separated by a fine ash bed. This 'fine ash bed' is here re-interpreted as a palaeosol which separates two fall deposits, a basal one (G) which in large part corresponds with material documented as 'Motutere Tephra Formation' by Froggatt (1981*c*), and an upper one (H) which is newly described. The basis for interpreting the 'fine ash bed' as a palaeosol is its similarity to other undoubted paleosols in the Holocene sequence, namely, its dark brown colour, the presence of carbonized vegetation fragments, and its slippery nature when rubbed between the fingers due to weathering of fine ash to clay minerals.

(i) *Unit G*

This is defined from a type locality at 7739 2518 (figure 17*a*) while its relationship to H is also well displayed at 7742 2529. Charcoal from the post-F, pre-G palaeosol at 7742 2529 gave an age of 6050±70 years BP, while charcoal from the post-G, pre-H palaeosol at 7837 2556 gave 5570±120 years BP (Appendix B). The adopted ages for G are thus estimated as 5800 years BP ($^{14}$C timescale), or 6650 years BP (calibrated timescale).

Unit G is subdivisible into two (figure 18). Subunit G1 is a well-sorted, poorly bedded pumice fall deposit with a moderately to well-developed inverse grading. Lithic clasts are dominated by foreign lithologies, suggesting open vent activity. At some localities the top contact with G2 is marked by a bed with variable quantities of a fine ash matrix. Isopach data from G1 (figure 19*b*) show a marked southerly dispersal from a vent inferred to be at 768 259, and the volume is estimated as 0.2 km$^3$.

Subunit G2 is very patchily preserved. Where most complete it consists of

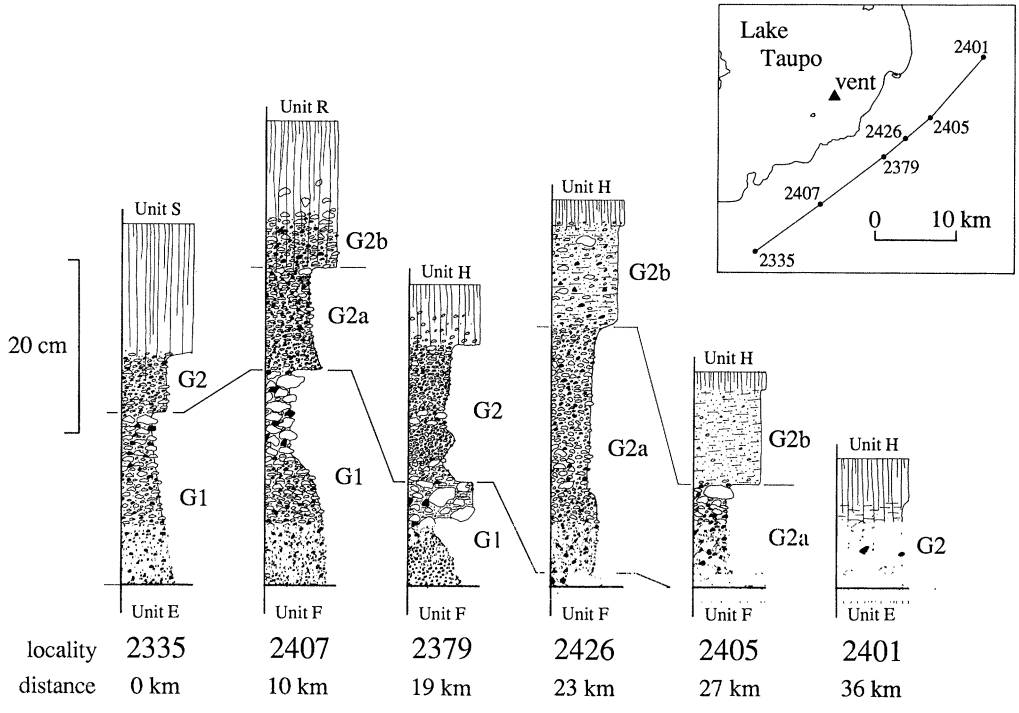


Figure 18. Stratigraphic columns to show the nature of and lateral correlations in Unit G. Locality 2379 is the designated type locality (Appendix A; see also figure 17*a*). Grid references for localities are: 7584 2404 (2335); 7663 2461 (2407); 7739 2518 (2379); 7766 2540 (2426); 7796 2565 (2405); 7861 2639 (2401).

a poorly bedded, well-sorted pumice fall unit (G2a) which is either ungraded or weakly normally graded in its upper part, overlain by a non-bedded, very poorly sorted, vesicular, fines-rich bed (G2b) interpreted as water-flushed. In southerly localities there is usually a marked drop in grainsize from G1 into G2a, but this distinction is not seen east of vent. The transition from G1 to G2a is thus interpreted as resulting from a change in dispersal direction rather than any change in eruptive vigour. Lithics in the basal part of G2a are dominated by older lavas, but obsidian proportions increase upwards, and in G2b obsidian is dominant, together with abundant grey, poorly vesicular juvenile material. Subtraction of the volume for G1 from that for G as a whole implies a volume for G2 of *ca.* 0.3 $km^3$.

Isopleth data (figure 19*c*, *d*) were inadvertantly collected from both G1 and G2; G1 is coarser to the south and G2 to the east. The Carey & Sparks (1986) method for estimating column height and vent position cannot therefore be used here, but the distribution of maximum clast sizes in G1 are similar to those in Unit C, and suggest a column height of 25–30 km. The vent position is constrained by the weakly bilobate nature of the isopachs, and the isopleth symmetry.

G began as an open-vent, dry eruption of increasing vigour (G1), and continued with similar vigour (G2a) after a change in dispersal direction. This change is accompanied by a water-flushed bed, suggesting that the change in wind directions may have accompanied the passage of a frontal system. The eruption

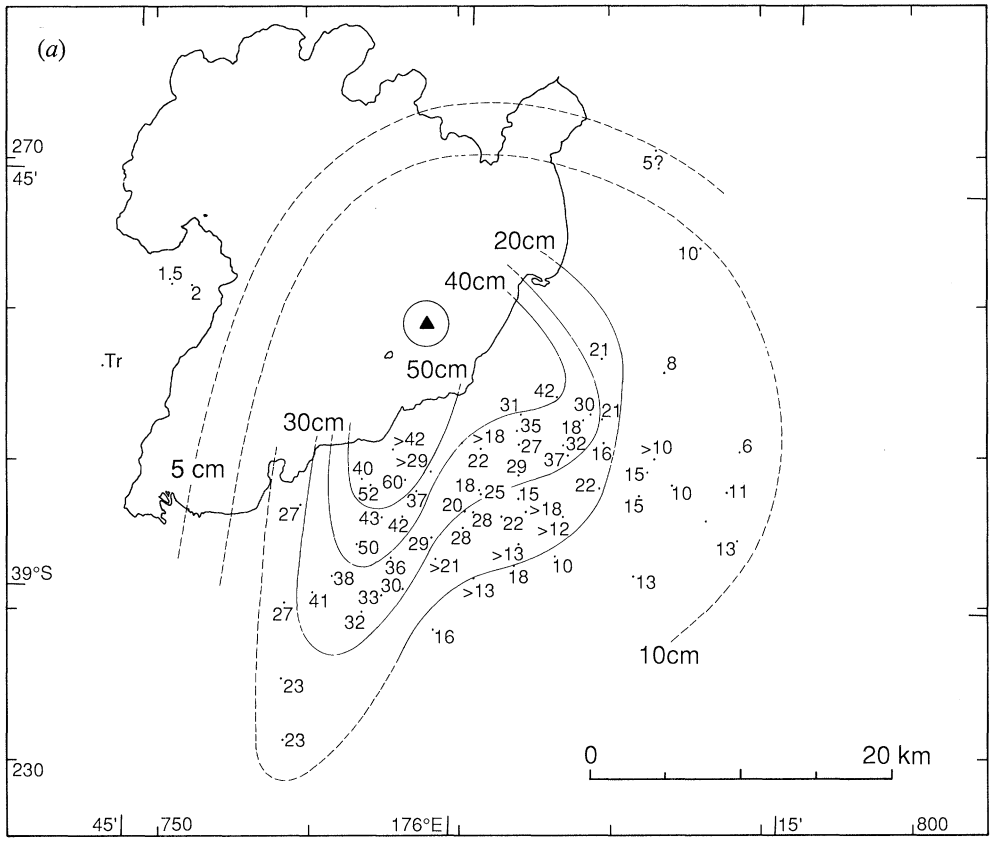


Figure 19. Isopach and isopleth data for Unit G. (*a*) G total thickness; values and isopachs in centimetres.

gradually weakened, as increasing amounts of obsidian were erupted, and terminated in 'wet' activity (G2b) as variably vesiculated magma interacted with water, possibly accompanying lava extrusion.

(ii) *Unit H*

A type locality for H is proposed at 7837 2556 where H is most complete (figure 20). Charcoal from the post-G, pre-H palaeosol here gave an age of 5570±120 years BP, while carbon in soil above Unit I (itself separated from H by a period of weathering) at 7739 2518 gave 4890±60 years BP (Appendix B). The degrees of palaeosol development with respect to these samples suggest adopted ages of 5300 years BP ($^{14}$C timescale) or 6050 years BP (calibrated timescale).

Unit H consists of two subunits (figure 20). H1 is a well sorted, normally graded pumice fall deposit. Lithic clasts are dominated by old lava, suggesting open-vent activity. Isopach data (figure 21*b*) yield a volume estimate of 0.10 km$^3$, and isopleths (figures 21*c*, *d*) are used to estimate a vent position at 770 263. H2 is poorly preserved. Where thickest it consists of a basal fines-rich, poorly sorted band, then a normally graded sequence which is generally matrix-rich and vesicular, but does sometimes contain fines-poor bands (e.g. at 7837 2556). H2 is inferred to be a mixture of waning episodic 'dry' activity interspersed with increasing amounts of

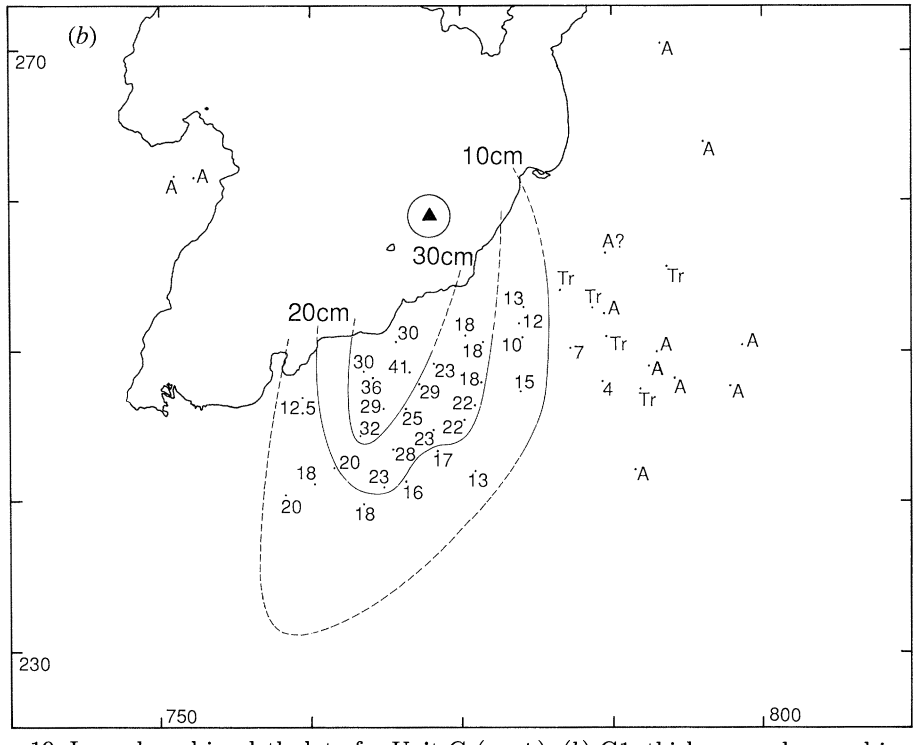


Figure 19. Isopach and isopleth data for Unit G (*cont.*). (*b*) G1, thickness; values and isopachs in centimetres.

magma–water interaction. H2 contains abundant poorly vesicular juvenile material and obsidian fragments, suggesting that it was accompanied and/or followed by lava extrusion. An estimated volume for H2 (from subtraction of H1 from total H data) is 0.1 $km^3$.

Eruption H was similar in overall terms though smaller than C and G, with open-vent, plinian activity (C1, G1, H1) being followed by less vigorous explosive activity, often 'wet' and possibly accompanying lava extrusion (C2, G2, H2). The only difference is that H1 is normally graded; the eruption column is estimated from isopach data to have reached a height of 23 km initially and thereafter declined.

### (*h*) *Units I to R (Hinemaiaia Tephra)*

Froggatt (1981*c*) redefined the Hinemaiaia Tephra Formation from the locality at 7742 2529. However, even at this locality, six deposits separated by palaeosols and/or periods of erosion/bioturbation can be distinguished (figure 17*b*, plate 3) and a new stratigraphy is proposed here. Based on the presence of palaeosols and/or erosion breaks, the material previously covered by the term 'Hinemaiaia Tephra' is divided into 10 units, I to R, which can be grouped into two intervals of more frequent activity separated (between Units M and N) by the best-developed palaeosol in the sequence. Correlation of individual units within the 'Hinemaiaia Tephra' (figure 22) is hampered by three factors.

1. Individual deposits rarely exceed 20 cm in thickness, and were thus often

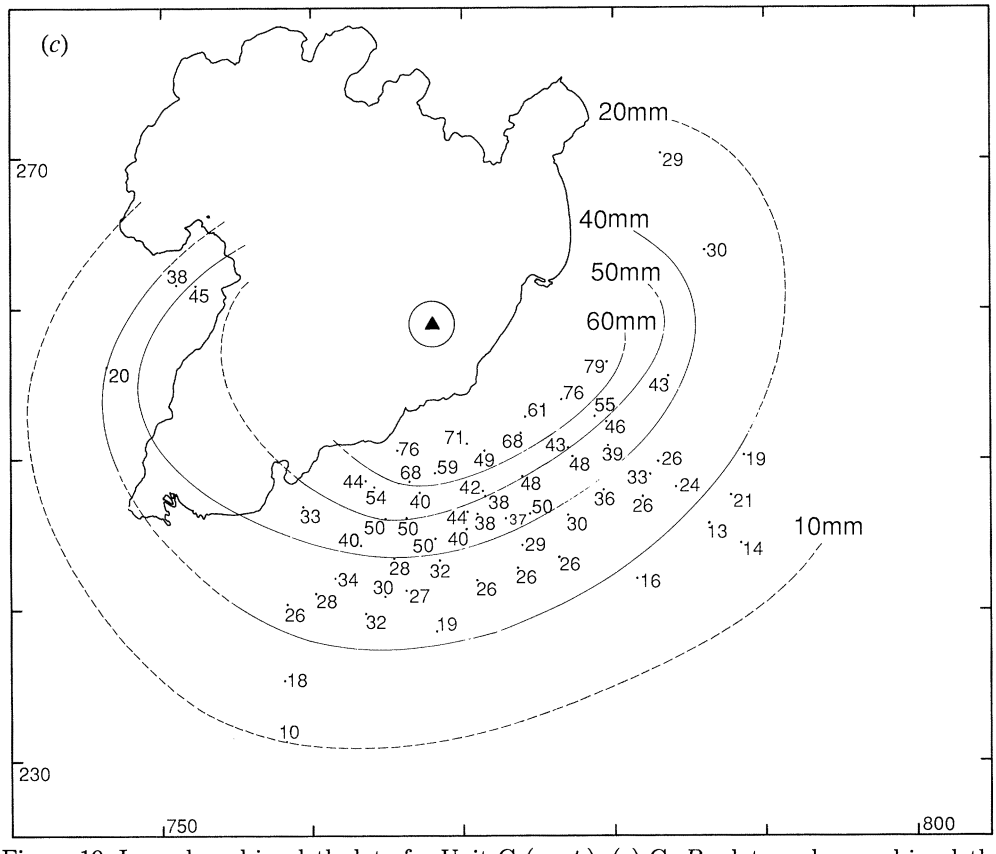


Figure 19. Isopach and isopleth data for Unit G (*cont.*). (*c*) G, $P_m$ data; values and isopleths in millimetres.

penecontemporaneously bioturbated to produce ashy, homogenized and weathered zones.

2. Exposures of the relevant stratigraphic level are preferentially seen either N or SE of Lake Taupo. Sparse intervening exposures are not good enough to establish unequivocal correlations between the two areas for some eruption units.

3. Only one unit (K) represents an eruption powerful enough to be clearly represented in both the northern and southern exposure areas.

Most of the 'Hinemaiaia' units were clearly only locally dispersed. Thus deposits which occur in the same relative stratigraphic position in the areas of better exposure N and SE of Lake Taupo are usually interpreted to represent separate eruptions. To illustrate this, compare Unit C, which is appreciably larger and more widely dispersed than any 'Hinemaiaia' unit, which is clearly present in the SE area, yet very poorly preserved to the N. Of the 10 'Hinemaiaia' units, four (J, L, Q, R) occur only in the southern area, three (M, O, P) occur primarily in the northern area, and three (I, K, N) together with the M-N palaeosol are found in both areas. $^{14}C$ age data imply that the earlier group (Units I to M) was erupted between *ca.* 5200 and 4500 $^{14}C$ years BP and the second (Units N to R) between *ca.* 4200 and 3950 $^{14}C$ years BP.

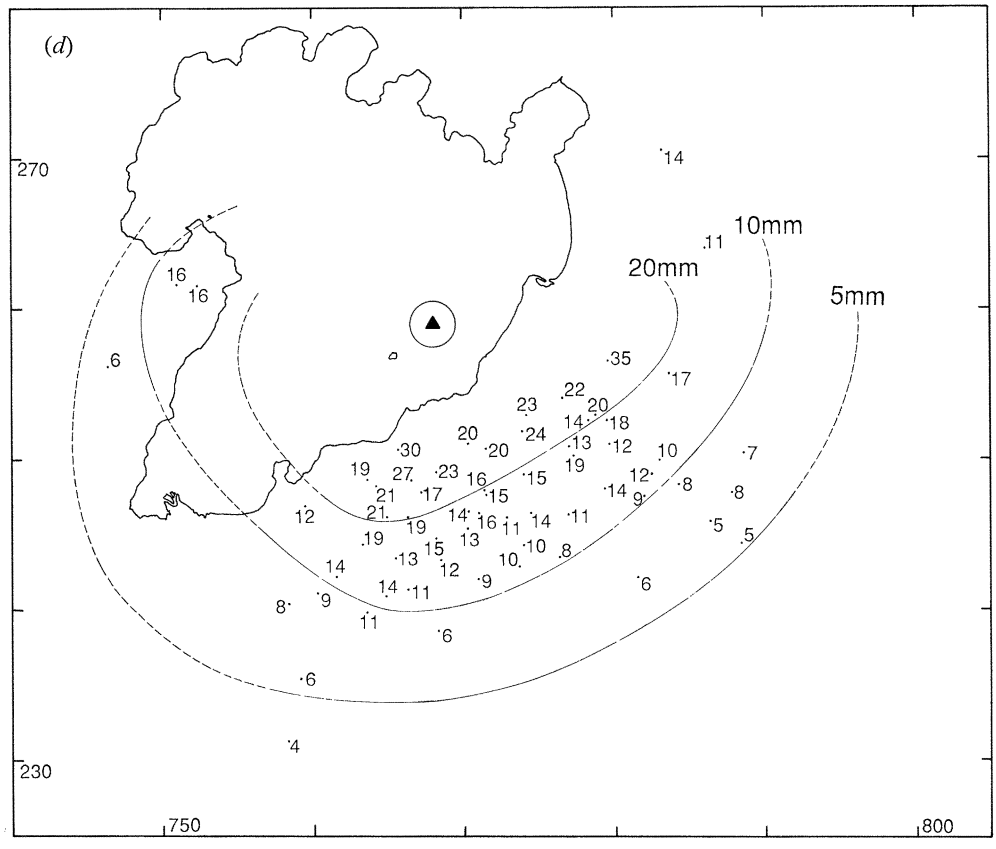


Figure 19. Isopach and isopleth data for Unit G (*cont.*). (*d*) G, $L_m$ data; values and isopleths in millimetres.

(i) *Unit I*

Unit I is a fall deposit defined from a type locality at 7798 2729 (figure 22, locality 39, and see figure 25), where it consists of 3 cm of mid-grey very-fine to fine ash with a thin bed of coarse ash to fine lapilli at the base. Unit I is separated from K by a palaeosol which is up to 10 cm thick at 7846 2647. Unit I is superficially similar to J, but the latter is separated from K by only a short period of bioturbation and weathering. I and J are seen together at 7739 2518 (figures 17*a*, 22); I occurs as patchy remnants below, and J as a discontinuous bed above, a carbonaceous palaeosol containing charcoal which gave an age of 4890±60 years BP (Appendix B). A weakly developed palaeosol separates I from H there. Adopted ages of I are thus estimated as *ca.* 5200 years BP ($^{14}$C timescale), or *ca.* 5950 years BP (calibrated timescale).

Unit I is rich in very fine ash, and dominated by poorly to non-vesicular juvenile material. It resembles Subunit Y4 (Rotongaio ash; Walker 1981*b*) and is similarly interpreted to represent a 'wet' eruption where non- to poorly vesiculated magma interacted with water, possibly accompanying lava extrusion. Isopach data (figure 23) poorly constrain the volume to (O) 0.02 km$^3$, and are consistent with a source in NE Lake Taupo.

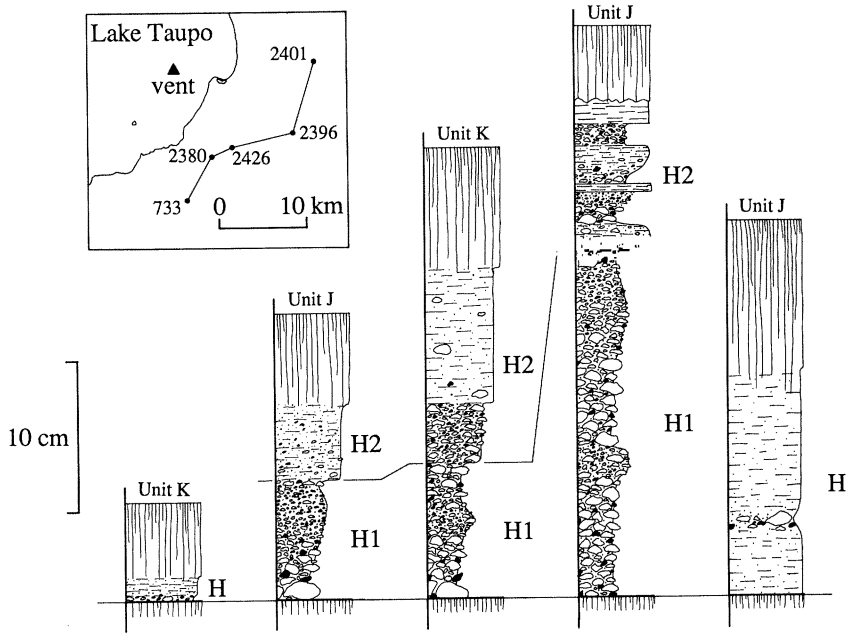


Figure 20. Stratigraphic columns to show the nature of and lateral correlations in Unit H. Locality 2396 is designated as the type locality (Appendix A). Grid references for localities are: 7714 2479 (733); 7742 2529 (2380); 7766 2540 (2426); 7837 2556 (2396); 7861 2639 (2401).

(ii) *Unit J*

Unit J is a fall deposit defined from a type locality at 7742 2529, where it is 1.5–2 cm thick (figures 17*b*; 19, locality 2380, and see figure 25). J lies above a carbonaceous palaeosol at 7739 2518, charcoal from which gave an age of 4890±60 years BP (Appendix B). J is separated from K by limited bioturbation or reworking, or is locally removed, which events are interpreted to represent a time period of years to a few decades. Ages are thus estimated as 4650 years ($^{14}$C timescale) or 5400 years BP (calibrated timescale). Isopach data are sparse (figure 24) but indicate a volume of (O) 0.015 km$^3$, and a source in the southern part of Lake Taupo. J, like I and Y4, is mid-grey and rich in very fine ash and dense juvenile ejecta, and is thus similarly interpreted to represent a small 'wet' eruption involving non- to poorly vesicular magma, possibly accompanying lava extrusion.

(iii) *Unit K*

Unit K is the largest and most widely dispersed of the 'Hinemaiaia' units. figure 25 shows correlations inferred for this unit between the proposed type locality at 7742 2529 and localities to the N of Taupo. The maximum age of K is constrained by $^{14}$C ages of 4890±60 years BP on charcoal from the pre-J palaeosol at 7739 2518 and 4630±200 years BP from charcoal in the pre-K palaeosol at 7713 2737 (Appendix B). Possible correlation of K with an ash bed found in peat bogs to the E (see below) makes relevant ages of 4530±60 and 4490±60 years BP from

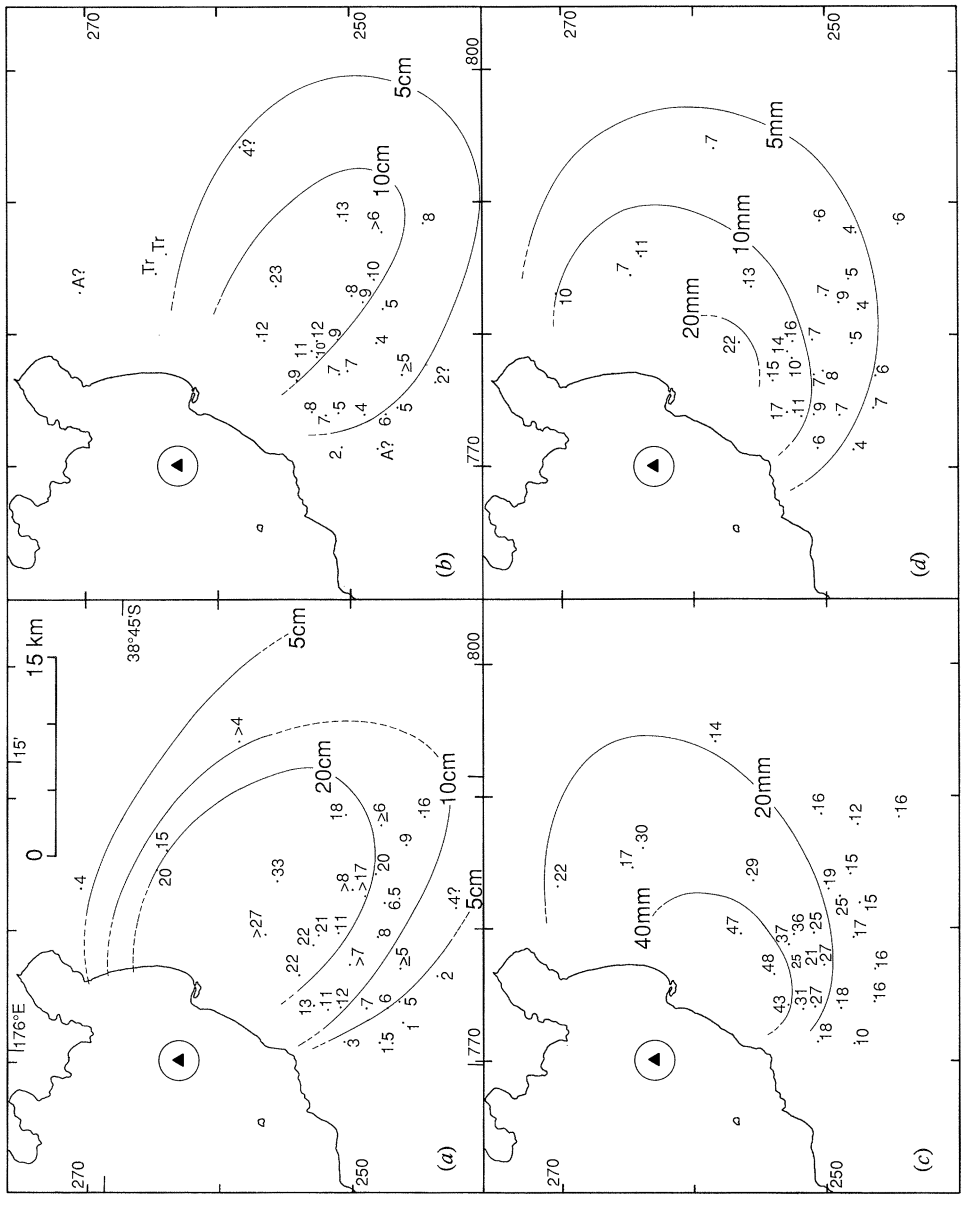


Figure 21. Isopach and isopleth maps for Unit H. (*a*) H total thickness; values and isopachs in centimetres. (*b*) H1, thickness; values and isopachs in centimetres. (*c*) H1, $P_m$ data; values and isopleths in millimetres. (*d*) H1, $L_m$ data; values and isopleths in millimetres.

underlying peat (Lowe & Hogg 1986), but from comparisons between peat and charcoal ages (Wilson *et al.* 1988) these are thought to be slightly young. Ages of 4600 years ($^{14}$C timescale), or 5350 years BP (calibrated timescale) are thus adopted here.

Unit K is a complexly bedded fall deposit which is divided on grainsize into two subunits. K1 has an overall normal grading. Much of K1 is well sorted, but some zones (especially the basal parts) are very poorly sorted, rich in very fine ash and are thus interpreted to have been water flushed. Lithics are mostly obsidian, suggesting that this phase may have been accompanied by lava extrusion.

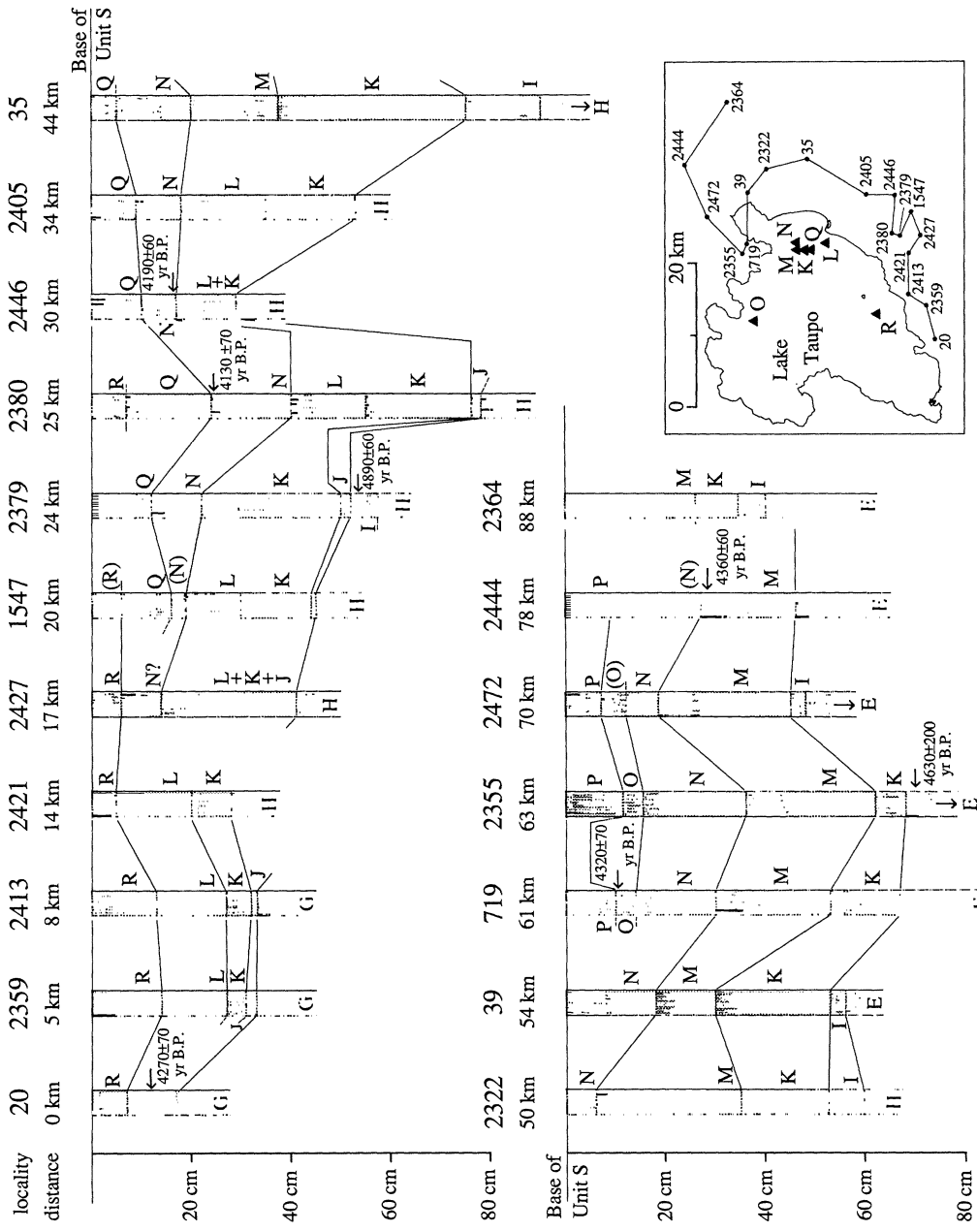


Figure 22. Schematic scaled stratigraphic columns to show lateral correlations between Units I to R previously mapped as a single 'Hinemaiaia Tephra' by Froggatt (1981*c*). Fresh tephra is represented by stippling, soilified ash and palaeosols by vertical lining. The contact at the base of S is taken as the upper datum for each column. See the text and relevant figures in the descriptions of I to R for details of each deposit. New $^{14}C$ age determinations (Appendix B) are shown. Because of inadequate data, no vent positions are shown on the inset map for I, J and P. Grid references for localities are: 7595 2469 (20); 7642 2482 (2359); 7657 2506 (2413); 7715 2506 (2421); 7740 2489 (2427); 7773 2502 (1547); 7739 2518 (2379);7742 2529 (2380); 7796 2525 (2446); 7796 2565 (2405); 7846 2647 (35); 7832 2704 (2322); 7798 2729 (39); 7727 2730 (719); 7713 2737 (2355); 7765 2786 (2472); 7837 2817 (2444); 7926 2758 (2364).

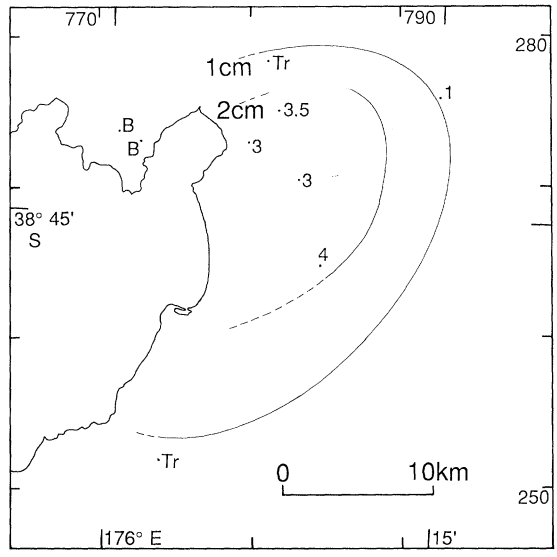


Figure 23. Isopach data for Unit I. Values and isopachs in centimetres.

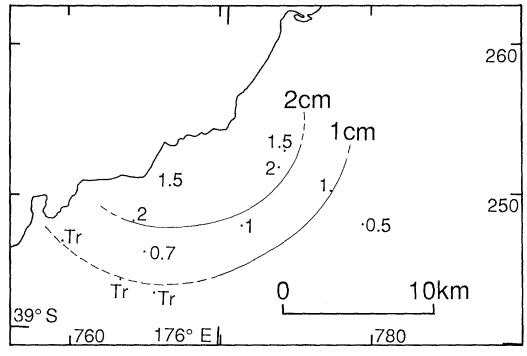


Figure 24. Isopach data for Unit J. Values and isopachs in centimetres.

Isopach data (figure 26*b*) poorly constrain the volume to *ca.* 0.13 km$^3$; these and isopleth data (figure 26*c*, *d*) are consistent with a vent position for K1 (and K2) at 772 265. K2 is often very poorly sorted. Its contact with K1 is marked by an increase in grainsize, then an influx of fines-rich matrix. Two bands within K2 are the coarsest beds in the deposit. Lithics are a mixture of obsidian and older lava, suggesting a more open-vent style of activity when compared to K1. The abundance of a fines-rich matrix suggests that this unit was water flushed and that magma–water interaction was important during this phase. Isopachs/isopleths (figure 26*e*–*g*) suggest a volume for K2 of *ca.* 0.22 km$^3$ and are consistent with the same vent as K1.

Unit K (specifically K2) is recognizable further from source than any other 'Hinemaiaia' unit, reflecting its relatively powerful dispersal. This, and available age data, are consistent with K being the 'newly recognized unnamed ash' at Tiniroto (Kohn *et al.* 1981), the 'Hinemaiaia Tephra' at Kaipo Lagoon (Lowe & Hogg 1986), and one of the 'Hinemaiaia Tephra' beds in the Waikato lakes (Lowe 1986).

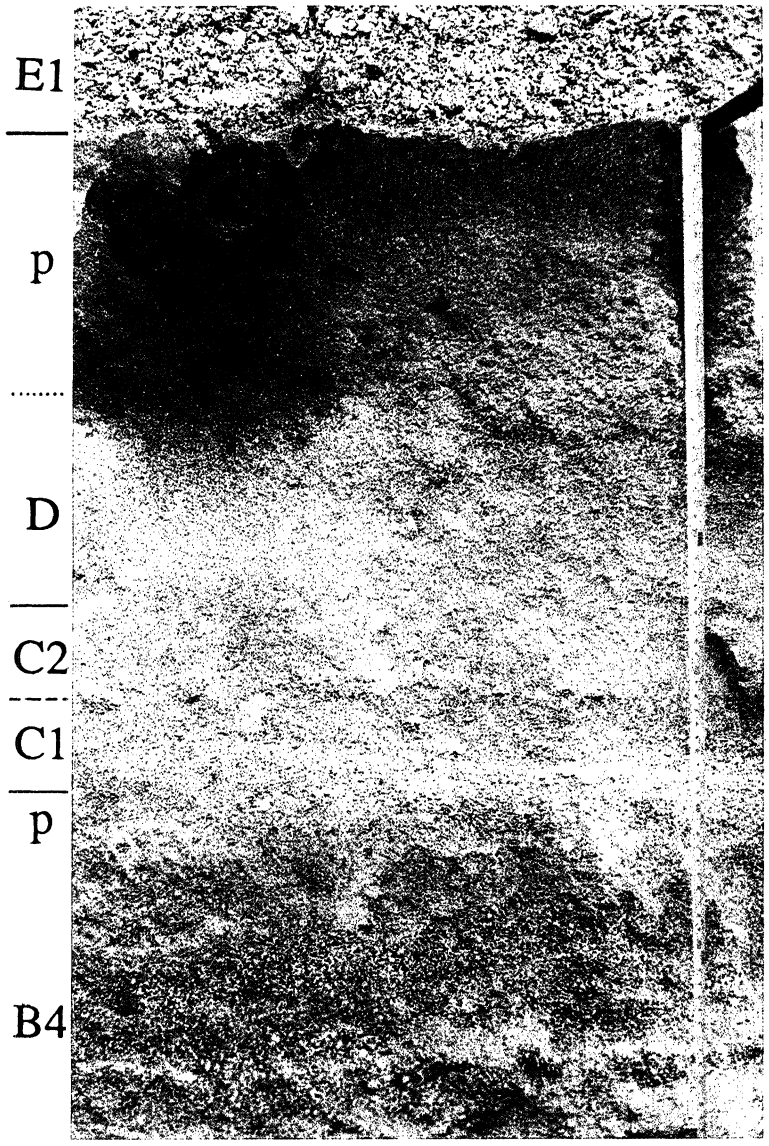


Figure 11. Photograph of Units C and D at the type locality for D (figure 9, locality 2394) at 7789 2729, to show the development of a weathered horizon (incipient palaeosol) between them. Fall deposits are designated by their letter, and p = palaeosol.

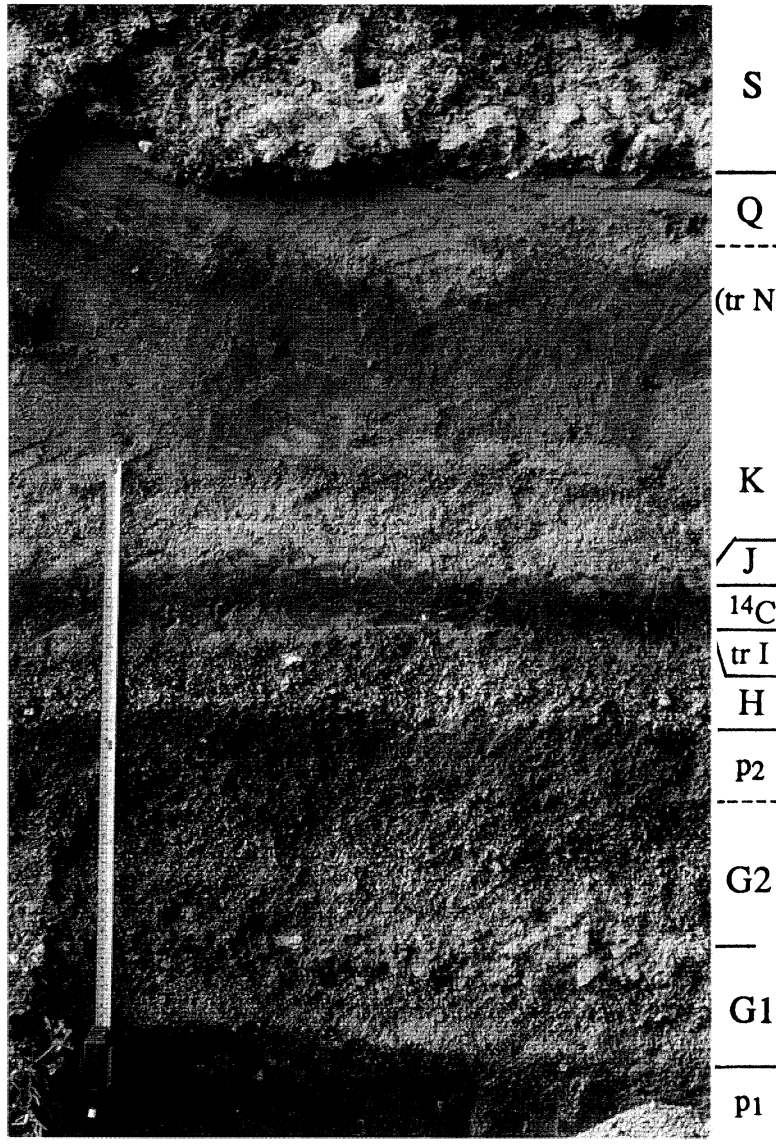


Figure 17. (*a*) Photograph of part of the section at 7739 2518 (figure 22, locality 2379) to show relationships between Units G and H, and units in the 'Hinemaiaia Tephra'. Eruption units are labelled in capitals, tr = trace, $p_1$ = pre-G palaeosol with traces of Unit F, $p_2$ = palaeosol separating G from H (see text), and $^{14}C$ = palaeosol where a $^{14}C$ age was obtained (Appendix B, sample 2379) (other palaeosols not labelled).

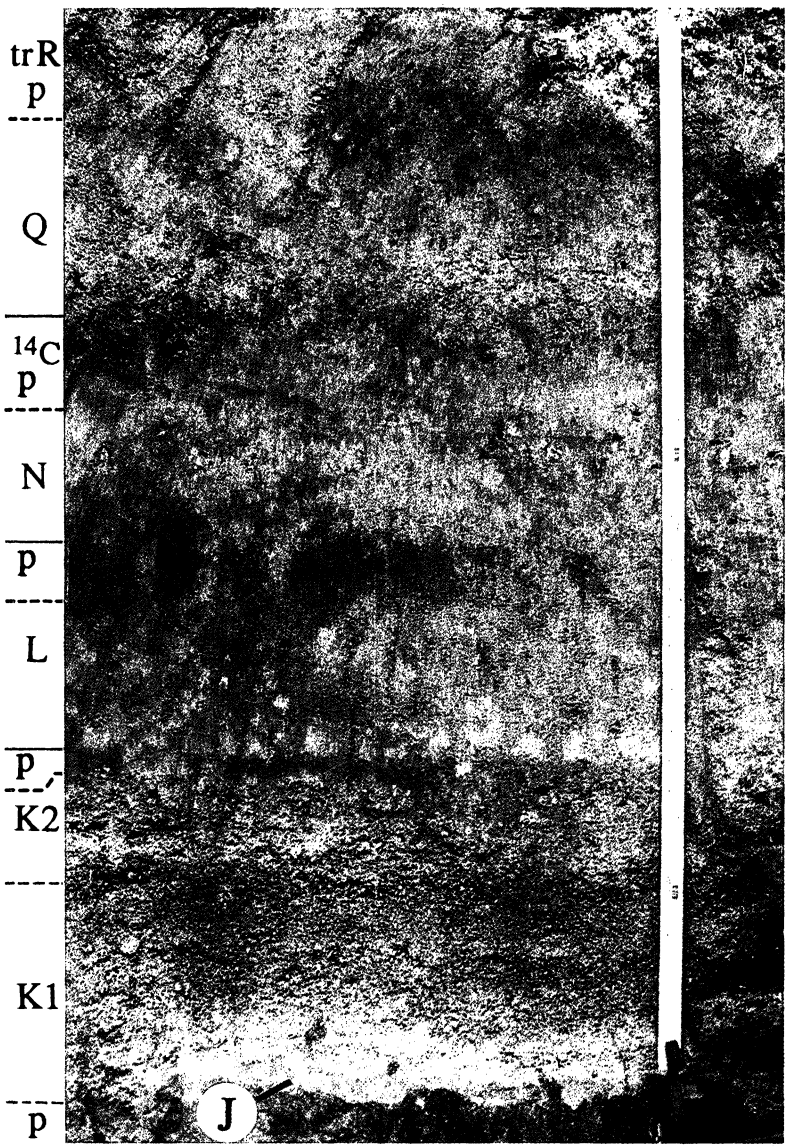


Figure 17. (*b*) Photograph of 'Hinemaiaia Tephra' at 7742 2529 (figure 22, locality 2380) to show units interpreted to be present. Lettering as in (*a*); the $^{14}C$ sample is 2380/C2 (Appendix B).


Figure 39. Photograph of Units T and U at 7827 2600, the type locality for T (Appendix A; figure 41, locality 2397), to show their relationships to each other, and to V and the post-S palaeosol. Palaeosols denoted by p.

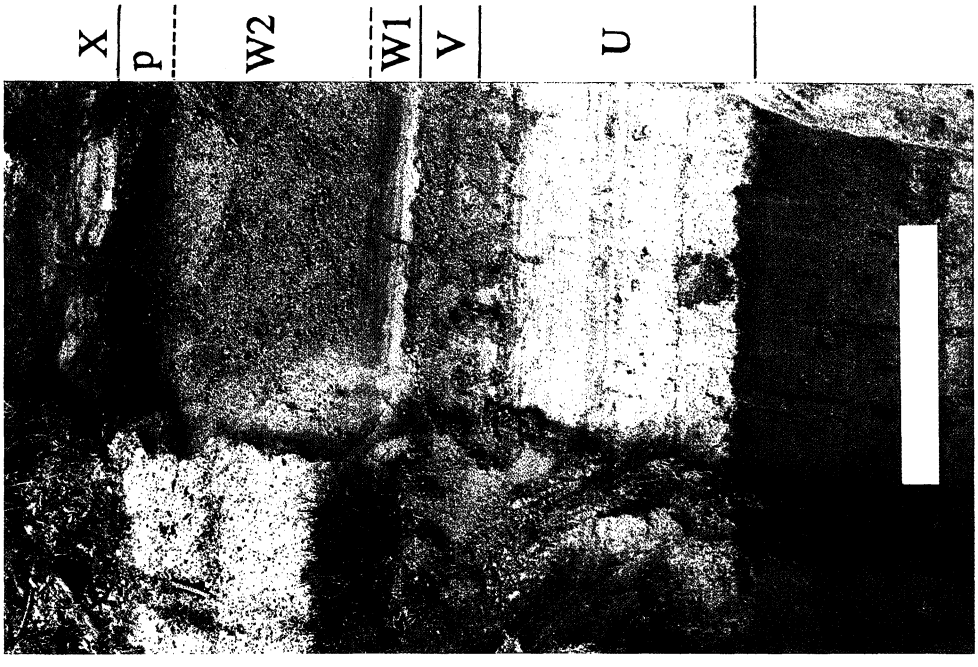


Figure 45. Photograph of the type locality of Unit W at 7739 2565 (Appendix A; figure 46). W rests on weathered (brown) U and V material which in turn overlie a palaeosol on reworked S material. W is separated from X by a clear palaeosol (p). Scale bar is 50 cm.

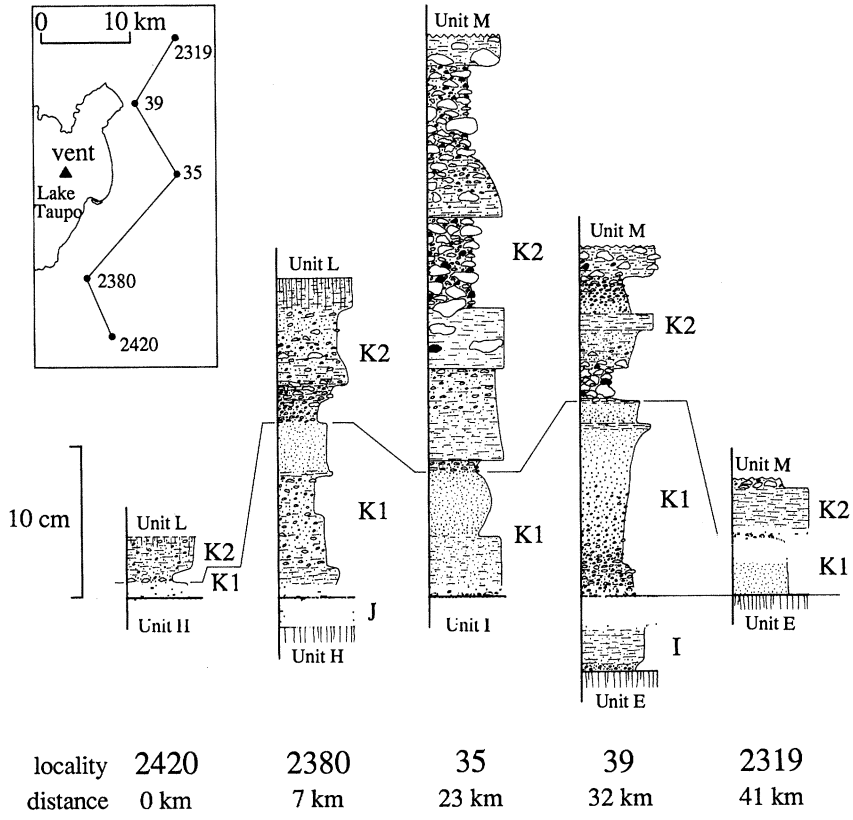


Figure 25. Stratigraphic columns to show the nature of and lateral correlations in Unit K, and the type localities of Units I and J. Locality 2380 (Appendix A, figures 17*b* and 22) is the type locality for K. Grid references for localities are: 7770 2463 (2420); 7742 2529 (2380); 7846 2647 (35); 7798 2729 (39); 7845 2803 (2319).

(iv) *Unit L*

This fall deposit is defined from a type locality at 7742 2529, where it consists of a 2 cm very-fine- to fine-ash bed overlain by up to 10 cm of poorly sorted very-fine- to coarse-ash (figures 17*b*; 27, locality 2380). Unit L is separated from K at the type locality by a thin, ginger-brown palaeosol whose colour is interpreted to reflect an influx of andesitic ash (cf. Vucetich & Pullar 1973). The degree of post-K, pre-L soil development here and elsewhere suggests a time break of a few decades; ages of 4550 years BP ($^{14}$C timescale) or 5350 years BP (calibrated timescale) are thus adopted here.

Unit L is found only in the south. Isopachs (figure 28) are poorly constrained but are consistent with S dispersal from a source in central E Lake Taupo at 773 262. L is always poorly sorted and rich in very fine ash, but moderately vesicular pumice also occurs. Lithics are dominated by obsidian. L is interpreted to represent a 'wet' eruption involving non- to moderately vesicular magma. Its volume can be only roughly estimated as 0.07 km$^3$.

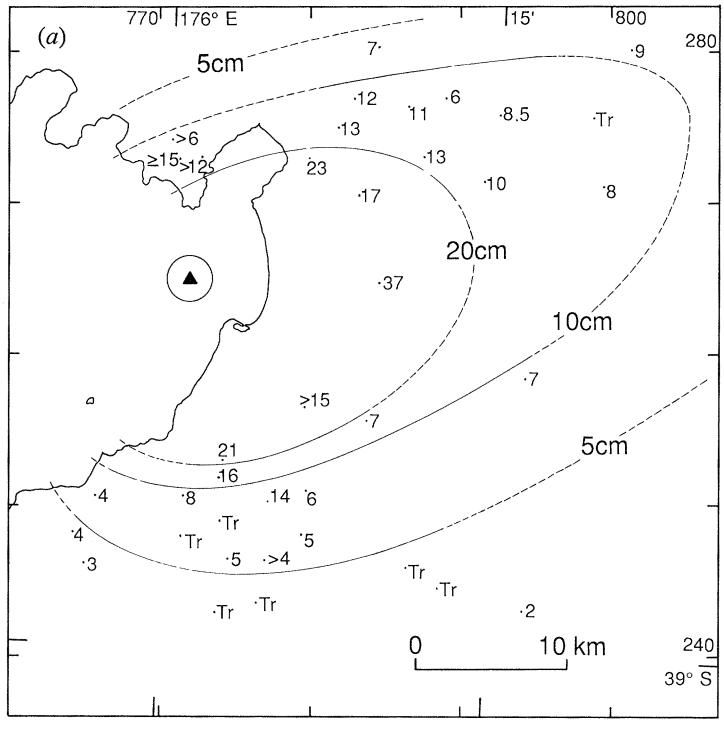


Figure 26. Isopach and isopleth data for Unit K. (*a*) K total thickness; values and isopachs in centimetres.

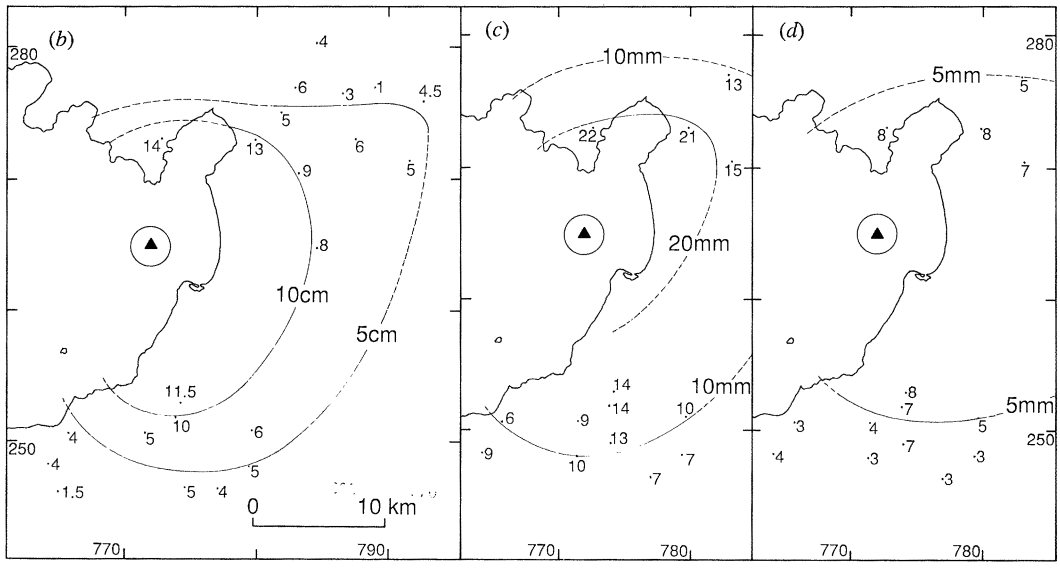


Figure 26. Isopach and isopleth data for Unit K (*cont.*). (*b*) K1, thickness; values and isopachs in centimetres. (*c*) K1, $P_m$ data; values and isopleths in millimetres. (*d*) K1, $L_m$ data; values and isopleths in millimetres.

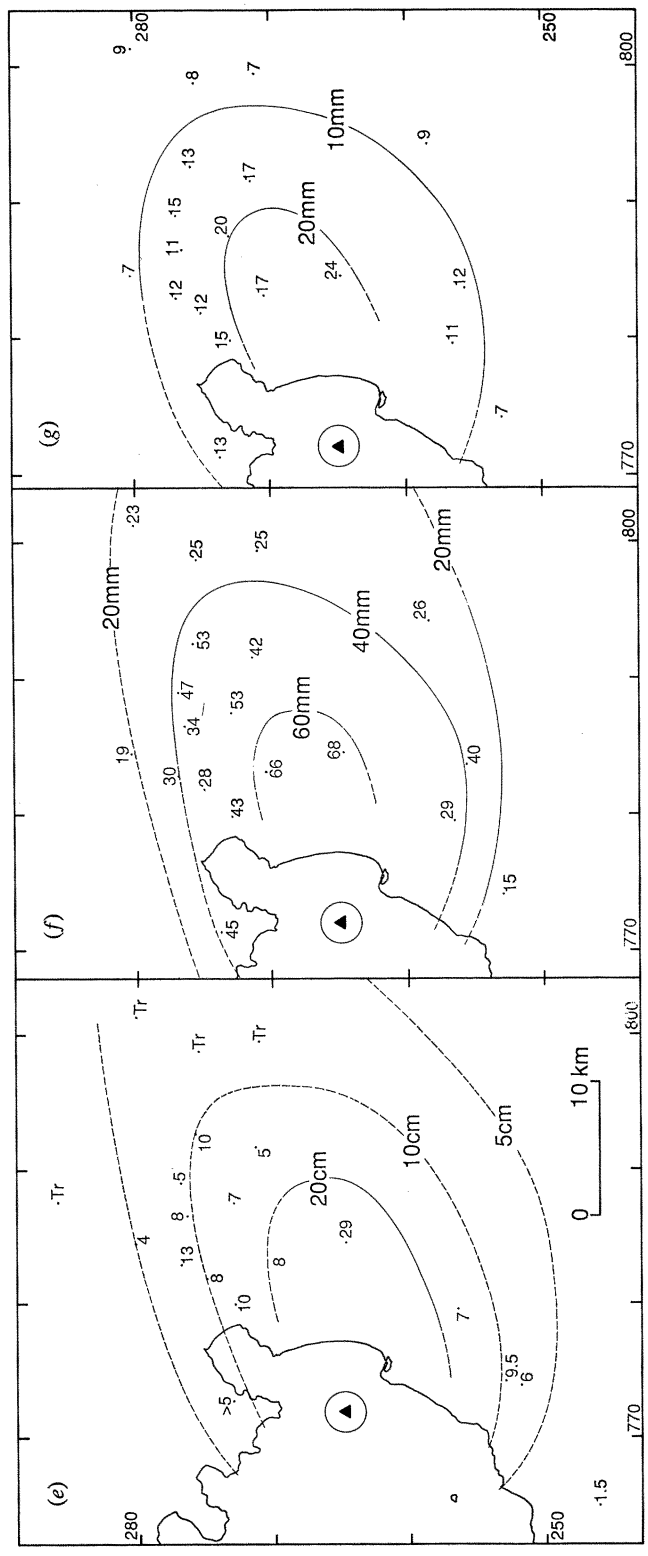


Figure 26. Isopach and isopleth data for Unit K (*cont.*). (*e*) K2, thickness; values and isopachs in centimetres. (*f*) K2, $P_{m}$ data; values and isopleths in millimetres. (*g*) K1, $L_{m}$ data; values and isopleths in millimetres.

Figure 27

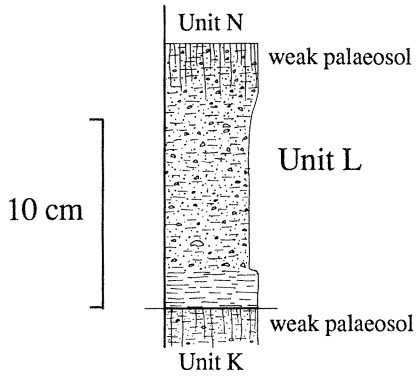


Figure 28

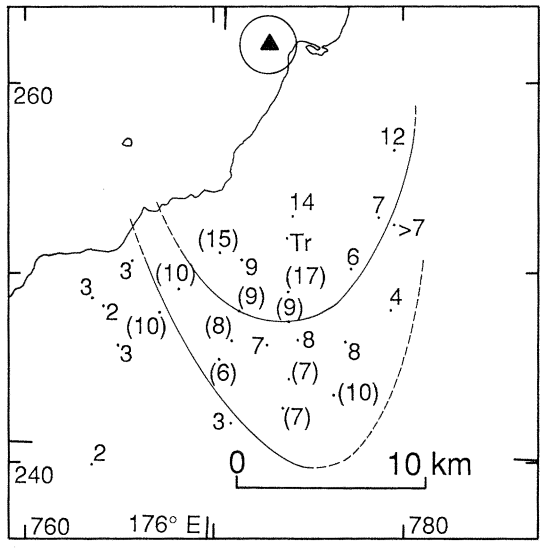


Figure 27. Stratigraphic column for the type locality of Unit L at 7742 2529 (Appendix A; figures 17*b* and 22, locality 2380).

Figure 28. Isopach data for Unit L. Values and isopachs in centimetres. Bracketed values are from localities where this unit is heavily bioturbated and are probably overestimates.

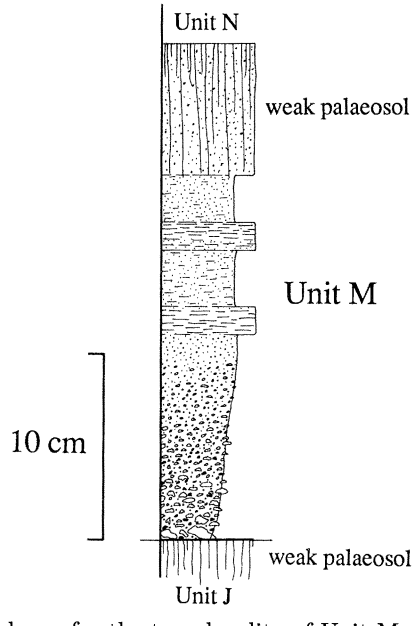


Figure 29. Stratigraphic column for the type locality of Unit M at 7765 2786 (Appendix A; figure 22, locality 2472).

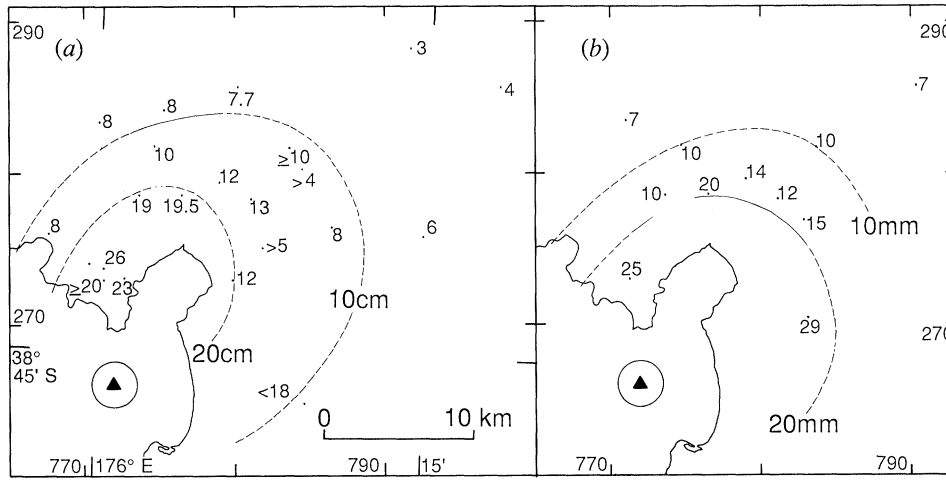


Figure 30. Isopach and isopleth data for Unit M. (*a*) thickness; values and isopachs in centimetres. (*b*) $P_m$ data; values and isopleths in millimetres.

(v) *Unit M*

Unit M is defined from a type locality at 7765 2786 (figure 22, locality 2472; figure 29). It consists of a normally graded, largely fines-poor fall deposit, with a number of ribs rich in very-fine ash towards the top. Units L and M have not been found juxtaposed, but they are interpreted to be separate because of (i) different eruptive styles; L was 'wet', M largely 'dry', and (ii) isopach (and, for M, isopleth) data which suggest different dispersal directions (south for L, NE for M) and which are not compatible with a common source. Unit M overlies a palaeosol developed on K (which is sometimes also severely bioturbated), while at 7837 2817 charcoal fragments in the post-M, pre-N palaeosol gave an age of 4330±60 years BP (Appendix B). Ages of 4500 years ($^{14}$C timescale) and 5250 years BP (calibrated timescale) are thus adopted here.

Unit M represents a largely 'dry' eruption, as evidenced by its general lack of an ash matrix. Limited isopach and isopleth data (figure 30) indicate a volume of roughly 0.2 km$^3$ and are consistent with a vent at *ca.* 772 266. Lithic clasts are dominantly obsidian; this and the abundance of grey, poorly to moderately vesicular juvenile material suggests M may have been accompanied by lava extrusion.

The eruptions of L (south) and M (north) were followed by a significant time break, during which Units I to M were bioturbated (and completely mixed at some localities) and locally a clear palaeosol was developed. The length of this time break is inferred to be *ca.* 300 years ($^{14}$C timescale) from available ages and this is broadly consistent with the degree of soil development.

(vi) *Unit N*

Unit N is a bedded fall deposit defined from a type locality at 7713 2737 (figure 22, locality 2355; figure 31) where its upper part and extreme base are very poorly sorted, with an intervening well-sorted fines-free zone. The inferred correlative of Unit N SE of Lake Taupo (figure 22) is poorly sorted and fines-rich throughout. This correlation is based on relative stratigraphic position, and the presence of scattered pumice lapilli, found above the well-sorted zone at 7798

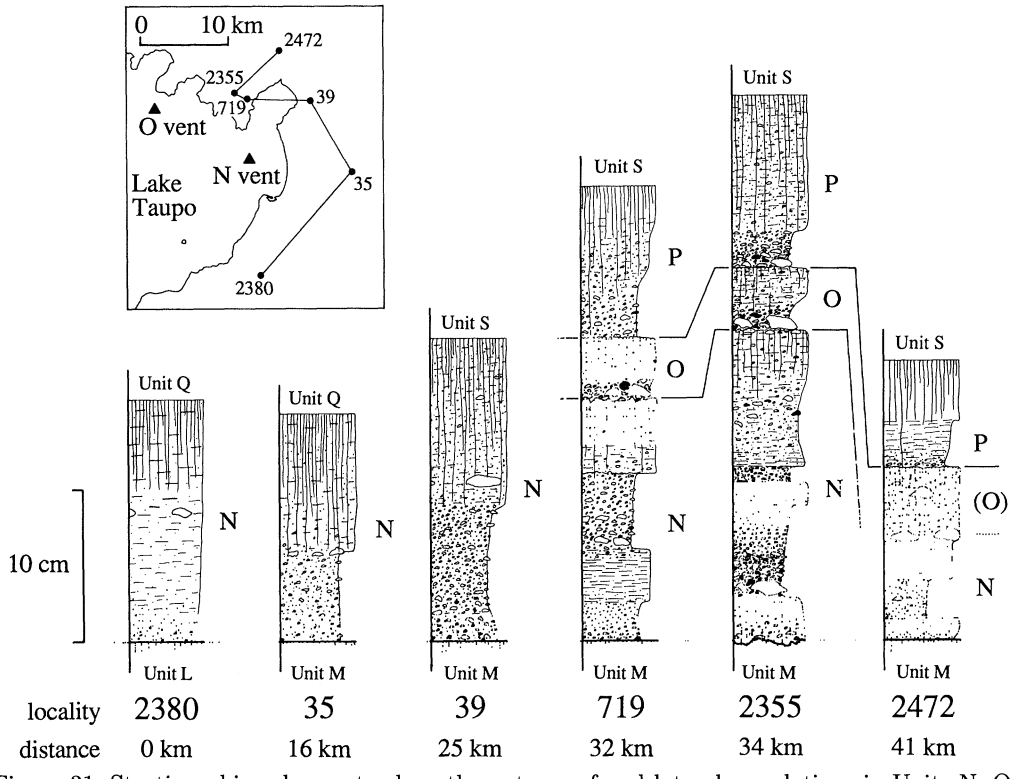


Figure 31. Stratigraphic columns to show the natures of and lateral correlations in Units N, O and P. Locality 2355 (Appendix A) is the type locality for all three units. Grid references for localities are: 7742 2529 (2380); 7846 2647 (35); 7798 2729 (39); 7727 2730 (719); 7713 2737 (2355); 7765 2786 (2472).

2729 and at an analogous position in the section at 7742 2529 (figures 17*b* and 22, locality 2380). One possible occurrence of N was also found west of Lake Taupo at 7523 2615. Unit N rests on a clear palaeosol developed on Units I to M; charcoal from within this soil at 7837 2817 yielded an age of 4330±60 years BP, while a carbonized branch in N at 7796 2525 gave an age of 4190±50 years BP (Appendix B). Adopted ages for N are thus 4200 years ($^{14}$C timescale) and 4850 years BP (calibrated timescale).

Unit N represents a mixed eruption, including both 'wet' and 'dry' activity. Lithic clasts are dominantly obsidian, and lava extrusion may have accompanied the explosive activity. Limited thickness and grainsize data (figure 32) suggest a volume of *ca.* 0.15 km$^3$, and a vent in the NE part of Lake Taupo at 773 266.

### (vii) *Unit O*

Unit O is is a fall deposit defined from a type locality at 7713 2737 (figure 31, locality 2355), where it overlies N, the contact between them being a zone of bioturbation and incipient soil formation, interpreted as a time gap of years to a few decades. Charcoal from the contact between Units O and P at 7727 2730 gave an age of 4320±70 years BP (Appendix B), but this is thought to be somewhat too old from the stratigraphic control. Ages of 4150 years BP ($^{14}$C timescale) and

4800 years BP (calibrated timescale) are adopted here, which assumes that the age for Unit N is more accurate.

Unit O, where best preserved, has a thin but coarse, fines-poor basal ash to lapilli zone overlain by very-poorly sorted, very-fine- to coarse-ash material. At most localities, O is only represented by a single-clast-thickness bed of pumice and obsidian fragments within a thick post-E, pre-S palaeosol. A volume of (O) 0.05 $km^3$ is indicated from isopach data (figure 33*a*). Unit O represents a moderately powerful eruption by 'Hinemaiaia' standards, and was dispersed to the NE from a vent inferred from isopleth data (figure 33*b*, *c*) to be in central N Lake Taupo at 762 262. Lithic clasts are dominated by obsidian, and lava extrusion may have accompanied this eruption.

Lowe (1986) recorded a 'Hinemaiaia Tephra' bed in peat in Lake Okoroire, *ca.* 90 km NNW of Taupo, with a $^{14}C$ age (Wk 662) of 4260±140 years BP below it. Lowe combined that age with others to obtain a 'mean age' for the 'Hinemaiaia Tephra', but it is possible that the younger age at Okoroire is real and the ash there is distal Unit O.

(viii) *Unit P*

Unit P is a fall deposit defined from a type locality at 7713 2737 (figure 31, locality 2355), where it consists of 10 cm of very-poorly sorted fall material which is coarser in the basal 4 cm. Unit P is distinguished from O because the two units appear to be separated by a period of bioturbation and incipient soil formation (best seen at 7765 2786), inferred to be a few decades in duration. Ages of 4100 years ($^{14}C$ timescale), or 4750 years BP (calibrated timescale) are adopted here.

Isopach/isopleth data for P are limited (figure 34), but imply that the deposit is of small volume, (O) 0.05 $km^3$, and that it rapidly thins and becomes finer N from Lake Taupo. Lithics are dominated by obsidian, suggesting lava extrusion may have accompanied this eruption.

(ix) *Unit Q*

This is a poorly preserved fall deposit seen east of Lake Taupo in the pre-S palaeosol. The type locality is at 7742 2529 (figures 17*b*, 22 and 35, locality 2380), where Q lies above N and is overlain by traces of R. Charcoal from within the post-N, pre-Q soil at 7742 2529 yielded an age of 4130±70 years BP (Appendix B), and ages of 4050 years ($^{14}C$ timescale) and 4550 years BP (calibrated timescale) are adopted for Q. The stratigraphic and chronological relationships between Q to the southeast and O and P to the north of Lake Taupo have not been resolved. Here, reliance is placed on the $^{14}C$ age data from 7742 2529 and the greater degree of palaeosol development between Units N and Q compared to that between N, O and P to suggest that Q is younger.

Unit Q is always very poorly sorted. Its thickness varies greatly (figure 36*a*) because of variable preservation, but a volume of (O) 0.15 $km^3$ is suggested. Isopleths (figure 36*b*, *c*) indicate a moderately powerful event by 'Hinemaiaia' standards, while a vent position at *ca.* 772 264 is indicated. Lithics are obsidian dominated, suggesting that lava extrusion may have accompanied this event.

(x) *Unit R*

Unit R is the youngest 'Hinemaiaia' fall unit to the S of Lake Taupo, and is defined from a type locality at 7642 2482 (figure 37). Where least bioturbated, R

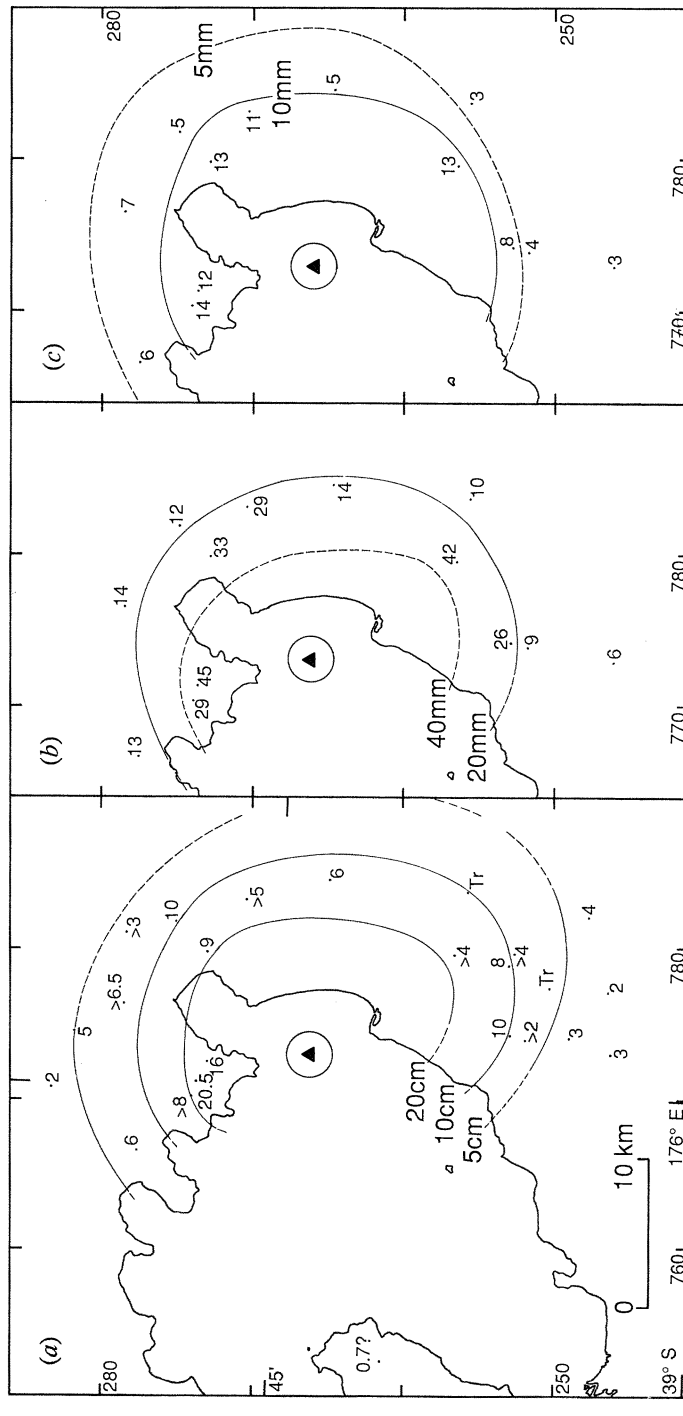


Figure 32. Isopach and isopleth maps for Unit N. (*a*) Thickness; values and isopachs in centimetres. (*b*) $P_m$ data; values and isopleths in millimetres. (*c*) $L_m$ data; values and isopleths in millimetres.

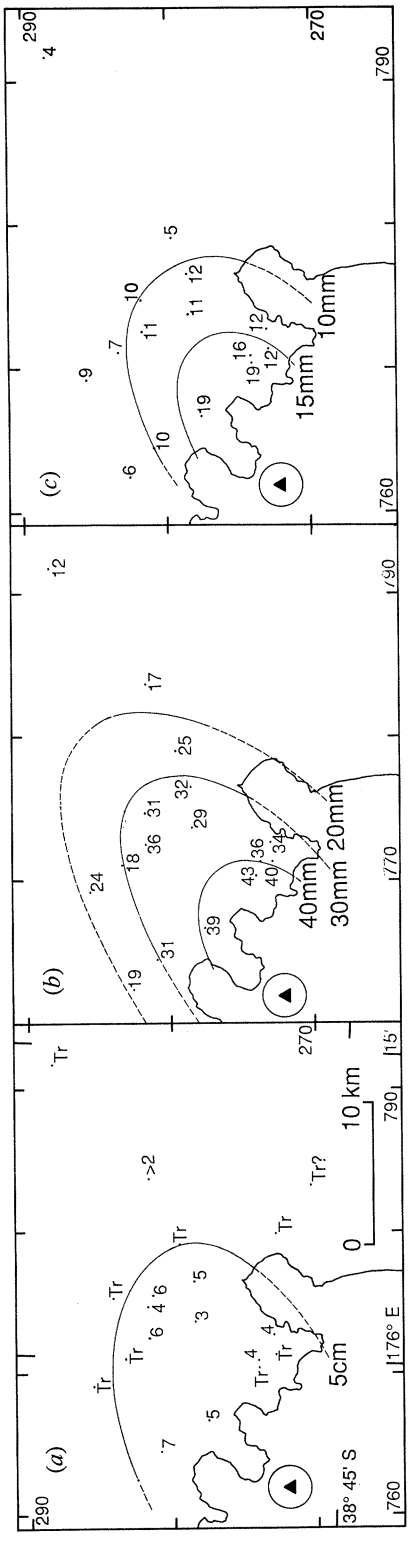


Figure 33. Isopach and isopleth maps for Unit O. (*a*) Thickness; values and isopleths in centimetres. (*b*) $P_m$ data; values and isopleths in millimetres. (*c*) $L_m$ data; values and isopleths in millimetres.

Figure 34

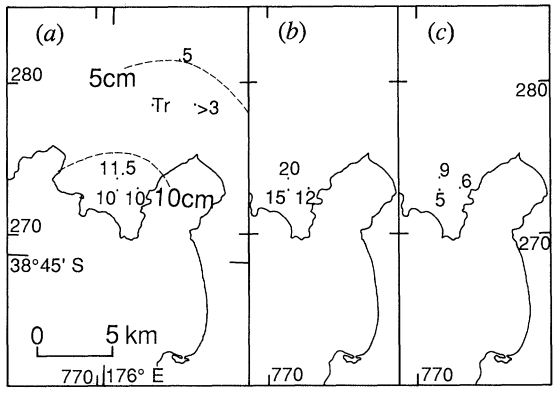


Figure 35

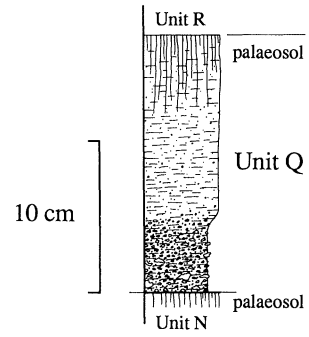


Figure 34. Isopach and maximum-clast size maps for Unit P. (*a*) Isopachs and thicknesses in centimetres. (*b*) $P_m$ data, values in millimetres. (*c*) $L_m$ data, values in millimetres.

Figure 35. Stratigraphic column for the type locality of Unit Q at 7742 2529 (Appendix A; figures 17*b* and 22, locality 2380).

consists of a fines-poor, normally graded bed overlain by very poorly sorted, fines-rich material which is interpreted to have been water-flushed. At most localities, only the bioturbated relicts of the basal unit are found, incorporated in the soil below Unit S. R overlies a palaeosol, charcoal from which gave ages of 4270±70 years BP at 7595 2469 and 4180±90 years BP at 7663 2461 (Appendix B). From the depths at which the charcoal was collected, and the degree of post-R, pre-S palaeosol development, ages of 3950 years BP ($^{14}$C timescale) and 4450 years BP (calibrated timescale) are adopted here.

Isopach/isopleth data from R (figure 38) show that it represents a small-volume (*ca.* 0.05 km$^3$), relatively weak fall eruption. Lithic clasts are mostly older lithologies, implying open-vent activity. The eruption started most powerfully and 'dry', then declined, and eventually became wet. A vent site at 763 255 is most consistent with isopach/isopleth data, and is the furthest-south active during the post-Oruanui period at Taupo.

### (*i*) *Unit S (Waimihia Tephra)*

The Waimihia Tephra Formation (Healy 1964) has long been recognized as including one of the largest young plinian fall deposits in New Zealand. Unit S is used in essentially the same sense here, except that a new deposit (T) is recognized in the post-S palaeosol. Froggatt & Lowe (1990) give an average $^{14}$C age of 3280±20 years BP Charcoal samples from the outer 5–10 growth rings of branches in the S3 ignimbrite at 7742 2529 and 7789 2729 yielded ages of 3340±50 and 3290±50 years BP respectively (Appendix B), and ages of 3300 years ($^{14}$C timescale) and 3550 years BP (calibrated timescale) are adopted here.

Unit S consists of a large pumice fall deposit (Walker 1981*a*) and a late-stage non-welded ignimbrite. Two fall subunits are recognized (S1 and S2; lower and upper Waimihia, respectively, of Walker (1981*a*) and Blake *et al.* (1992)), which are of similar volume and dispersal characteristics. S1 contains almost purely rhyolitic pumice, while S2 contains dominantly rhyolitic pumice but with subordinate quantities of streaky and grey rhyodacitic pumice and trace amounts of andesitic

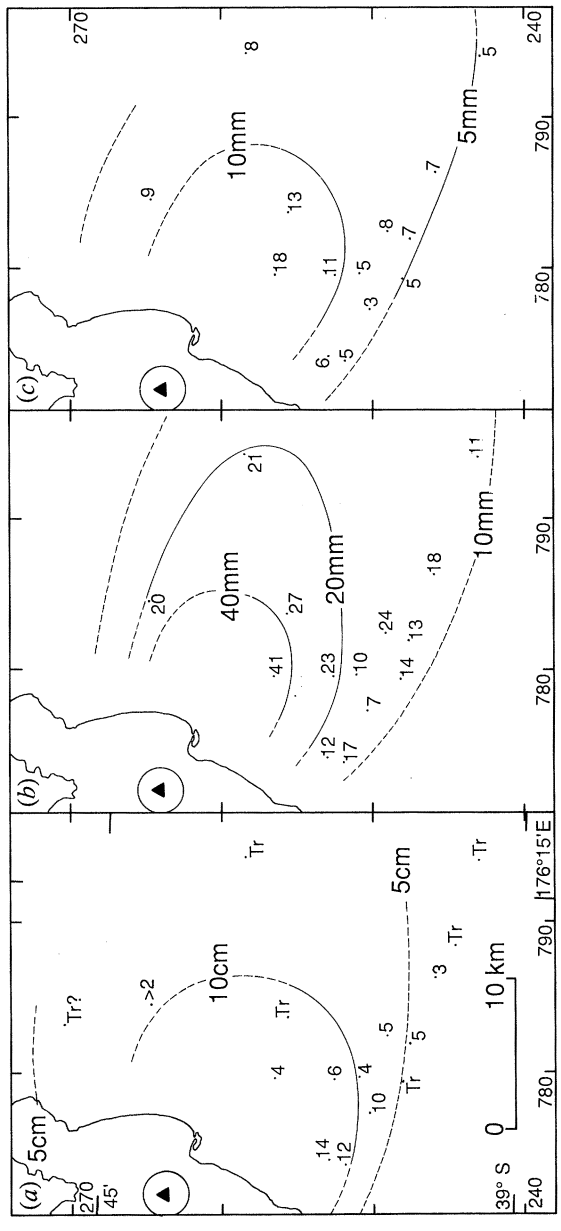


Figure 36. Isopach and isopleth maps for Unit Q. (*a*) Thickness; values and isopachs in centimetres. (*b*) $P_m$ data; values and isopleths in millimetres. (*c*) $L_m$ data; values and isopleths in millimetres.

scoria (Blake *et al.* 1992). Isopleth data (Walker 1981*a*) indicate a vent position for both S1 and S2 at 769 261. The volume of Units S1 and S2 is controversial. Integration of isopach data (as used elsewhere in this paper) yields volume estimates of 8.2 km$^3$ (S1) and 7.9 km$^3$ (S2) (Blake *et al.* 1992), while mass-balance calculations utilizing the phenocryst contents of pumice versus the free-crystal content of the deposits imply a bulk volume of 29 km$^3$ (Walker 1981*a*).

Subunit S3 is a non-welded ignimbrite, found up to 20 km from source, which has two distinct facies. A conventional non-welded ignimbrite occurs in proximal areas out to 10 km from vent, for example, four flow units totalling 12 m

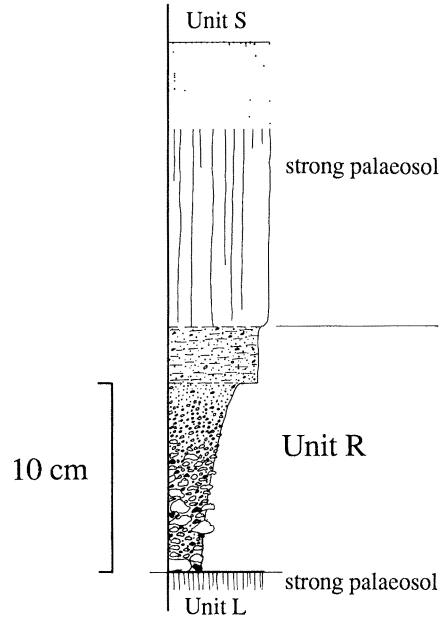


Figure 37. Stratigraphic column for the type locality of Unit R at 7642 2482 (Appendix A; figure 22, locality 2359).

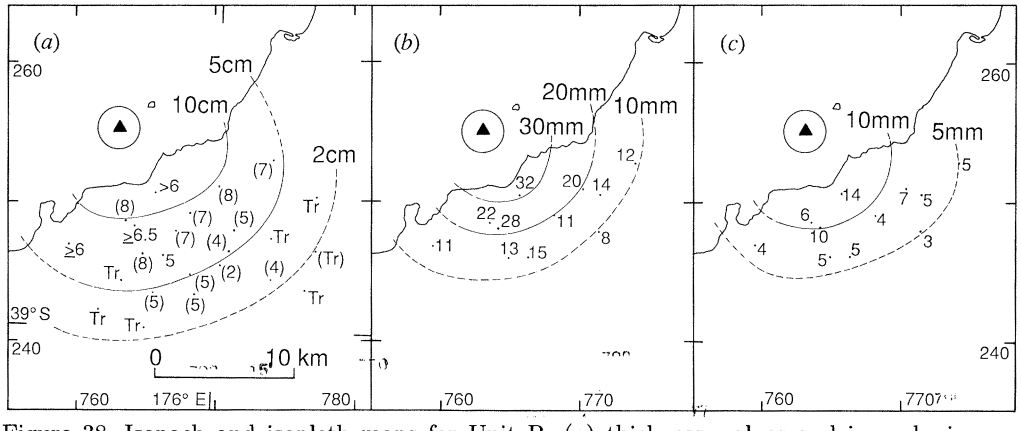


Figure 38. Isopach and isopleth maps for Unit R. (*a*) thickness; values and isopachs in centimetres. (*b*) $P_m$ data; values and isopleths in millimetres. (*c*) $L_m$ data; values and isopleths in millimetres.

thickness are exposed at 7787 2607. The distal facies consists of low-angle cross bedded deposits, including some fines-poor material, which are rich in fragments of carbonized vegetation (e.g. at 7798 2729). The distal deposits may represent more energetic, more-dilute flows or surges around the margins of the conventional ignimbrite, or could in part reflect interaction of thin flows with abundant vegetation (cf. Walker *et al.* 1980*a*). Sections around the distal margin of S3 (e.g. at 7742 2529) and the proportions of rhyodacite pumice and andesite scoria show that flow activity commenced during the later stages of S2 and that waning of the S2 plume accompanied the production of increasing quantities of S3 ignimbrite.

Eruption S contrasts with most other post-Oruanui events at Taupo in its

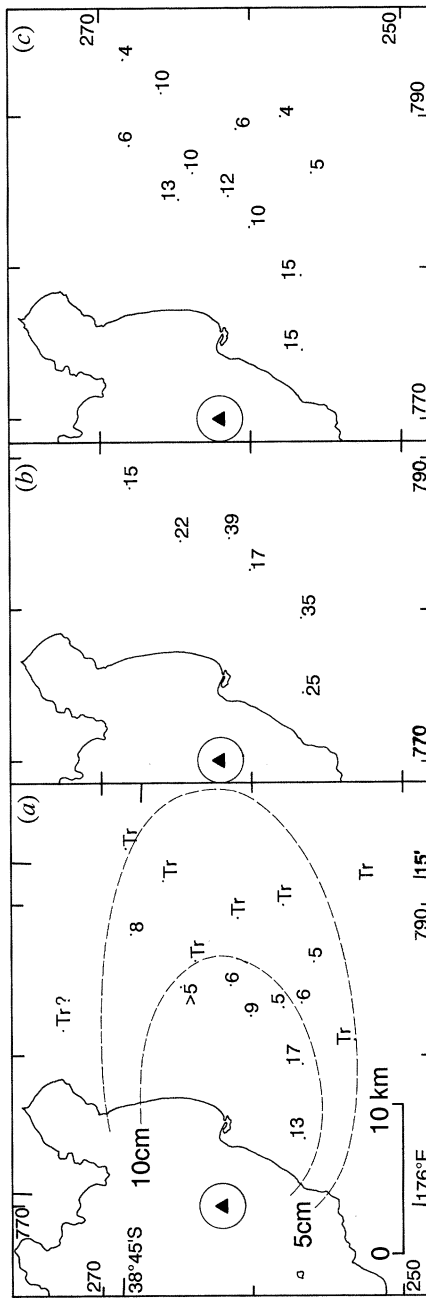


Figure 40. Isopach and maximum-clast size maps for Unit T. (*a*) Isopachs and thicknesses in centimetres. (*b*) $P_m$ data; values in millimetres. (*c*) $L_m$ data; values in millimetres.

large volume and the steadily maintained nature of the plinian plume. The only sign of any magma-water interaction is the presence of several centimetre-thick matrix-rich beds of water-flushed material in the upper part of S2. At 7742 2529 these beds are seen to post-date the onset of ignimbrite activity and any putative magma–water interaction could simply reflect passage of flows into remnants of the penecontemporaneous Lake Taupo. Lithic clasts in S are almost entirely

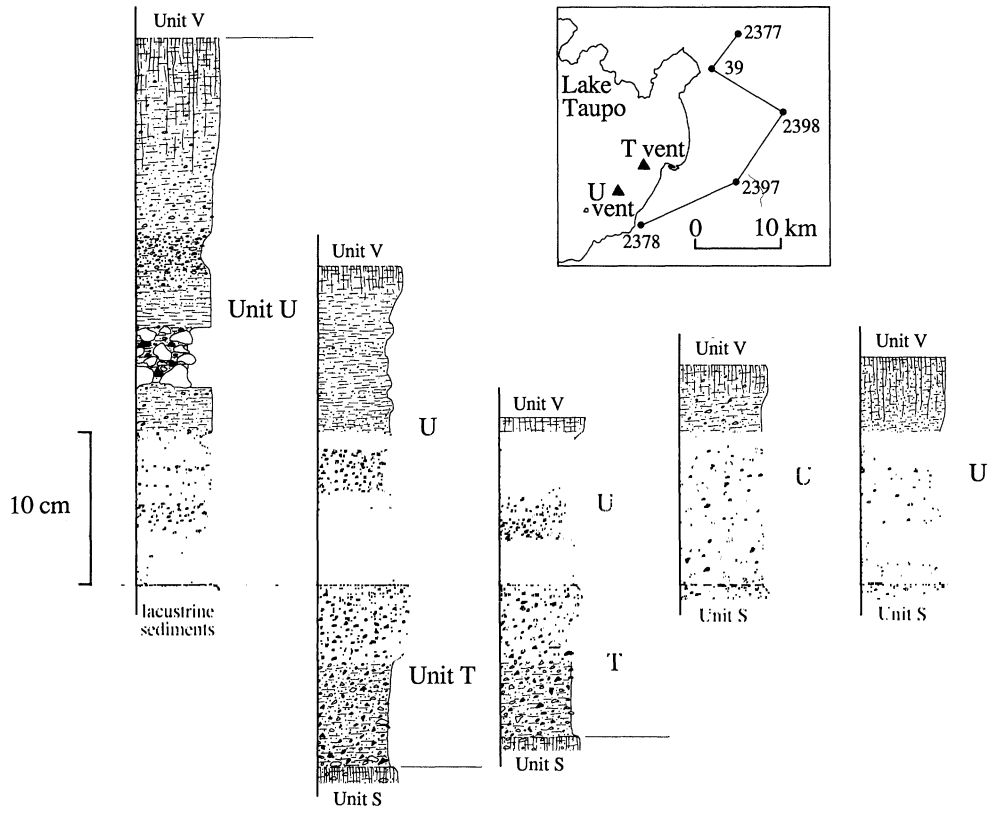


Figure 41. Stratigraphic columns to show the natures of and lateral correlations in Units T and U. 2397 and 2378 are the type localities for T (figure 39, plate 4) and U, respectively (Appendix A). Grid references for localities are: 7717 2551 (2378); 7827 2600 (2397); 7881 2680 (2398); 7798 2729 (39); 7829 2769 (2377).

foreign, and obsidian contents are so low that there is no evidence for any lava extrusion during or following this eruption.

### (*j*) *Unit T*

This new fall deposit is recognized within the palaeosol developed on Unit S. The type locality is at 7827 2600 (figure 39, plate 4; figure 41, locality 2397) where T is separated above and below by palaeosols from U and S, respectively. Charcoal fragments from the post-T, pre-U palaeosol at 7795 2566 and 7836 2567, gave ages of 3280±110 years BP and 2930±70 years BP, respectively (Appendix B). The older age is considered anomalous, from the degree of post-S, pre-T palaeosol development (figure 39), and ages of 3000 years ($^{14}$C timescale) and 3200 years BP (calibrated timescale) adopted here.

Where best preserved (e.g. 7795 2566), T is very poorly sorted and matrix rich. The lithic component is purely angular black obsidian fragments and these stand out in the post-S palaeosol at localities where otherwise T has been destroyed by weathering or bioturbation (e.g. 7892 2609). Isopach and isopleth data are

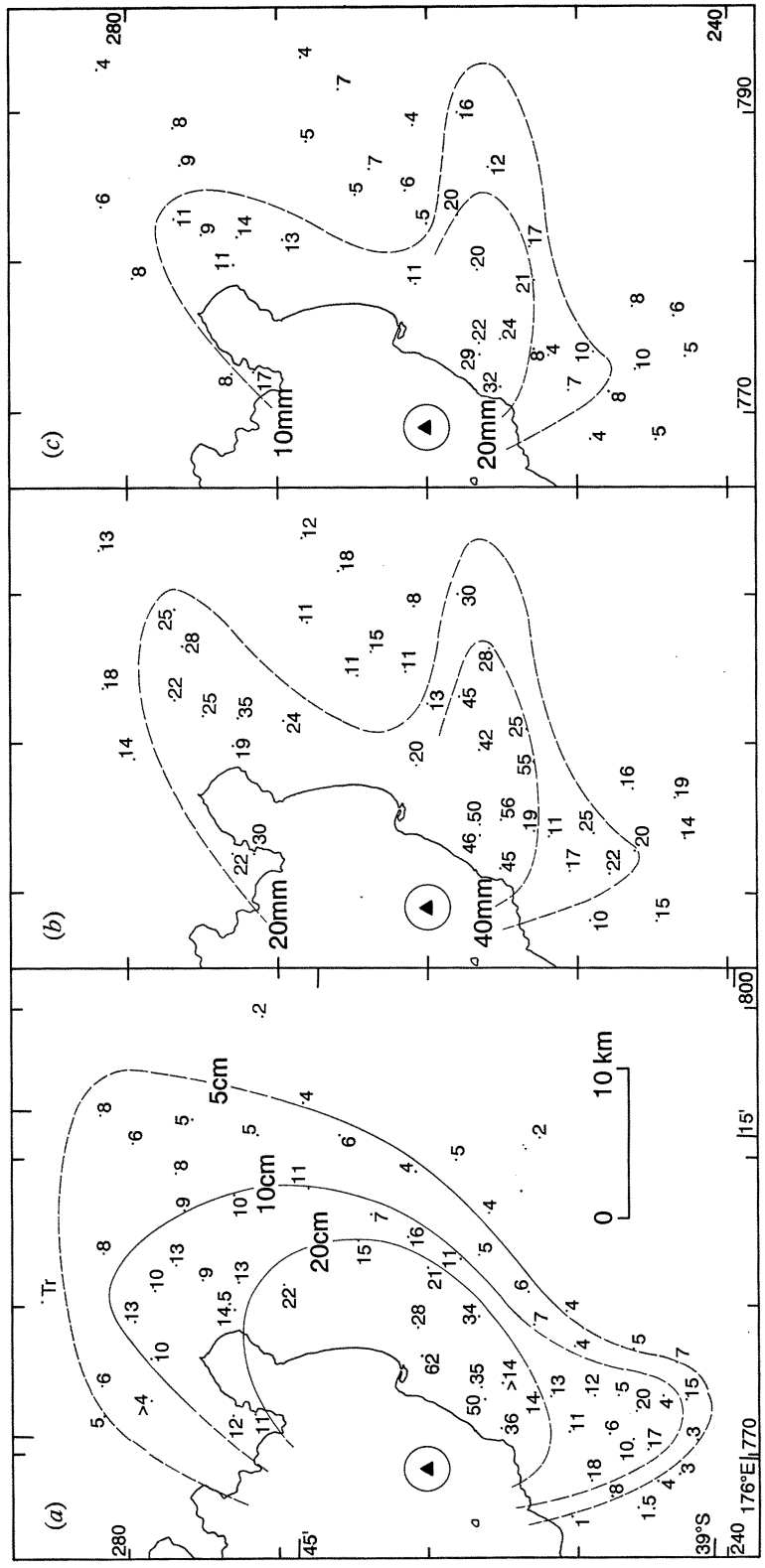


Figure 42. Isopach and isopleth maps for Unit U. (*a*) Thickness; values and isopachs in centimetres. (*b*) $P_m$ data; values and isopleths in millimetres. (*c*) $L_m$ data; values and isopleths in millimetres.

limited (figure 40), but indicate a bulk volume of *ca.* 0.08 $km^3$ and are consistent with the same vent position at 769 261 as for eruption S.

Unit T is interpreted as the product of 'wet' explosive activity which possibly accompanied extrusion of lava. The $^{14}C$ age data and palaeosol separating T from S count against any extrusive activity simply being part of the closing stages of the S eruption.

### (*k*) *Unit U*

This is a fall deposit which (from their thickness data) was previously included in the Whakaipo Tephra Formation (see Unit V, below) by Vucetich & Pullar (1973). Unit U is treated separately here because at most localities its top surface was weathered to form a weak palaeosol and/or eroded before emplacement of V. The type locality for U is at 7717 2551 (figure 41, locality 2378), while evidence for the time breaks sufficient to form palaeosols between U and V (above) and S (below) is well shown at 7795 2566. $^{14}C$ ages (Appendix B) from charcoal in the pre-U palaeosol are 2930±70 years BP (at 7836 2567) and 2890±60 years BP (at 7788 2529) which are considered valid, and 3280±110 years BP (at 7795 2566) which is thought to be recycled older carbon (possibly killed during eruption S?). Charcoal in U at 7929 2819 gave an age of 3210±60 years BP, but again this is considered anomalous when field relations with respect to V are considered. Adopted ages for Unit U are 2750 years ($^{14}C$ timescale) and 2850 years BP (calibrated timescale).

Unit U is very poorly sorted and rich in a vesicular ash matrix. A crude bedding is defined in proximal areas by variations in lapilli content, and also elsewhere by variations in the sizes and proportions of vesicles in the matrix (figure 39). Lithic clasts are dominated by grey to black obsidian. Isopach data (figure 42*a*) show a weakly bilobate distribution, and indicate a bulk volume of 0.2 $km^3$. The major NNE lobe is confidently correlated, but part of the minor southerly lobe is only tentatively identified as U from its characteristics; it lies between definite S and X, but could in part be confused with Units V and W. Isopleth data (figure 42*b*, *c*) show two lobes, but there is a wide scatter in values.

Unit U is interpreted as a water-flushed deposit from its characteristics and similarity in appearance to Y3 (Hatepe ash; Walker 1980*b*), and is interpreted to reflect interaction of a variably vesiculated magma body with abundant water. The bilobate distribution could reflect wind shear or a change in wind direction during the eruption. The abundance of obsidian in the lithic fraction suggests that lava extrusion may have occurred during or after this eruption. A vent position at 769 260, further SW than that for Unit V, is suggested from isopach and isopleth data.

### (*l*) *Unit V (Whakaipo Tephra)*

The Whakaipo Tephra Formation was defined by Vucetich & Pullar (1973) from a type locality at 7798 2729 (figure 43, locality 39), but their data make it apparent that Unit U was included as well. Units U and V are considered to represent independent eruptions from evidence of the time break between them, namely the weak palaeosol developed on U, and the observation at 7774 2676 that V rests on weakly weathered post-S lake sediments with no sign of U. Unit V is defined from the locality at 7798 2729, and correlation lines used to establish lateral changes (figure 43). Froggatt & Lowe (1990) give an average $^{14}C$ age of

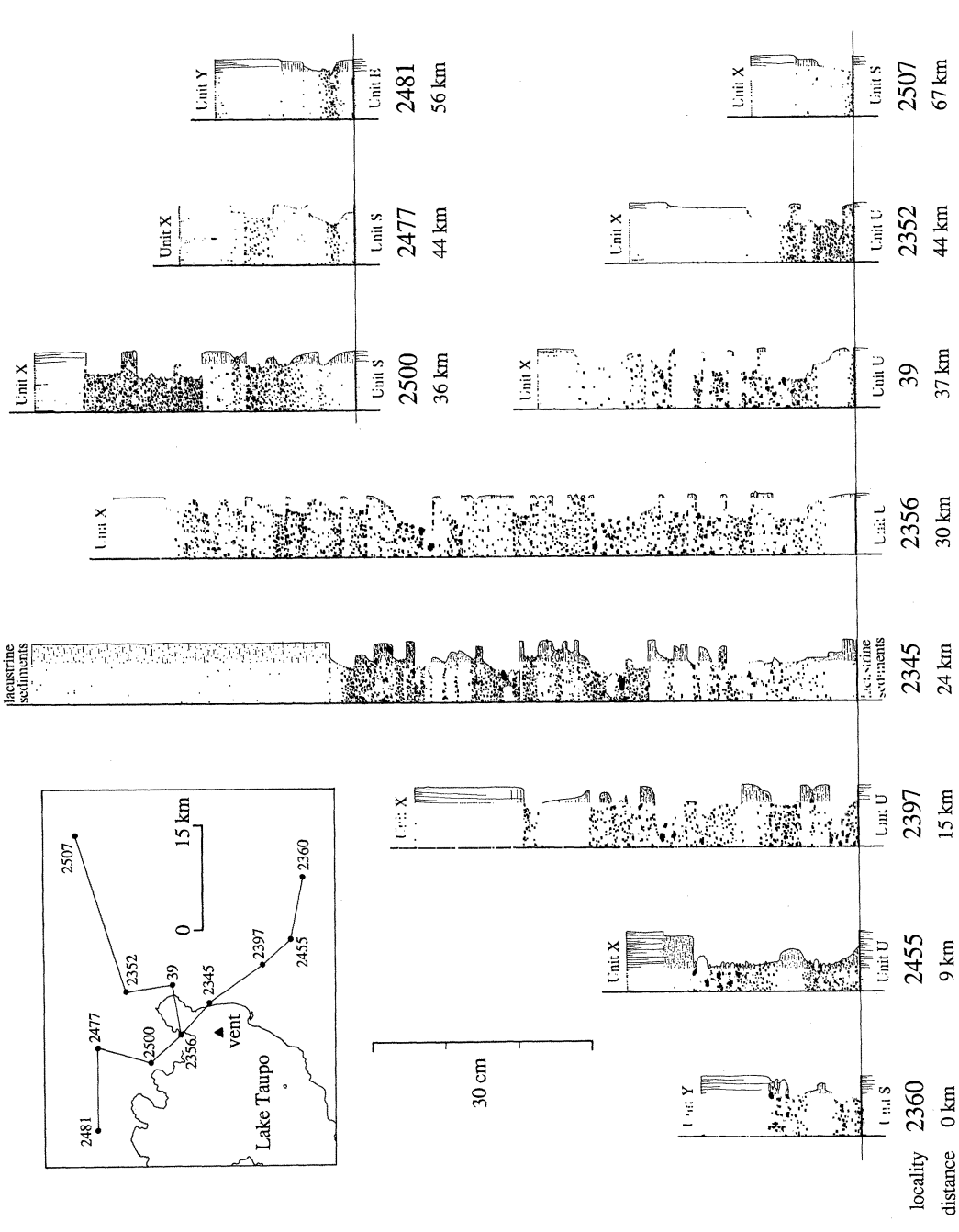


Figure 43. Stratigraphic columns to show the nature of and lateral correlations in Unit V. Localities 39 and 2345 are the type and reference sections, respectively (Appendix A). Grid references for localities are: 7953 2541 (2360); 7864 2559 (2455); 7827 2600 (2397); 7774 2676 (2345); 7727 2716 (2356); 7798 2729 (39); 7790 2796 (2352); 8014 2866 (2507); 7688 2759 (2500); 7710 2834 (2477); 7591 2834 (2481).

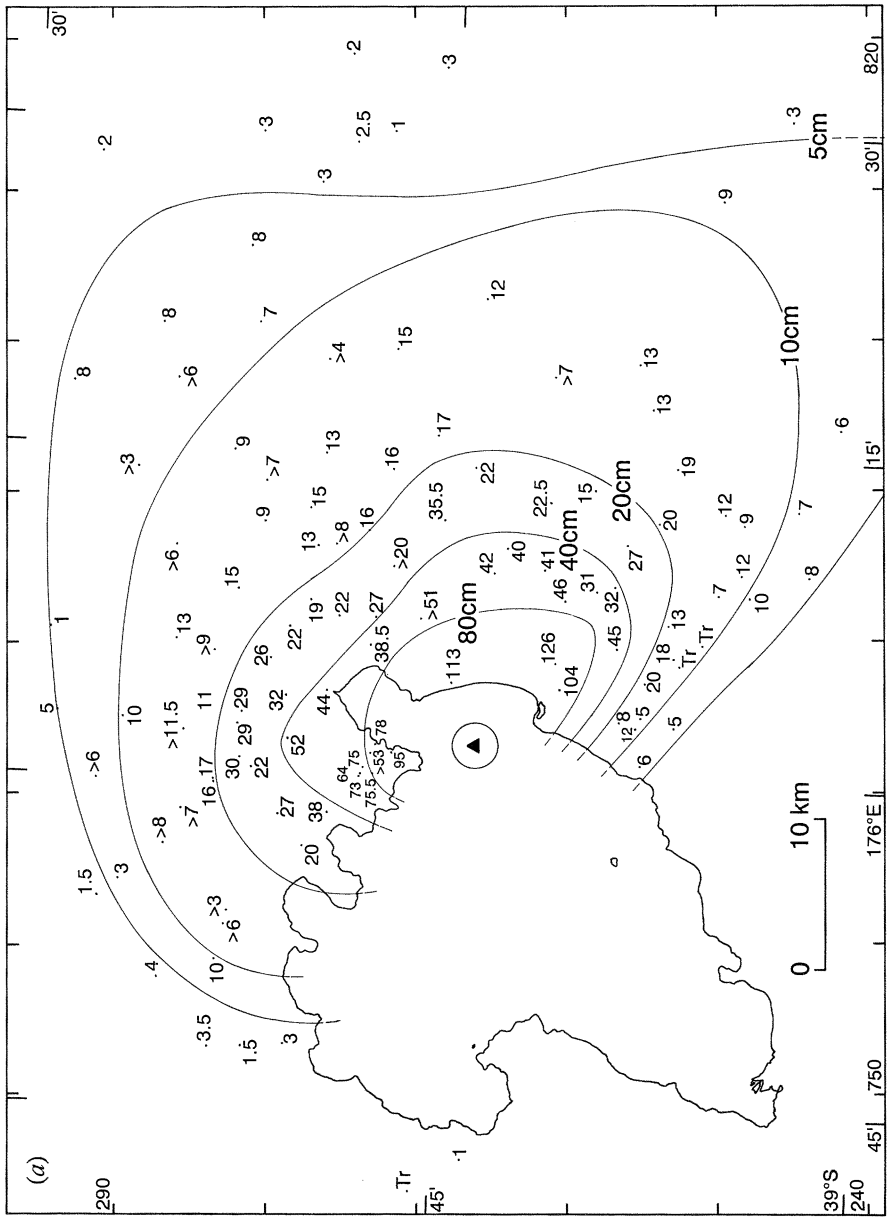


Figure 44. Isopach and isopleth maps for Unit V. (*a*) Thickness; values and isopachs in centimetres.

2685±20 years BP, and ages of 2700 $^{14}$C years (2800 calibrated years) BP are adopted here.

Unit V is a characteristically well-bedded fall deposit, which weathers to give a ribbed appearance on exposed surfaces. A detailed subdivision of V is not attempted here as the bedding is unusually complex, and beyond *ca.* 20 km from source many of the internal contacts become gradational. In proximal areas, the deposit consists of four coarser zones (figure 43) which are separated by multiple-

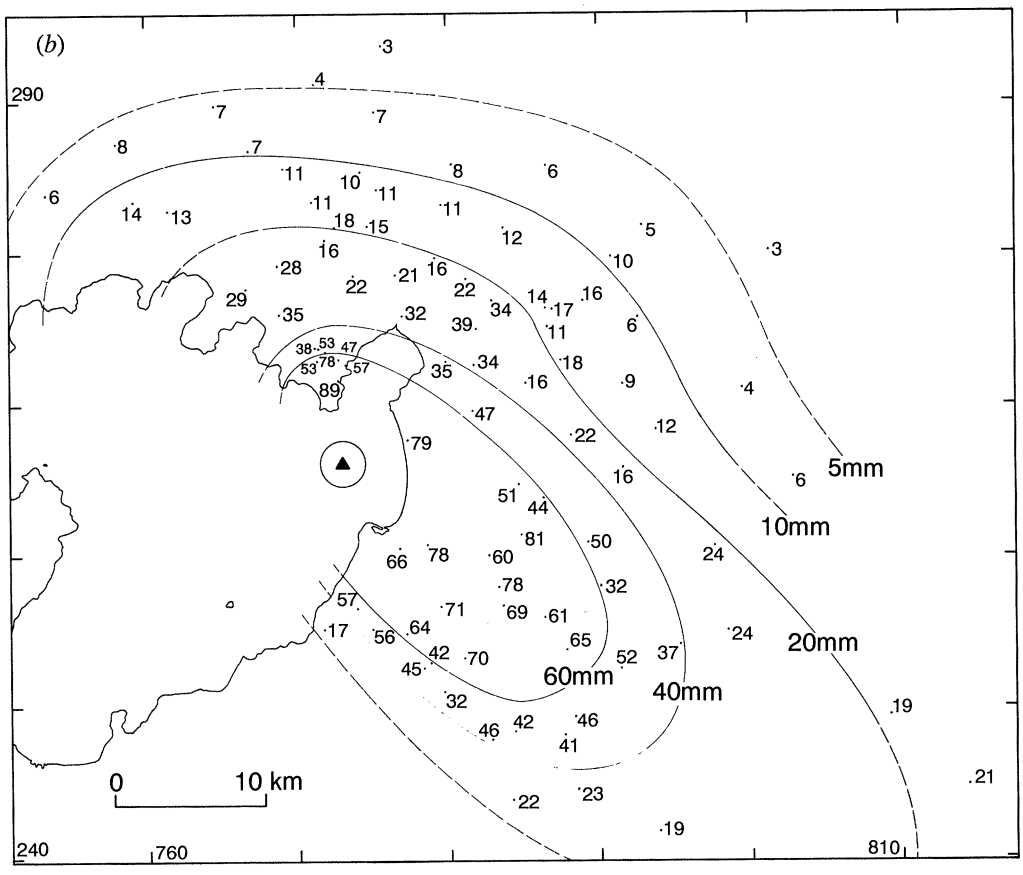


Figure 44. Isopach and isopleth maps for Unit V (*cont.*). (*b*) $P_m$ data; values and isopleths in millimetres.

bedded bands, each band being made up of numerous beds defined on a centimetre scale by fluctuations in overall grainsize and the abundance of a vesicular, fines-rich matrix. Moving away from vent, the fines-rich beds either coalesce, or fade away, to leave fewer but thicker, fine grained beds (figure 43). The overall grading in the medial to distal deposits implies that the lowest two coarse beds persist most strongly to the N and NE, while the third coarse bed is strongly directed to the SE.

Isopach data for V (figure 44*a*) are bilobate, and yield a volume estimate of 0.8 km$^3$. Isopleth data (figure 44*b*, *c*) also are bilobate; the N lobe reflects the dispersal of the lower two coarse beds, while the prominent SE lobe is from the third coarse band. Lithic isopleths from the SE lobe yield a column height estimate (a maximum for the eruption) of 26 km, and a vent position at 773 266 which is compatible with the grainsize and dispersal characteristics of other parts of V. Lithic clast proportions change through the deposit from roughly 50/50 juvenile/foreign in the lowest coarse band to juvenile (obsidian) dominated in the third and fourth coarse bands, suggesting that the magma fragmentation level rose during the eruption and that lava extrusion may have accompanied the later stages.

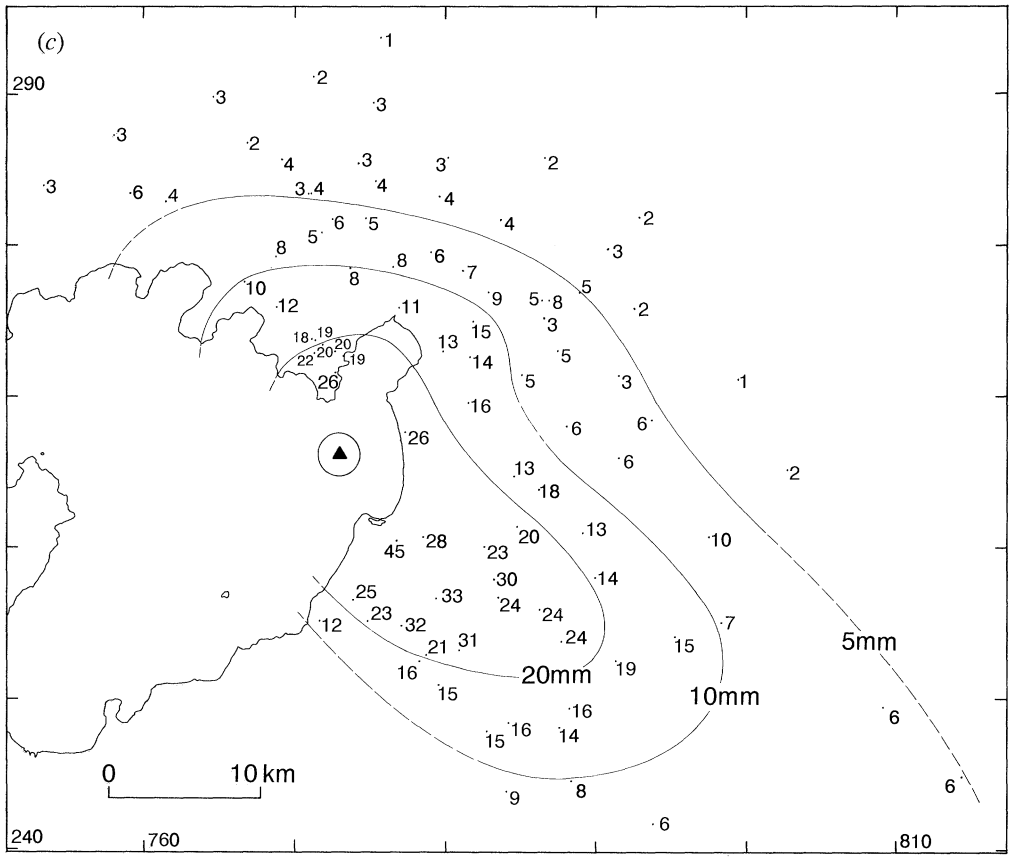


Figure 44. Isopach and isopleth maps for Unit V (*cont.*). (*c*) $L_m$ data; values and isopleths in millimetres.

Eruption V was very complex and episodic when compared with similar-volume units earlier in the Taupo sequence (e.g. E1, C). The relatively high visual abundance of lithics in the coarse bands and the abundance of water-flushed beds in proximal localities suggest that a combination of vent wall instability and a highly variable influx of water contributed to the spasmodic nature of the eruption. The coarser bands imply that the eruption column height and hence the magma supply rate may also have fluctuated widely (though on a longer timescale), but no beds equivalent to Subunit C2a have been recognized to suggest that the eruption paused for any significant period.

### (*m*) *Unit W*

This is a new, very locally dispersed fall deposit found overlying V. The type locality is at 7739 2565 (figures 45, plate 4, and 46) where W rests conformably on brown-stained V material. The brown staining is interpreted to represent a weak palaeosol, perhaps enhanced by incorporation of distal andesitic ash (from the colour; cf. Vucetich & Pullar 1973). A well-developed palaeosol then separates W from X. No $^{14}C$ ages relevant to Unit W are known, but the field relationships

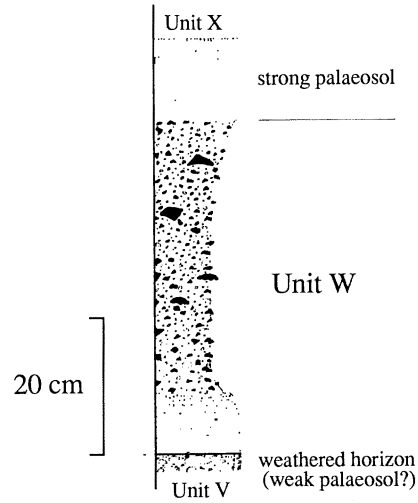


Figure 46. Stratigraphic column for the type locality of Unit W at 7739 2565 (Appendix A; figure 45, plate 4).

imply a time break of a few decades at most after Unit V. Ages of 2650 years BP ($^{14}$C timescale) and 2750 years BP (calibrated timescale) are thus adopted.

Unit W consists of two beds, a basal purplish-grey or -brown ash bed (W1) and an upper bed (W2) of ash to lapilli. W1 thins extremely rapidly S of vent and is not found to the N. It is weakly bedded and poorly sorted but contains no material coarser than ash-grade. W2 is non-bedded, non-graded and poorly sorted, with fine ash to medium lapilli and scattered coarse lapilli to blocks at the type locality. Foreign lithics are rare and small, rounded (accidental?) pumices are subordinate, while most of the bed is non- to poorly vesicular black juvenile obsidian. W2 thins and fines rapidly from the type locality; 3.5 km away at 7742 2529 it is only 7 cm thick and lacks lapilli-grade material.

The nature, grainsize and rapid lateral changes in W imply a source close to the type locality. The Ouaha Hills (figure 47) are an elongate ridge composed of pre-1800 year BP but very young lava, and it is thought that Unit W represents explosive activity preceeding or accompanying the lava extrusion, though not necessarily from the same vent. Unit W is seen S and N of Ouaha Hills and is noticeably absent above Unit V in sections to the E (the obsidian-bearing top parts of V are still dominantly composed of moderately to highly vesicular pumice), implying a restricted dispersal and correspondingly small volume, estimated as (O) 0.003 km$^3$. The Ouaha Hills lava volume is roughly 0.02 km$^3$.

Unit W is interpreted to represent very weak explosive activity where poorly to non-vesiculated magma interacted with water at shallow levels. The N15° W alignment of the Ouaha Hills ridge is unusual, and the extension of this alignment passes close enough to the inferred vent site for Units V and X (figure 47) to suggest there may be some some tectonic relationship.

### (*n*) *Unit X (Mapara Tephra)*

The Mapara Tephra Formation was defined by Vucetich & Pullar (1973) from a type locality at 7798 2729. Their definition remains valid for Unit X, except that the post-X palaeosol is not included here. An average age of 2160±25 years

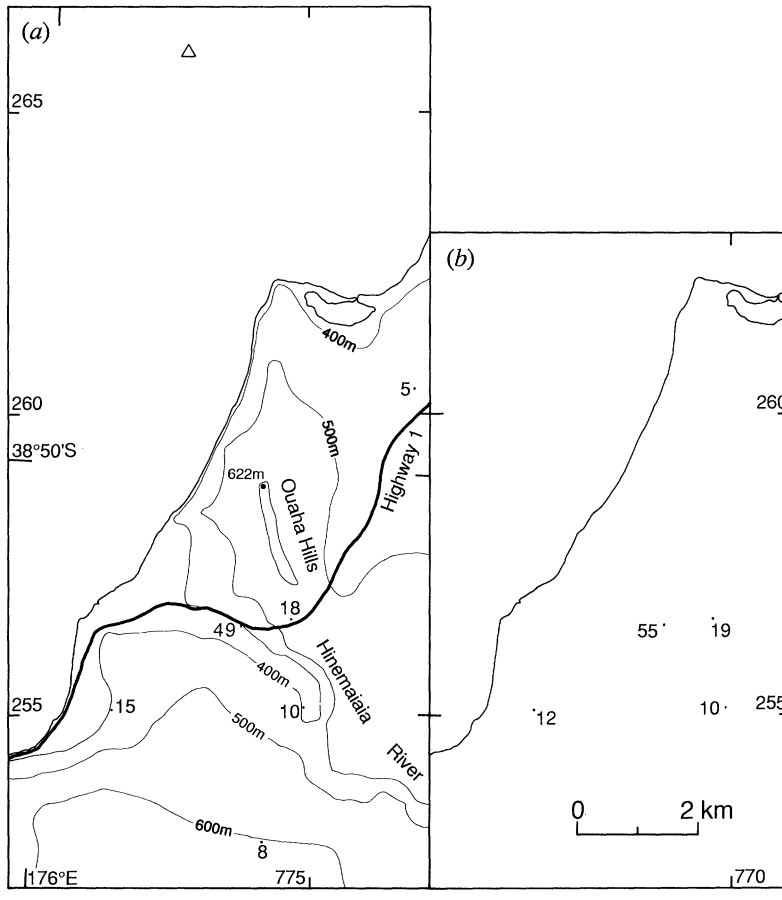


Figure 47. (*a*) Map of part of the E shoreline of Lake Taupo. Thickness values for Unit W are in centimetres, contours and spot height in metres above sea level, and the open triangle represents the inferred vent for Units V and X. (*b*) $L_m$ data; values in millimetres.

BP is given by Froggatt & Lowe (1990), and an age of 2150 years BP ($^{14}C$ and calibrated timescales) adopted here.

Unit X is a fall deposit which, like V, shows marked lateral changes in appearance. The thickest section is at 7774 2676 (figure 48, locality 2345) where 23 fines-rich beds alternate with fines-poor beds. The former are plane-parallel bedded, often vesicular, are very poorly sorted, and are interpreted as water-flushed beds; however, a lack of draping over coarse pumices suggests that these beds may have been emplaced with a significant lateral component of movement. Away from this locality, the numbers of water-flushed beds diminishes (figure 48) and so the water source is considered to have been Lake Taupo. However, the percentage of X that is inferred to have been water-flushed varies widely and non-systematically (figure 49), interpreted to reflect the importance of low-level (tropospheric) weather patterns. The whole deposit shows a systematic dispersal (figure 50*a*), and is divided into three main subunits, X1 to X3.

Subunit X1 consists of a variable number (1–6) of normally graded to non-graded beds. This subunit is the thinnest, contains the least amount of water-

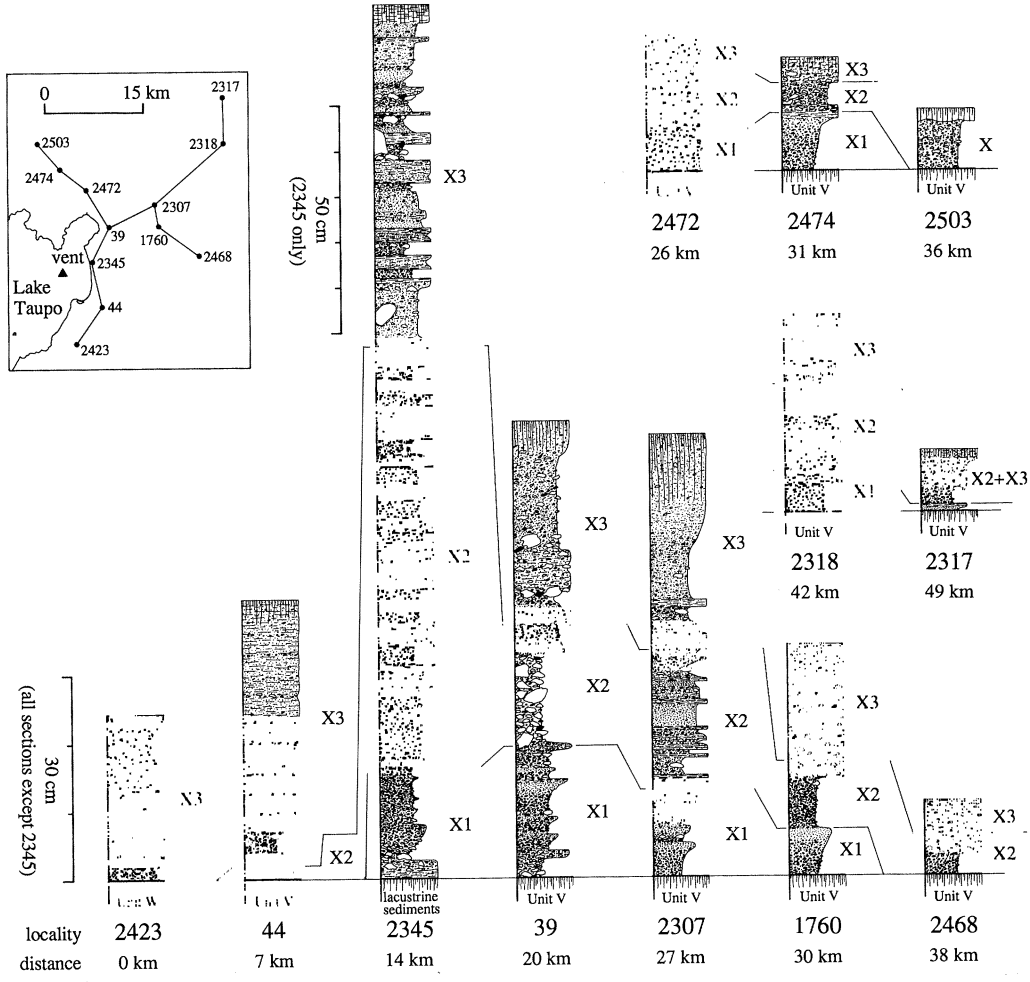


Figure 48. Stratigraphic columns to show the nature of and lateral correlations in Unit X. Localities 39 and 2345 are the type and reference sections, respectively (Appendix A). Grid references for localities are: 7749 2551 (2423); 7786 2607 (44); 7774 2676 (2345); 7798 2729 (39); 7867 2763 (2307); 7875 2730 (1760); 7938 2684 (2468); 7977 2856 (2318); 7976 2925 (2317); 7765 2786 (2472); 7725 2817 (2474); 7691 2856 (2503).

flushed material, and has a lithics dominated by foreign lithologies. X1 is demarcated from X2 by the onset of water-flushing at many localities or, where water-flushing was less pronounced (e.g. figure 48, localities 39, 1760), by a marked upwards increase in grainsize.

Subunit X2 is the thickest part of the deposit along the overall dispersal axis. X2 varies widely in appearance from mostly dry-deposited material, via a pronounced ribbed appearance caused by up to 10 poorly sorted intrabeds of flushed material, to a vaguely bedded, very poorly sorted unit which was largely to wholly water-flushed. Pumices in X2 are often sub-rounded, in contrast to angular in X1; this difference is also seen between Y2 and Y3, and is similarly attributed (Walker 1981*b*) to abrasion during magma–water interaction. Lithics are a mixture of comparable proportions of foreign lithologies and juvenile obsidian.

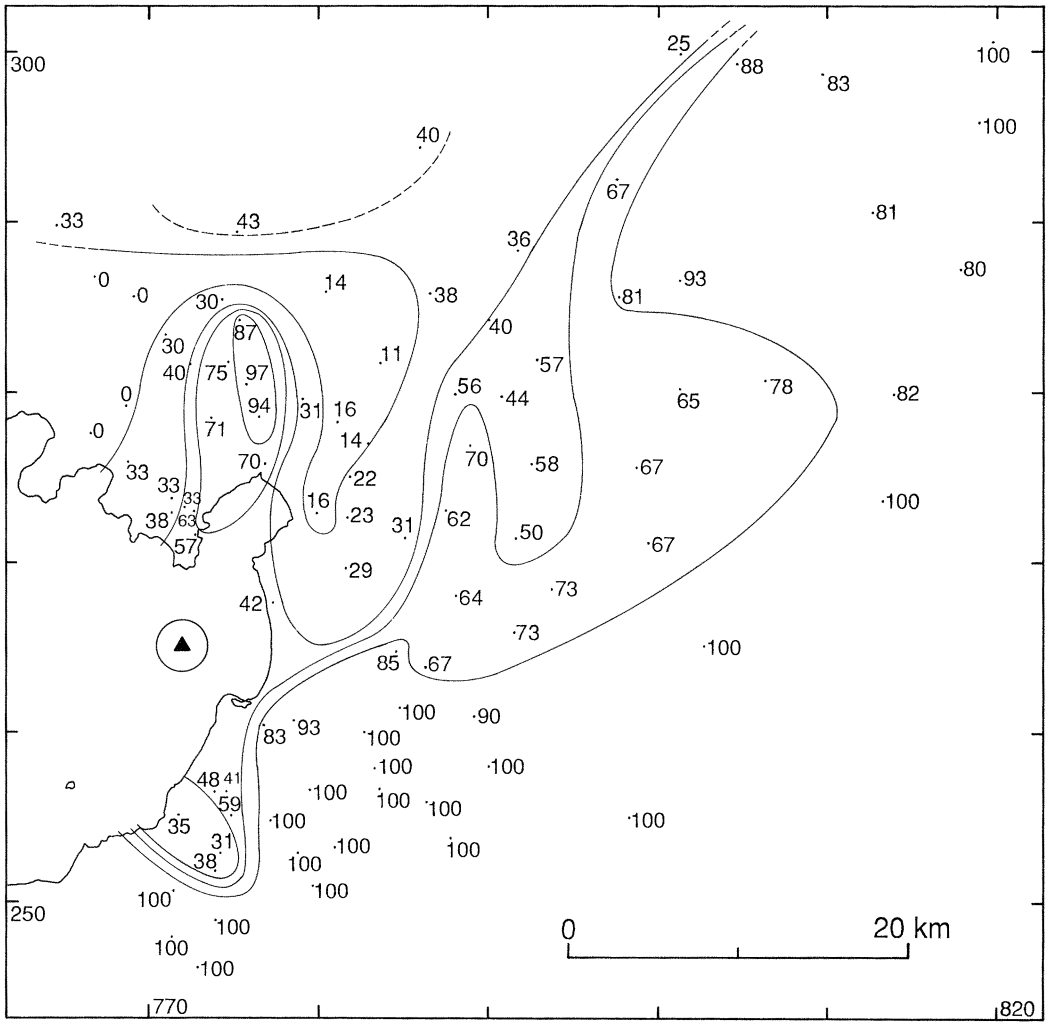


Figure 49. Map to show the percentage of Unit X which is cohesive, fines-rich and poorly sorted, and is hence inferred to have been water-flushed.

Subunit X3 is distinguished from X2 by its lithic-rich nature and the dominance of obsidian in the lithic fraction. The change in lithic proportions can be sharply defined, even in proximal localities, but is less obviously revealed in heavily water-flushed material by a change in colour from brown to grey hues. At many localities, the base of X3 is marked by a fines-poorer, lapilli-rich bed with abundant black obsidian chips, which is usually the single coarsest bed in X. X3 is dispersed more to the S and SE than X1 and X2 (figure 48), causing a southerly bulge in the isopachs (figure 50*a*). In proximal areas where the proportion of flushed material in X is less than 50%, Unit X3 characteristically terminates in a poorly sorted, dusty but non-cohesive, ash to lapilli bed rich in fragments of non- to moderately vesicular juvenile material which possibly represents explosive activity accompanying lava extrusion.

Although X1 to X3 can be defined and laterally correlated (figure 48), varia-

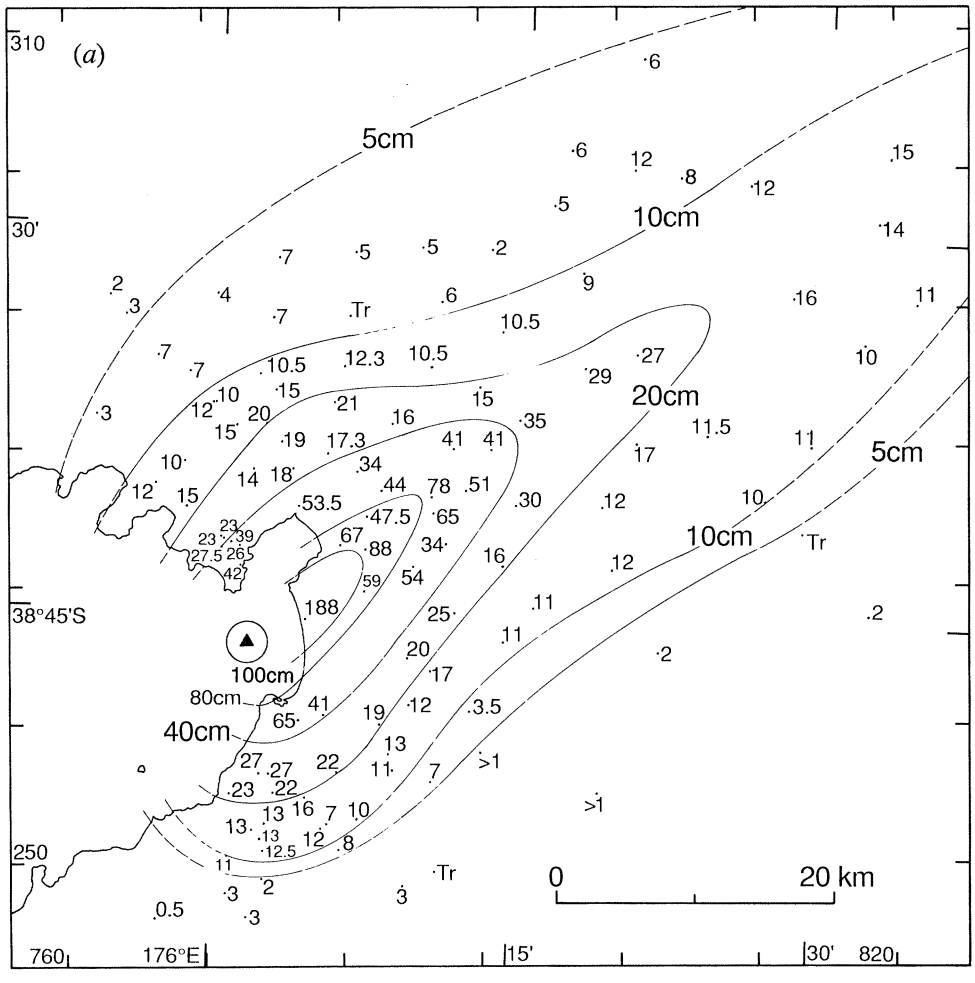


Figure 50. Isopach and isopleth maps for Unit X. (*a*) Unit X, total thickness; values and isopachs in centimetres.

tions in the frequency and amounts of water-flushing make it impossible to draw separate isopach maps for these subunits. Overall isopachs for X (figure 50*a*) yield a volume estimate of 0.8 $km^3$. Isopleth data from subunits X2 and X3 (figure 50*b*, *c*) represent moderately powerful activity, with a maximum column height of 35 km, but at no stage was this sustained for any significant time. Isopach and isopleth data are most consistent with a source at *ca.* 773 266, the same as for V. The isopleth data and lack of ballistic clasts preclude any vent further NE towards Taupo township as suggested by Vucetich & Pullar (1973).

Unit X represents an extremely complex episodic eruption in which a magma body, with an overall progression from volatile rich to volatile poor, interacted with very variable proportions of external water (i.e. Lake Taupo). The overall similarities in eruptive styles and inferred vent positions of Units V and X are striking.

### (o) Unit Y (Taupo Tephra)

Deposits of the youngest pyroclastic eruption at Taupo are described in detail elsewhere; summaries here are only modified in the light of new information (notably that supplied by the deep road cutting at 7773 2623). The type locality for this formation was originally at 7798 2729 (Healy 1964), but this has since been destroyed and a new type locality proposed by Froggatt (1981*d*) in a cliff section at 7877 2607. However, the latter is extremely difficult to get to, most of the contacts cannot be examined in close up, and several aspects of the stratigraphy are not representative. An accessible and more representative section is now available on Highway 1 at 7773 2623, and this is proposed here as a type locality. The vent position for all the major phases of this eruption was inferred by Walker (1980) to be at Horomatangi Reefs (centred on 769 261), although the reefs themselves are here interpreted as a younger lava (see eruption Z, below). The average of 41 $^{14}$C ages considered by Froggatt & Lowe (1990) is 1850±10 years BP. A putative correlation betwen Roman and Chinese records of atmospheric phenomena was used by Wilson *et al.* (1980) to suggest a calendar date of *ca.* AD 186. Although disputed (Froggatt 1981*e*; Stothers & Rampino 1983) this date is consistent with curve matching on a sequence of $^{14}$C ages on a floating tree-ring sequence from a forest buried by the Taupo ignimbrite (Y7, below) which yields a date of AD 177 (1 s.d. range AD 166–195; Palmer *et al.* 1988, and J. G. Palmer, personal communication quoted in Froggatt & Lowe 1990).

Subunit Y1 (initial ash) represents relatively minor 'wet' activity (Wilson & Walker 1985). The juvenile material is moderately to highly vesicular pumice (Houghton & Wilson 1989), and the lithics are a mixture of inferred juvenile and foreign lithologies. New exposures limit the N extent of the ash (it is absent at 7774 2676) and imply a bulk volume of 0.05 km$^3$. In overall terms, Y1 is comparable in size and inferred eruptive style to some of the 'Hinemaiaia' events.

Subunit Y2 (Hatepe plinian pumice (Walker 1981*a*), Hatepe Lapilli (Froggatt & Lowe 1990)) is mostly a uniform, non-graded, well- sorted fall deposit. Integration of the isopach data of Walker (1981*a*) yields a bulk volume of 2.5 km$^3$, but the crystal mass balance method used by Walker (1981*a*) suggested a bulk volume of 6 km$^3$. Lithic clasts are almost entirely foreign, juvenile obsidian fragments being uncommon and small. During early stages of this episode, some fines-rich, poorly sorted beds were deposited in the northerly part of the dispersal area. These are interpreted to reflect water flushing of material and to be due to minor magma–water interaction around the fringes of the eruption column (Talbot 1988).

Subunit Y3 (Hatepe ash) represents a period of vigorous 'wet' activity when moderately to highly vesiculated magma interacted with abundant external water (Walker 1981*b*; Houghton & Wilson 1989). Isopach data (Walker 1981*b*) yield a volume of 1.9 km$^3$. Foreign lithologies remain dominant in the lithic fraction, but juvenile obsidian fragments are common. This deposit is an archetypal 'phreatoplinian' water-flushed fall deposit (Self & Sparks 1978; Walker 1981*b*) with evidence that the water source was the proto-Lake Taupo, and that the ash was washed out of the plume by liquid water. Y3 is anomalously thin at 7773 2623 and in part is represented by obsidian-rich water-reworked material; it appears that this close to vent the tephra was too rich in water to accumulate as a deposit. Further gullying of Y3, by water inferred to have been ejected from the

lake, occurred during a short time break (probably less than *ca.* 3 weeks) between Y3 and Y4 (Walker 1981*b*).

Subunit Y4 (Rotongaio ash) represents another 'wet' fall event, but is mainly composed of poorly to non-vesicular juvenile material and dominated by fine to very fine ash material even at the most proximal exposures (Self & Sparks 1978; Walker 1981*b*). Foreign lithic clasts are very rare. At 7773 2623, Y4 is more than 6 m thick and contains intraformational erosion gullies with penecontemporaneous slumping of mobile ash-mud material. At this locality Y4 is mostly plane-parallel bedded, but on an unusually fine scale of mm to cm. Many of the beds are vesicular and are seen to be composed of 2–3 mm ash pellets which have partly to wholly coalesced. More-distal exposures show fewer but often coarser vesicles, and some beds locally adhering to $\geq 70°$ slopes, implying deposition as a cohesive mud, while others are represented by penecontemporaneously water-reworked material (R. Smith, work in progress). A coarser (ash to lapilli), better sorted bed occurs about 3.2 m below the top of Y4 at 7773 2623 and its probable equivalent is prominent (and coarser) in sections W of Taupo township. Isopach data for this unit (Walker 1981*b*) represent the only example among all the deposits considered in this paper which requires more than two straight-line segments on a plot of ln(thickness) against $\sqrt{}$area (Pyle 1989); three straight-line segments yield a volume of 1.1 $km^3$. However, the thickening of this unit to 7773 2623 suggests that either this volume is a significant underestimate, or a vent closer to this locality that that proposed by Walker (1981*b*) was involved.

Subunit Y5 (Taupo plinian pumice (Walker 1980), Taupo Lapilli (Froggatt & Lowe 1990)) represents a rapid change from the 'wet', dense-clast-rich Y4 conditions to a 'dry' eruption involving highly vesicular pumice. This change is accomplished over a stratigraphic interval that represents less than 0.1 $km^3$ of material. Y5 was deposited dry , except for a thin, localized, poorly sorted, fines-rich bed interpreted as due to low-level (tropospheric) water flushing, found near the base of the unit northeast of Lake Taupo (Talbot 1988). Y5 is notable for its wide dispersal (Walker 1980); despite a maximum observed thickness of only 2.1 m (C. J. N. Wilson and B.F. Houghton, unpublished data), the deposit shows the slowest rate of thinning of any 'dry' fall deposit so far documented, and was termed 'ultraplinian' by Walker (1980) as a consequence. Integration of Walker's isopach data yields a bulk volume of 7.7 $km^3$, but mass-balance calculations led Walker (1980) to postulate a bulk volume of 23 $km^3$. Lithic clasts are mostly foreign, but include sparse breadcrusted vitrophyric welded tuff which is interpreted as recycled material from the vent walls (see Y6, below). Isopleth data and the absence of ballistic lithics in this unit led Walker (1980) to first postulate the Horomatangi Reefs as the vent site for the Y eruption products.

Subunit Y6 (early ignimbrite flow units; Wilson & Walker 1985) represents ignimbrite generated synchronously with Y5. The coeval nature of Y5 and Y6 is shown at 7773 2623, where beds of Y5 less than 30 cm thick are intercalated with multiple 5–10 m flow units of non-welded to sintered Y6 ignimbrite. As with the S3 ignimbrite, two facies of Y6 are recognized, *proximal*, weakly emplaced metre-thick flow units like those at 7773 2623 where ignimbrite dominates over fall material, and *distal*, energetically emplaced dm-thick flow units which form thin intercalations in the Y5 fall material (e.g. at 7726 2730). The volume of Y6 is estimated to be *ca.* 1.5 $km^3$ (Wilson & Walker 1985).

Subunit Y7 (Taupo ignimbrite) formed during the climax of the eruption, and

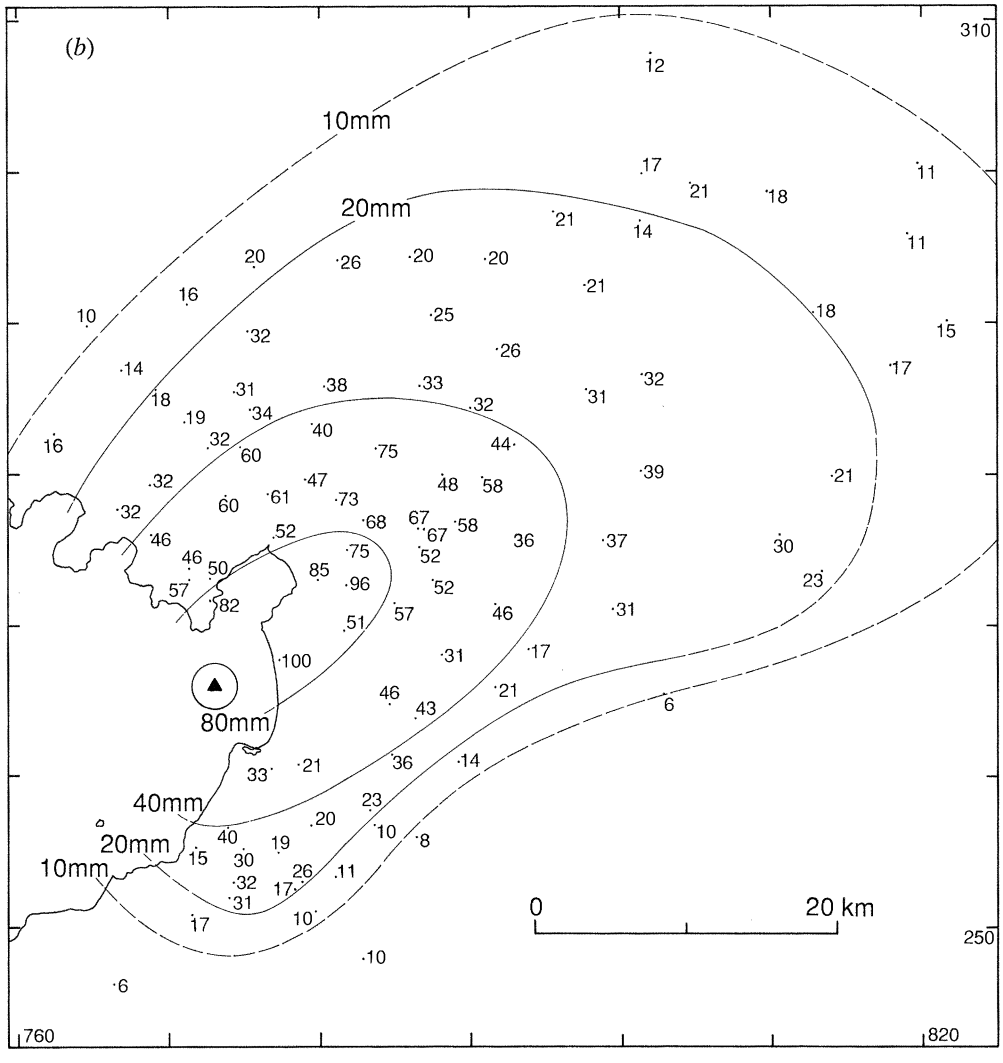


Figure 50. Isopach and isopleth maps for Unit X (*cont.*). (*b*) Units X2 and X3, $P_m$ data; values and isopleths in millimetres.

represents a volume (30 $km^3$) at least as great as all the earlier phases combined. Field observations have been used to suggest that the ignimbrite resulted from a single pyroclastic flow whose eruption was triggered by incipient caldera collapse and unroofing of the magma chamber (Wilson & Walker 1985). The flow is estimated to have been erupted over roughly 400 s (Wilson & Walker 1981) as a series of batches of material which coalesced to form a concentrated flow which travelled essentially radially outwards (Froggatt *et al.* 1981) at speeds exceeding 200–300 m $s^{-1}$(Wilson 1985). The extreme violence of the flow caused it to be spread thinly over the landscape to generate an archetypal low-aspect ratio ignimbrite (Walker *et al.* 1980*b*) and form a remarkable range of facies and lateral variations (Walker *et al.* 1980*a*, 1981*a*, *b*; Wilson & Walker 1982; Walker & Wilson 1983; Wilson 1985).

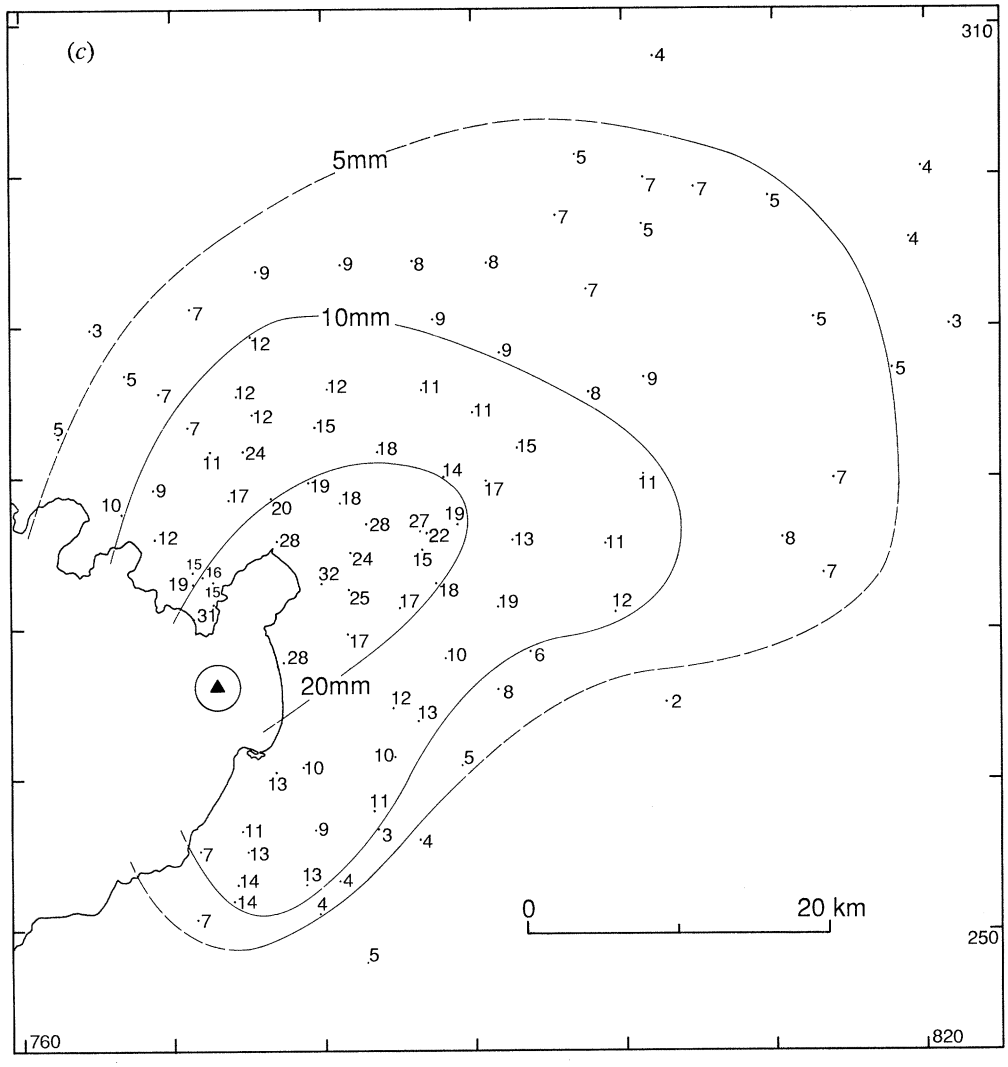


Figure 50. Isopach and isopleth maps for Unit X (*cont.*). (*c*) Units X2 and X3, $L_m$ data; values and isopleths in millimetres.

The Y eruption is most unusual in the post-Oruanui activity at Taupo, not only for its size but also the comparatively uniform conditions which prevailed during each phase. Whereas eruptions V and X fluctuated rapidly between 'wet' and 'dry' deposition (and inferred activity) on a volume scale of not more than 0.05 $km^3$, the Y events fluctuated most between phases of not less than 1 $km^3$. In Y, conditions changed sharply and irreversibly across eruption unit boundaries, for example, from Y4 to Y5. The Y eruption is the only post-Oruanui event for which caldera collapse is inferred, by wholesale collapse of an area of *ca.* 100 $km^2$ delineated by seismic evidence (Northey 1983) in the NE part of Lake Taupo and by warping of an adjacent onshore area (Walker 1984).

### (p) *Eruption Z*

Wilson & Walker (1985) described large blocks of pumiceous rhyolite (floated giant pumices) found associated with post-Y lake sediments at exposures of less than 10 m above modern lake along the E side of Lake Taupo. These blocks were inferred to be fragments of a subaqueous dome that had spalled off and were floated into place. It was inferred that Lake Taupo had re-filled after the Y eruption, reached a high level at +33 m, then fallen significantly before eruption of the dome. From comparisons with modern flow rates of streams feeding the lake, these events must have taken 20–30 years. This time period is comparable with other inferred breaks between eruptions considered here (e.g. C to D and J to K), and so the dome emplacement event is here designated as a separate eruption, with ages of 1820 years ($^{14}$C timescale) and 1740 years BP (calibrated timescale) adopted here. Potential sources for the pumiceous blocks are the arcuate structures of Horomatangi Reefs (centred on 7690 2610) and Waitahanui Bank (7699 2634). Both are young structures, by inference post-dating any putative Y-eruption related caldera collapse, and are covered in pumiceous glassy rhyolite debris (P. M. Otway, personal communication). Their volumes above local base level are *ca.* 0.25 km$^3$ (Horomatangi Reefs) and 0.03 km$^3$ (Waitahanui Bank).

## 3. Discussion

The post-Oruanui pyroclastic sequence at Taupo represents one of the most complex successions of explosive rhyolitic volcanism yet found. The output and frequency of eruptions at Taupo make it the most active and productive rhyolitic volcano in the world, but the information presented here also emphasizes the wide range of behaviour possible from a compositionally uniform magma. Eruptions in the last 20 500 years alone have varied over more than three and not less than two orders of magnitude in size and repose period, respectively. Furthermore, the styles of eruptions have varied widely with respect to such parameters as the dispersal characteristics of the fall deposits, the presence or absence of intra-eruptive time breaks, the formation of pyroclastic flows, the degree of magma-water interaction, the vesiculation state of the magma on fragmentation, and the relative proportions of juvenile versus foreign lithics. The key to understanding the dynamics of this or any other volcano, and hence in trying to predict future activity, lies in being able to explain and model these variables.

### (a) *How complete is the eruption record?*

The deposits described here are believed to represent a fairly complete record of explosive activity at Taupo from *ca.* 21 500 years BP (calibrated timescale) up to the present day. However, two groups of eruptions may well have escaped notice.

First, any purely effusive eruption would not be noticed because of burial and/or destruction of the lava by younger eruptions and submergence beneath Lake Taupo. For example, the only evidence for eruption Z is floated blocks of pumiceous rhyolite which are fortuitously preserved in lacustrine shoreline sediments. There is some evidence from the lithics in the pyroclastic deposits

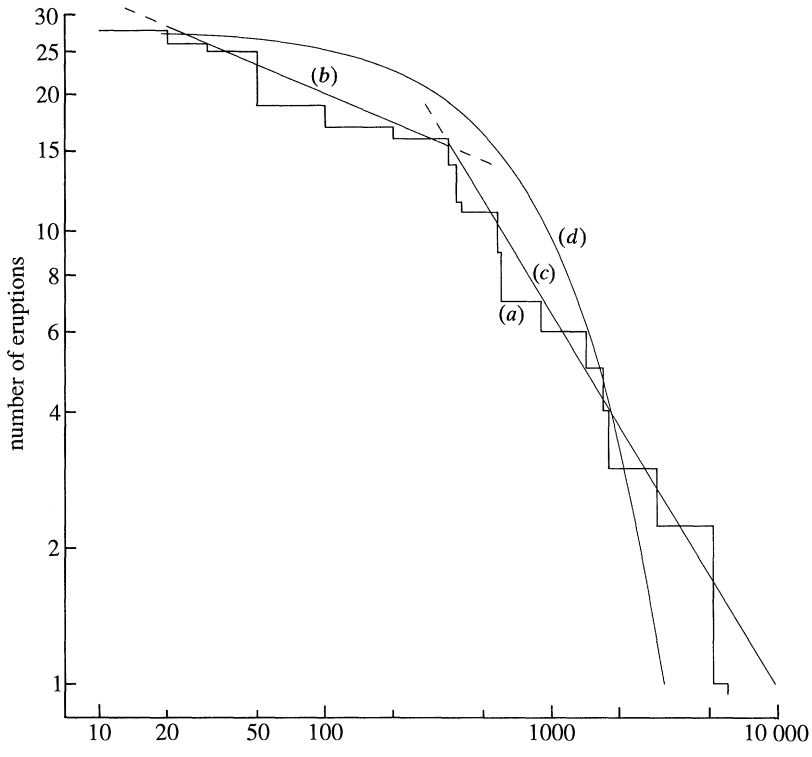


Figure 51. Plot of the cumulative number of eruptions ($n$) against their preceding repose periods ($r$, calibrated timescale). (*a*) Line representing raw data compiled from table 1. (*b*) Best-fit straight line to data for repose periods of not more than 350 years, given by $n = 53.5r^{-0.21}$, where $n$ is the number of eruptions and $r$ the repose period. (*c*) Best-fit straight line to data for repose periods of not less than 350 years, given by $n = 2096r^{-0.83}$. (*d*) Theoretical relationship for $n$ against $r$ if it is assumed the eruptions follow a gaussian distribution (Wickmann 1966) with the relationship $\text{Prob}(T \geq t) = \text{e}^{-\alpha t}$, where $\alpha$ is taken as the reciprocal average repose period of post-Oruanui eruptions, i.e. $(28/26\,500)\ \text{a}^{-1}$ .

(§3*e*(vi), below) for effusive activity between *ca.* 26 500 and 11 800 calibrated years BP.

Second, the Oruanui eruption was followed by severe erosion due to burial and destruction of vegetation which would otherwise have anchored the deposits, the non-indurated nature of the deposits themselves and the severe climate during the following glacial maximum. The tephrochronological record in surrounding areas (e.g. Vucetich & Pullar 1964; Topping & Kohn 1973; Lowe 1988; Froggatt & Lowe 1990) is complete enough to imply that no pyroclastic eruption of more than 0.3 $\text{km}^3$ could have occurred without leaving a record. However, eruptions smaller than this, like Units Ψ, Ω and A, possibly accompanying lava extrusions, could have occurred and no traces would be preserved.

### (*b*) *Eruption timing*

The repose periods between eruptions given in table 1 range from 20 to 6000 years. All of these represent time periods at least an order of magnitude longer

than the probable duration of any explosive eruption (see § 3*e*(iii), below) and so the eruptions are treated as point events in time. Two distinct models for repose periods are available. The first (Wickmann 1966) treats eruptions as random events, so that the probability of a repose period $T$ longer than any time period $t$ is given by

$$\text{Prob}\,(T \geq t) = \mathrm{e}^{-\alpha t}$$

and a plot of $\ln n$ (where $n$ is the number of repose intervals of duration greater than $t$) against $t$ will yield a linear relationship with slope $-\alpha$. The second approach (Dubois & Cheminée 1988, 1991) considers the data to show self-similar properties and have a fractal dimension $D$ such that

$$\text{Prob}\,(T \geq t) = t^{-D},$$

where $0 < D < 1$, and a log–log plot of $n$ against $t$ will yield a linear relationship with slope $-D$ (Mandelbrot 1982). The lower the value of $D$, the less uniform the eruptions are spaced in time and vice versa. Despite uncertainties and potential errors in estimates of the repose periods, especially those of not more than 100 years, it is clear that the lengths of repose periods ($r$) are best fitted by lines of the form $n = kr^{-D}$, where $n$ is the number of eruptions and $k$ a constant (figure 51). Repose periods of not more than 350 years are most-closely fitted by a line with $k = 53.5$ and $D = 0.21$, and those of not less than 350 years by one with $k = 2096$ and $D = 0.83$ (figure 51). The presence of two linear segments was noted for several basaltic volcanoes by Dubois & Cheminée (1991), but in those cases the transition between shorter (lower $D$) and longer (higher $D$) repose periods occurred at $10 < r < 72$ months. A model random (gaussian) distribution (cf. Wickman 1966) departs noticeably from the data (figure 51).

The controls on lengths of repose periods are potentially complicated. Historical earthquakes (and any surface faulting) at Taupo have been clustered into swarms with 'repose periods' of a few decades (activity in 1895, 1922, 1964/5 and 1983; Grindley & Hull 1986), and it is plausible that the shorter-timescale control on eruptions ($D = 0.21$) is regional tectonics accompanying rifting in the Lake Taupo area. Longer-timescale controls may also reflect episodicity in rifting events, or the frequency with which magma bodies are supplied. These relationships are currently being tested by seeing if the products of successive eruptions represent aliquots of a single magma batch, or if they represent separate magma bodies (A. Sutton, work in progress). Note that any differences between magma batches may be subtle, as in overall terms the post-Oruanui rhyolites at Taupo form a remarkably uniform suite (Ewart 1963; Dunbar *et al.* 1989*a*).

### (*c*) *Eruption volumes*

Eruption volumes (as listed in table 2 and using the lower figures for eruptions S and Y for consistency) show wide variations. In general, the volumes are markedly smaller than those proposed by other workers, for two reasons. First, most values given by Vucetich & Pullar (1973), Froggatt (1981*b*, 1982) and Froggatt & Lowe (1990) are based on isopachs which include both the overlying palaeosol, as well as estimates of apparent thicknesses of tephra inferred to be present in distal palaeosol horizons (Vucetich & Pullar 1964), and are thus considered to be overestimated. Second, Walker's (1980) technique of comparing crystal contents in the deposit versus in the magma yields significantly larger

Table 2. *Summary of volumes for post-Oruanui eruptions at Taupo volano*

(All volumes refer to the bulk volume of pyroclastic material, except where noted as including lava as well. Superscripts refer to references for data not presented in this paper, as follows: 1. Wilson & Walker (1985), 2. Froggatt (1981*d*), 3. Froggatt (1982), 4. Walker (1980), 5. Froggatt & Lowe (1990), 6. Walker (1981*b*), 7. Walker (1981*a*), 8. Vucetich & Pullar (1973), 9. Froggatt (1981*c*).)

| unit, or subunit | volume, bulk/km$^3$ | other estimates | unit, or subunit | volume, bulk/km$^3$ | other estimates |
|---|---|---|---|---|---|
| (Z) | 0.28[a] | — | K | 0.35 | |
| Y | 44.75 | 65[1,b] | K2 | 0.22 | |
| Y | — | 105[1,c] | K1 | 0.13 | |
| Y7 | 30.0[1] | 70[2,3,5] | J | 0.015 | |
| Y6 | 1.5[1] | | I | 0.02 | |
| Y5 | 7.7 | 23[4], 12[3,5] | H | 0.2 | note f |
| Y4 | 1.1 | 1.3[6], 2[2], 1[3,5] | H2 | 0.1 | |
| Y3 | 1.9 | 2.5[6], 2[2] | H1 | 0.1 | |
| Y2 | 2.5 | 6[7], 2[3] | G | 0.5 | |
| Y1 | 0.05 | 0.015[1] | G2 | 0.3 | |
| X | 0.8 | 0.65[8], 2[3,5], 6[2] | G1 | 0.2 | |
| W | 0.023[d] | | F | 0.12[g] | |
| V | 0.8 | 0.8[8], 1.5[3], 2[5], 6[2] | E | 4.8 | 4[3,5], 5[5], 12[2] |
| U | 0.2 | | E5 | 0.2 | |
| T | 0.08 | | E4 | 1.5 | |
| S | 16.9 | 15[8], 17[2], 19[5] | E3 | 1.95 | |
| S3 | 0.8 | 5[2,3,5] | E2 | 0.15 | |
| S1 plus S2 | 16.1 | 12[2], 14[3,5], 29[7] | E1 | 1.0 | |
| S2 | 7.9 | | D | 0.2[h] | |
| S1 | 8.2 | | C | 0.75 | 3[3,5], 3.5[8], 7[2] |
| R | 0.05 | note e | C2 | 0.2 | |
| Q | 0.15 | | C1 | 0.55 | |
| P | 0.05 | | B | 1.4 | 2[3,5], 5[8], 6[2] |
| O | 0.05 | | B4 | 0.82 | |
| N | 0.15 | | B3 | 0.15 | |
| M | 0.2 | | B2 | 0.1 | |
| L | 0.07 | | B1 | 0.23 | |
| | | | A | (0.01) | |
| | | | Ω | 0.1 | |
| | | | Ψ | (0.05) | |

[a]Volume of lavas of Horomatangi Reefs and Waitahanui Bank, inferred to be from this eruption. [b]Excludes co-ignimbrite ash fall, and material beneath Lake Taupo. [c]Includes co-ignimbrite ash fall, and material beneath Lake Taupo. [d]Includes volume of Ouaha Hills lava (0.02 km$^3$). [e]Volume estimates for the 'Hinemaiaia Tephra' are 3 km$^3$(for Units I to R, inclusive; refs 2, 3, 5) and 4.7 km$^3$(for Units G to R, inclusive; ref. 8). [f]Volume estimates for 'Motutere Tephra' (Units G and H, inclusive) are 0.5 km$^3$(ref. 3) and 1 km$^3$(refs 2, 5 and 9). [g]Includes volume of Motutaiko Island dome (0.05 km$^3$). [h]Includes volume of Acacia Bay dome (*ca.* 0.05 km$^3$).

volume estimates for Subunits S1, S2, Y2 and Y5, but these are subject to some uncertainties. These include adoption of a value for the magmatic crystal content, distinguishing between phenocrysts and xenocrysts in the loose-crystal population, and converting isopach and componentry data to isomass contours for each component. The errors inherent in the techniques of Walker (1980) and Pyle

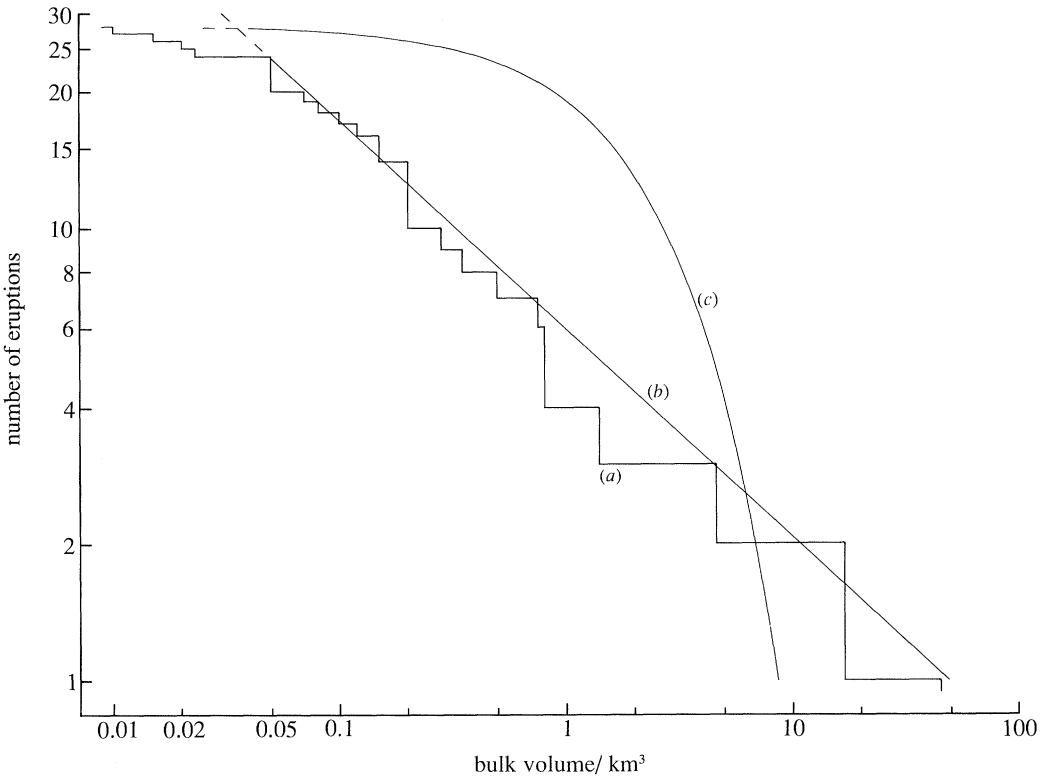


Figure 52. Plot of the cumulative number of eruptions ($n$) against their volumes ($v$). ($a$) Line representing raw data compiled from table 2. ($b$) Best-fit straight line to data for volumes of not less than 0.05 km$^3$, given by $n = 6.17v^{-0.46}$ (lines were fitted to the volume data at various lower cut-offs, and the best fit was given by this line). ($c$) Theoretical relationship for $n$ against $v$ if it is assumed the volumes follow a gaussian distribution (cf. figure 51) with the relationship Prob $(V \geq v) = e^{-\beta v}$, where $\beta$ is taken as the reciprocal of the average volume of post-Oruanui eruptions, i.e. (28/73) km$^{-3}$. See text for discussion.

(1989) are not established and differences cannot be assessed, but the volumes given in table 2 are reliable minima. Conversions to magma volumes are difficult because of lack of data on the *in situ* bulk densities of the deposits and their proportions of foreign lithics, but to a first approximation, magma volumes will be 25–33% of the bulk volumes reported. In addition, the volumes of any putative co-eruptive lavas are generally unknown. However, in similar fashion to repose intervals, eruption volumes ($v$) are best fitted by a line of the form $n = kv^{-D}$ (figure 52), with $D = 0.46$. A departure from the self-similar trend for volumes not greater than 0.05 km$^3$ is in part an artefact, because rounding-off of volume estimates will have caused more clustering of data (i.e. lower $D$) and also because volume estimates are less accurate because volumes of any co-eruptive lavas (whose presence is suggested by high juvenile obsidian proportions in most of these small deposits) are unknown.

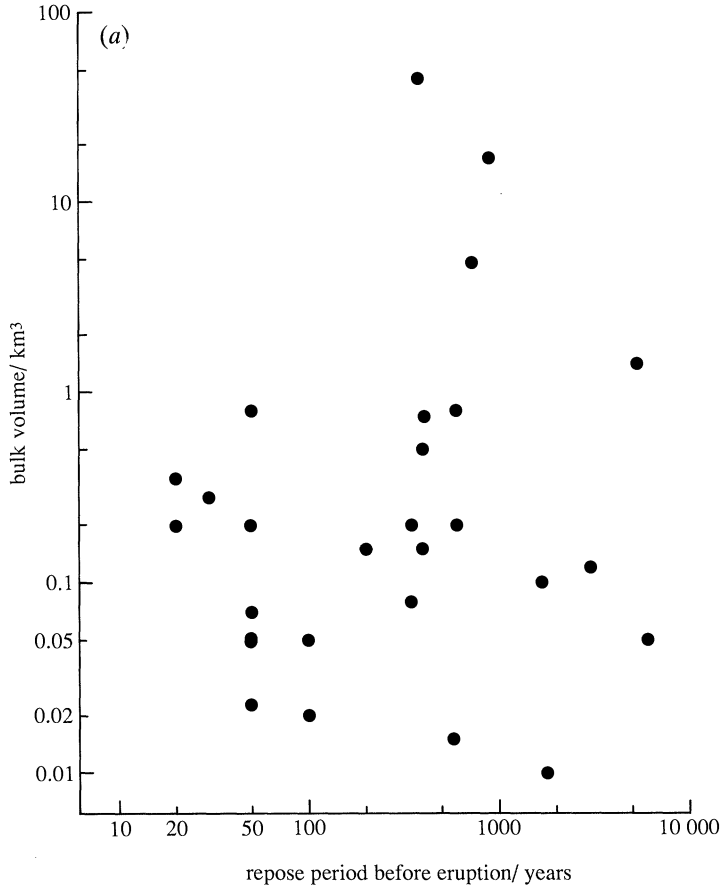


Figure 53. Plots of the volumes of the post-Oruanui eruptions at Taupo against the repose periods (calibrated timescale) (*a*) before that eruption.

### (*d*) *Time-predictable volcanism at Taupo?*

A detailed sequence of eruption volumes and ages begs the question whether volumes are consistently related to repose period, both to suggest an underlying causal relationship and to predict the size and/or return interval of the next eruption (Bacon 1982). This has been attempted by Froggatt (1982) but his conclusions about the size and timing of the next Taupo eruption are questionable because the graph used (his fig. 5) would yield a strong positive correlation even with wholly random values of eruption volume and repose intervals simply because cumulative values are used. A better alternative is to plot eruption size versus the preceding or following repose period (figure 53); in either case a strong correlation would imply a uniform magma supply rate and a uniform proportion of the magma chamber being evacuated, with eruptions being triggered by one of the following.

1. Rupture of an overpressured chamber; the eruption volume reflects the repose period required to build up the overpressure, i.e. volumes are related to the preceding repose period.

2. Eruption from a weak chamber that ruptures as soon as it is filled; the

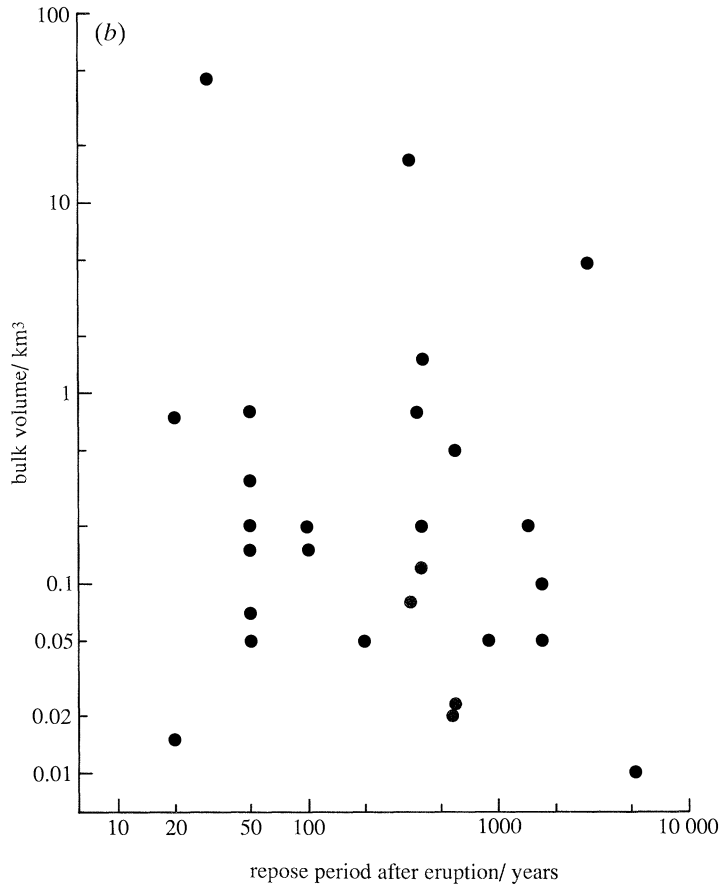


Figure 53. Plots of the volumes of the post-Oruanui eruptions at Taupo against the repose periods (calibrated timescale) (*b*) following that eruption.

eruption volume represents what can be evacuated from the chamber and thus controls the time period before the chamber re-fills, i.e. the repose period is proportional to the size of the preceeding eruption.

However, the Taupo data show no clear relationships between eruption volumes and before subsequent repose periods (figure 53). Unfortunately the number of eruptions is inadequate to determine whether the behaviour is deterministically chaotic or truly random (cf. Sornette *et al.* 1991). An overall eruption rate at Taupo can be calculated over any time period simply by dividing cumulative volume by elapsed time, but the relationships expressed in figures 51–53 imply that such an eruption rate may be misleading when used to predict either when the next eruption will occur, or the size of the next eruption, regardless of when it occurs.

Geochemical studies of the post-Oruanui eruptives at Taupo have demonstrated how compositionally uniform they are from Unit B onwards (Ewart 1963, Dunbar *et al.* 1989*a*; A. Sutton, personal communication), with maximum variations of 10–15 relative % through time. These data could be interpreted in terms of either a uniform source region, or that the magmas were erupted from a chamber of

remarkably uniform composition of such a size that the volumes removed were insufficient to tap through any hypothetical compositional zonation (cf. Smith 1979; Hildreth 1981). Data from Unit S suggest that this eruption occurred from a flat-lying discoidal magma body of thickness (O) 350 m and radius (O) 3.5 km, and that most of this magma body was ejected during the eruption (Blake *et al.* 1992). If eruption S is representative in terms of the proportion of the magma chamber that was ejected, then the hypothesis of the uniform source region is more favoured to explain the uniformity in Taupo compositions.

The magma source in the Taupo Volcanic Zone (TVZ) is poorly constrained, but current models consider it to be a deep (*ca.* 5 kb) complex system in which primitive mafic melts hybridize with fused material from intrusions of the Miocene-Pliocene Coromandel arc and differentiate to yield high-silica magmas (Conrad *et al.* 1988; Corlett *et al.* 1990; Cole 1990). During the whole 1.6 Ma lifetime of the TVZ by far the dominant proportion of rhyolite has been erupted as large welded ignimbrites or their phreatomagmatic equivalents with individual bulk volumes of 100 to more than 1000 $km^3$ (Wilson *et al.* 1984), the latest being the Oruanui eruption at Taupo. Work in progress by B. F. Houghton and the author on the chronology of these large events implies that they are more regularly spaced in time (averaging one per 40–60 000 years) and have to be included in any assessment of the steady-state condition for the zone as a whole. Thus on the timescale considered in this paper, although the eruptions concerned may represent devastating events (especially Y) they represent inter-caldera (in time) and intra-caldera (in space) activity when placed in context in the whole TVZ.

### (*e*) *Eruption styles*

The sequence of deposits shows a wide variation of eruptive styles and behaviour. Variables noted in the deposits include (i) the dispersal characteristics of beds, subunits, or units, (ii) the continuity or otherwise of eruptions, (iii) the presence or absence of pyroclastic flow deposits, (iv) the relative abundances and stratigraphic positions of water-flushed material (in most cases reflecting magma-water interaction at vent), (v) the vesicularity spectrum of the juvenile component, and (vi) the relative proportions of juvenile to foreign material in the lithic fraction.

With each variable, there is a spectrum of behaviour which sheds light on aspects of the eruption dynamics.

#### (i) *Dispersal characteristics and eruption column heights*

Two techniques are available to quantify the dispersal of fall deposits (Walker 1973; Pyle 1989). By using plots of ln(thickness, or maximum clast size) against $\sqrt{\text{area}}$, three parameters can be defined for most of the fall deposits (table 3).

1. The dispersal index ($I_d$) of Walker (1973), where $I_d$ is the area enclosed by the $T = 0.01T_{max}$ isopach ($T_{max}$ is the maximum thickness, obtained here by extrapolation).

2. The thickness decay constant ($b_t$) of Pyle (1989), where $b_t$ is the average distance over which the thickness diminishes by one half.

3. The grainsize decay constant ($b_c$) of Pyle (1989). In this case, $b_c$ is the average distance over which maximum pumice or lithic sizes (see § 1*c*(iii)) diminish by one half.

Most of the Taupo fall units are plinian in dispersal, but it is not feasible to

Table 3. *Summary of dispersal parameters for post-Oruanui pyroclastic deposits at Taupo volcano*

(For definitions of parameters, see text. Data are inadequate to define dispersal parameters for Units Ψ, A and W.)

| deposit | $I_d$/km$^2$ | $b_t$/m | | pumice $b_c$/m | lithic $b_c$/m |
|---|---|---|---|---|---|
| Y5 | 40900 | 17200 | | 17300 | 11300 |
| Y4 | 1540 | — | | — | — |
| Y3 | 7200 | 5700 | (proximal) | — | — |
| | | 10400 | (distal) | — | — |
| Y2 | 5500 | 5500 | (proximal) | 6100 | 4800 |
| | | 15100 | (distal) | | |
| Y1 | 140 | — | | — | — |
| X | 6200 | 4400 | (proximal) | 8000 | 8900 |
| | | 8900 | (distal) | | |
| V | 4600 | 3600 | (proximal) | 6400 | 5400 |
| | | 8800 | (distal) | | |
| U | 2200 | 4000 | | — | — |
| T | 2400 | 4100 | | — | — |
| S1 plus S2 | 16400 | 7700 | (proximal) | — | — |
| | | 27500 | (distal) | | |
| S2 | 16900 | 8100 | (proximal) | 10500 | 9300 |
| | | 27200 | (distal) | | |
| S1 | 16300 | 7300 | (proximal) | 12100 | 10700 |
| | | 28500 | (distal) | | |
| R | 1300 | 3100 | | 3300 | 3400 |
| Q | 7200 | 7200 | | 6400 | 7000 |
| P | *ca.* 3900 | *ca.* 5300 | | — | — |
| O | *ca.* 2700 | *ca.* 4400 | | *ca.* 7700 | *ca.* 3800 |
| N | 1800 | 3600 | | 3900 | 4100 |
| M | 4200 | 5500 | | 4300 | — |
| L | 1100 | 2800 | | — | — |
| K | 5200 | 4900 | (proximal) | — | — |
| | | 7400 | (distal) | | |
| K2 | 4100 | 5500 | | 12 000 | 6200 |
| K1 | 1900 | 3700 | | 6500 | 7700 |
| J | *ca.* 1700 | *ca.* 3500 | | — | — |
| I | *ca.* 3000 | *ca.* 4600 | | — | — |
| H | 1900 | 3700 | | — | — |
| H1 | 4200 | 5500 | | 5900 | 4500 |
| G | 5200 | 6100 | | *ca.* 6000 | *ca.* 5900 |
| G1 | 2300 | 4100 | | — | — |
| F | 890 | 2500 | | — | — |
| E3 | 12100 | 10200 | | 11600 | 8700 |
| E1 | 4200 | 5500 | | 6800 | 6200 |
| D | 2200 | 4000 | | — | — |
| C | 7300 | 7300 | | — | — |
| C2 | 8200 | 7700 | | — | — |
| C1 | 5000 | 6000 | | 7100 | 6500 |
| B | 4700 | 4700 | (proximal) | — | — |
| | | 6700 | (distal) | | |
| B4 | 4700 | 5800 | | 5000 | 4800 |
| B3 | 1600 | 3400 | | — | — |
| B2 | 3500 | 5000 | | — | — |
| B1 | 1300 | 3100 | | 3000 | 3100 |
| Ω | 860 | 2500 | | — | — |

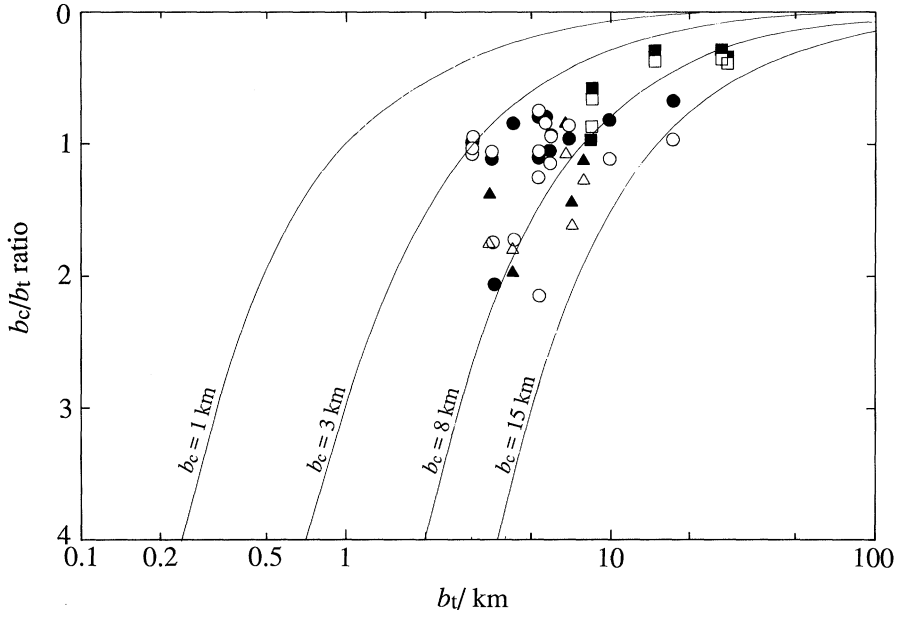


Figure 54. Plot of parameter $b_t$ against the $b_c/b_t$ ratio, after Pyle (1989), showing values where they can be defined for post-Oruanui eruptions at Taupo (data values from table 3). Open and closed symbols represent $b_c$ values defined from measurements on pumice and lithic clasts, respectively (see text), circles are from deposits with a single $b_t$ value; where separate proximal and distal $b_t$ values were defined, the triangles denote proximal data and squares distal data.

represent them on a $I_d$–$F$ plot (where $F$ is the mass % of the deposit less than 1 mm on the dispersal axis where $T = 0.1T_{max}$; Walker 1973) for two reasons. First, the variably water-flushed nature of many units means that the $F$ value may vary widely between otherwise similar units because of local depositional conditions. Second, many of the tephras are not preserved out to their $T = 0.1T_{max}$ isopachs. However, if it is accepted that the maximum-clast-size data can be used to derive $b_c$ values then many deposits can be plotted on a figure of $b_t$ against $b_c/b_t$ (figure 54). Note that $b_c$ values derived from $P_m$ and $L_m$ data often differ; in most cases this is apparently due to the increasing density of pumice clasts with decreasing size so that $(b_c)_{pumice} > (b_c)_{lithic}$.

Isopleth data can in some examples be used to infer maximum or sustained eruption column heights using the method of Sparks & Carey (1986). Results are summarized in figure 55, where column heights are plotted versus the bulk volume of eruptions (cf. Carey & Sigurdsson 1989).

(ii) *Eruption continuity*

This term is used to describe whether an eruption represents continuous activity or whether short time breaks (weeks or less) can be inferred. Evidence for time breaks of the order of hours to tens of hours is given by widespread but fine-grained ash beds which are interpreted (following Fierstein & Hildreth 1992) as representing ash settling out when no significant eruption column was present. Longer time breaks are inferred from erosion between fall units; the best and probably the longest example of this being the gullying between Y3 and Y4 which may represent a period of up to a few weeks (Walker 1981*b*). Otherwise, most of

the eruptions appear to have been continuous and hence occupied hours to tens of hours by analogy with historic eruptions. In a few cases (notably D) the fine grainsize of a deposit coupled with its wide dispersal suggests that it represents the product of multiple but weak explosions. In all such deposits, the abundances of dense to non-vesicular juvenile material suggest that they accompanied lava extrusion which may have been prolonged for weeks to months.

(iii) *Ignimbrites*

Four ignimbrites are found in the post-Oruanui sequence, associated with the three largest eruptions. Three of these ignimbrites are demonstrably (S3, Y6) or inferred (E5) to be intraplinian and generated by partial collapse of a flourishing (Y6) or waning (E5, S3) plinian column. With E5 and S3 this may reflect vent widening and resulting column instability towards the close of an eruption, but in Y6 the flows are demonstrably coeval with almost the entire history of the plume generating the Y5 'ultraplinian' fall deposit.

The fourth ignimbrite is Y7, the Taupo ignimbrite itself, which is exceptional in its volume (more than 20 times those of the other three) and emplacement violence. The formation of its parental flow as a result of incipient caldera collapse is supported by field evidence and inferred magma-chamber conditions (Wilson & Walker 1985; Dunbar *et al.* 1989*b*), and so on that basis can be considered unusual. However, in any future eruption in which a comparable-sized body of magma is available, a repeat performance is possible if the only requirement is for caldera collapse to occur during rather than after the eruption.

(iv) *Magma–water interaction*

There two end-members to a spectrum of magma–water interaction in fall eruptions.

1. Well-sorted pumice fall deposits, generated by 'dry' activity driven solely by internal gas sources, i.e. volatiles dissolved in the magma (Walker 1980, 1981*a*). Lithics are exclusively foreign.

2. Very poorly sorted fall deposits, generated by 'wet' activity driven solely by steam generated by boiling of external water (Self & Sparks 1978; Walker 1981*b*). Lithics are exclusively juvenile.

With few exceptions (e.g. G), evidence for wet deposition is taken as indicative of 'wet' conditions at the vent on the basis that the amounts and/or complexities of the water-flushed beds generally increase towards the vent. A spectrum can then be established on the grounds of the continuity and persistence of 'wet' activity (table 4). Two points are noticeable.

1. Only a few units (B2, E1, H1, S1, Y5) represent consistently 'dry' activity which was evenly sustained or changed in vigour slowly. Most of the medium-sized fall units show strongly fluctuating activity (notably V and X), with 'wet' and 'dry' phases alternating on such a fine scale (e.g. figures 43, 48, section 2345) that conditions must have switched on a timescale of the order of a few minutes. A similarly rapid fluctuation, but between more- and less-'wet' activity can also be inferred within some dominantly 'wet' deposits, as seen in the fine-scale bedding in Y3 and Y4 (Walker 1981*b*).

2. Several eruptions start off with mostly dry activity and become progressively 'wetter' (notably $\Psi$, $\Omega$, B, C, E, G, H, K and X). In some cases this could be due to subsidence of an initially subaerial vent area during the eruption, and is

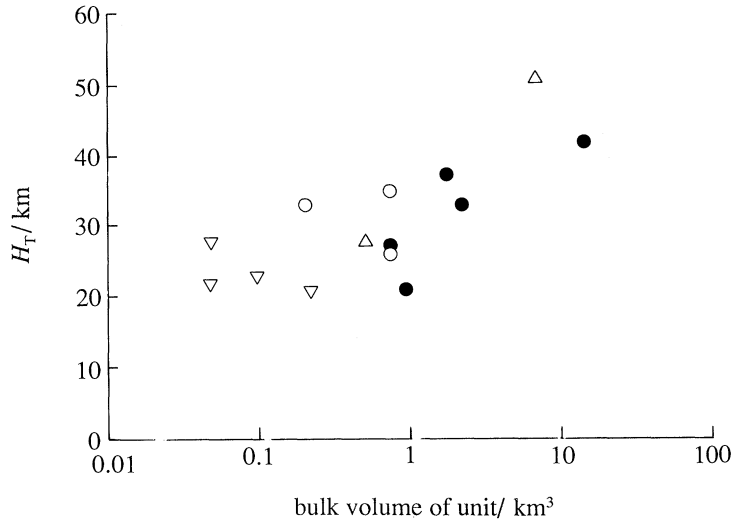


Figure 55. Plot of eruption column heights, inferred from isopleth data using the method of Sparks & Carey (1986), versus the bulk volume of eruptions. Symbols are: filled circles, sustained columns; open circles, episodically generated columns to similar heights; upright triangles, column building up to the maximum given; inverted triangles, column declining from the maximum given.

favoured for Ψ, B, K and X because the switch from 'drier' to 'wetter' activity accompanied an increase in eruptive power (as measured by maximum clast sizes). In other cases it could reflect the earlier, more powerful activity holding back lake water, then water entering the vent as the column weakened, and this is considered likely for Units Ω, C, G and H because of an accompanying diminution in maximum clast sizes and/or change in lithic lithologies (see § 3*e*(vi), below). In E the situation is complicated by a change in vent areas during the eruption.

(v) *Juvenile clast vesicularity*

The vesicularity of the juvenile clasts in a deposit is a useful tool to examine when the vesiculation history of the magma was interrupted by fragmentation (Houghton & Wilson 1989). Houghton & Wilson published detailed data for the deposits of eruption Y and comparisons with these units and others allow a spectrum of clast vesicularities to be constructed for the Taupo sequence (table 5) with Y4 and Y5 as end members.

1. Y5 is dominated by uniformly highly- to extremely vesicular pumice, and the eruption is inferred to have been driven solely by internal volatiles, with no signs of magma-water interaction. Lithics are overwhelmingly foreign.

2. Y4 is dominated by non- to poorly vesiculated juvenile material and is interpreted to represent material that had largely de-gassed before magma–water interaction. In this case, essentially all the volatiles involved represent external water which was flashed to steam, and foreign lithics are rare.

The spectrum observed in the other Taupo deposits matches that inferred for the peralkaline rhyolite sequences on Mayor Island (Houghton & Wilson 1986, 1989; see table 5), but the sizes of eruptions at Taupo are typically an order of magnitude larger.

Table 4. *Summary of the spectrum of magma–water interaction in all deposits from post-Oruanui eruptions at Taupo volcano*

| categories of activity | deposits |
|---|---|
| purely 'dry'; no evidence for any magma–water interaction | B2, E1, H1, S1 |
| mostly 'dry', but with episodic premature deposition of fine ash by clumping or water flushing; this may or may not be due to magma:water interaction (some examples are inferred to be due to passage of a weather system) | Ψ1, B3, C2a, C2c, G1, M, S2, X1, Y5 |
| mostly 'dry', but with episodic water-flushing of fine ash; an increase in the degree of flushing towards vent is taken to indicate this is due to magma–water interaction: | |
| (i) at the start of the eruption | B1 |
| (ii) during the eruption | B4 (northeast lobe), E3, K1, Y2 |
| (iii) at the close of the eruption | C1, G2, R |
| mostly or completely deposited 'dry' and lacking an abundant fine ash matrix, but evidence (e.g. high juvenile clast densities) for magma:water interaction driving explosive activity | C2b, D, W, X3 (part) |
| comparable proportions of material deposited 'dry' and water-flushed; evidence for rapid, reversible changes in the degree of magma–water interaction | E2, H2, K2, N, O, P, X2, V |
| mostly to entirely deposited by water flushing; eruption dominated by magma–water interaction with comparable volumes of magma and water | Ψ2, Ω, A, B4 (southeast lobe), E4, F, I, J, L, Q, T, U, X3 (part), Y1, Y3, Y4 |

(vi) *Lithic lithologies*

The lithologies of the dense-clast fractions of the fall deposits at Taupo are notable for two reasons.

First, although lithics in the Oruanui deposits are of many lithologies (among them andesite lava, welded tuff, metasediments, lacustrine sediment (some syn-eruptive), low to high grade (epidote-bearing) hydrothermally altered clasts, and fluvially rounded pebbles to cobbles), those in the post-Oruanui sequence are dominantly types of rhyolite lava (notably in Y7). This suggests that although the Oruanui eruption (with its accompanying caldera collapse) excavated lithics from the surface down to depths of at least 2–3 km (from comparison of the hydrothermally altered lithics with their equivalents in present-day nearby geothermal fields (e.g. Henley & Hedenquist 1986), the younger eruptions have excavated only to shallower levels (most lithics are fresh, or show low-grade hydrothermal alteration). The contrast in lithic types between the Oruanui and younger deposits is most marked SE of Lake Taupo where the lithic-rich facies in the Oruanui ignimbrite typically contain more than 30–40 mass % andesite and less than 10 mass % rhyolite, while lithic-rich material in Y7 contains more than 70% rhyolite (Chernet 1987). It is thought that the younger eruptives are excavating lithics from rhyolite lavas which must realistically have been extruded after the Oruanui

Table 5. *Summary of the spectrum of juvenile clast vesicularities in fall deposits from post-Oruanui eruptions at Taupo volcano*

| categories of juvenile clast vesicularity | deposits | published examples (Houghton & Wilson 1989) |
|---|---|---|
| mode of highly to extremely vesicular pumice, with a narrow range of vesicularities. Magma fragmented purely by rupturing of bubbles | Ψ1, B1, B2, B3, B4 (northeast lobe), C1, E1, E2, E3, G1, G2a, H1, S1, S2, X1, Y2, Y5 | Y2 (Hatepe plinian pumice) Y5 (Taupo plinian pumice) Oira cone (Mayor Island) |
| mode of moderately to highly vesicular pumice, with a moderate range of vesicularities. Magma fragmented both by rupturing of vesicles and by quenching on interaction with water. Lithic clasts dominated by foreign lithologies; open vent activity | Ω, B4a (southeast lobe, earlier stages), E4, K2, R, V (earlier stages), X2, Y1, Y3 | Y1 (initial ash) Y3 (Hatepe ash) |
| mode of moderately to highly vesicular pumice, with a moderate range of vesicularities. Magma fragmented both by rupturing of vesicles and by quenching on interaction with water. Lithic clasts dominated by juvenile obsidian; activity accompanying lava extrusion | A, B4a (southeast lobe, later stages), G2b, K1, L, U, V (later stages) | |
| mode of poorly to moderately vesicular juvenile material, with a wide range of vesicularities. Magma fragmented mainly by quenching on interaction with water. Lithic clasts dominated by juvenile obsidian; activity accompanying lava extrusion | Ψ2, B4b (southeast lobe), C2, D, F, H2, M, N, O, P, Q, T, X3 | Ruamata cone (Mayor Island) |
| mode of non- to poorly vesicular juvenile material, with a moderate to wide range of vesicularities. Foreign lithic clasts are rare; explosive activity may be in place of, or be followed or accompanied by lava extrusion | I, J, W, Y4 | Y4 (Rotongaio ash) Opo Bay cone (Mayor Island) |

eruption. That this is true even for early post-Oruanui events (e.g. Ω and B) suggests there may have been significant rhyolitic effusive activity between *ca.* 26 500 and 12 000 calibrated years BP in the area occupied by Lake Taupo for which no co-eruptive pyroclastic material is known. Second, the rhyolite clasts which dominate lithic assemblages in the post-Oruanui deposits can be divided into two types: (1) inferred juvenile: grey to black, angular, fresh glassy obsidian, and (2) inferred foreign–hydrated obsidian, devitrified lava (sometimes flow-banded and/or spherulitic), usually fresh, but sometimes brown and hydrothermally altered.

The relative proportions of these two groups suggest another spectrum, of lithic types, with two end-members.

Table 6. *Summary of the spectrum of lithic lithologies in deposits from post-Oruanui eruptions at Taupo volcano*

(The lithic lithologies refer to those dense clasts which are visible in hand specimen. See text for discussion.)

| categories of lithic assemblages | deposits |
|---|---|
| almost entirely foreign lithologies. Juvenile obsidian fragments rare ($\ll 0.1\%$) and small ($< 1$ cm) | Ψ1, Ω, B1, B2, B3, C1, E2, E3, E4, E5, S1, S2, S3, X1, Y2, Y5, Y6, Y7 |
| foreign lithologies dominate over juvenile obsidian | B4 (northwest lobe), B4a (southeast lobe, lower parts), E1, G1, G2 (lower parts), H1, R, X2, Y1, Y3 |
| sub-equal proportions of foreign lithologies and juvenile obsidian | B4a (southeast lobe, upper parts), C2, V (lower parts) |
| juvenile obsidian dominates over foreign lithologies | Ψ2, A, B4b (southeast lobe), G2 (upper parts), H2, K1, M, N, O, P, Q, V (upper parts), X3 |
| almost entirely or completely juvenile obsidian | D, F, I, J, L, T, U, W, Y4 |

1. Lithics that are purely foreign. This is inferred to reflect open-vent activity, in which the magma is vesiculating to form pumice (i.e. 'dry' activity), and the walls of the conduit are exposed to and eroded by the erupting pyroclastic mixture.

2. Lithics that are purely juvenile obsidian. By analogy with other deposits (e.g. Heiken & Wohletz 1987) such an assemblage is interpreted to reflect a closed-vent system, in which explosions (usually driven by magma–water interaction) are occurring through extruding lava.

The Taupo deposits cover the complete spectrum between these two extremes (table 6), except that deposits dominated by foreign lithologies usually have a trace fraction (very much less than 0.1 mass %) of less than 5–10 mm obsidian chips. Volatile content and D/H isotopic determinations on these chips (Dunbar 1985) imply that these are quenched magma fragments which did not vesiculate, perhaps due to rapid chilling. In the Taupo deposits there is a correspondence between eruption size and the lithic assemblage; smaller eruptions are dominated by juvenile obsidian, while the largest eruptions (E, S and most of Y) are essentially devoid of juvenile obsidian. In between there is a group of intermediate-sized deposits (0.2–1.4 $km^3$ bulk volume) which start out obsidian poor, then gradually or suddenly become obsidian-dominated. This systematic change in lithic types (and concomitant juvenile-clast density populations; § 3*e*(v), above) is a feature common to many explosive eruptions, reflecting the upwards concentration of volatiles in a magma body (e.g. Hildreth 1981). However, the nature and relative volumes of explosive versus effusive activity (which can only be inferred for D, F and W), and the spectrum of juvenile clast densities reflect many influences (e.g. Eichelberger *et al.* 1986; Heiken & Wohletz 1987; Houghton & Wilson 1986, 1989) which cannot be quantified further with the data available here.

### (*f*) *Vent positions and their tectonic control*

The vent positions compiled from this work (and Walker 1980, 1981*a*, *b*, for eruptions S and Y) are noticeably concentrated in a linear area (figure 56) within a 55 km long lineament previously postulated as a fundamental structure at Taupo (Wilson *et al.* 1984). Vents which fall outside this lineament are close enough to two other young structural elements identified by bathymetric or seismic evidence, the Horomatangi Fault (E1) and the Northern Bays Fault ($\Omega$, O (and P?)), to suggest some causal relationship. The Horomatangi Fault is one of several NW-trending structural elements in the central TVZ (Wan & Hedenquist 1981), and the opening pyroclastic fall phases of the Oruanui eruption occurred from a vent close to or on this fault (figure 56; Self 1983; C. J. N. Wilson, unpublished data). The Northern Bays Fault is an arcuate caldera-bounding fault (Northey 1983) now interpreted (Wilson *et al.* 1984, 1986) as dating from the Oruanui eruption.

Of the vents along the NNE lineament, nine (32%), including the two most voluminous events (S and Y) occur at or within *ca.* 3 km (i.e. approximately the error in estimating positions) of the modern Horomatangi Reefs which lie at the intersection of the Horomatangi Fault and the lineament. Thus on a simple probabilistic basis this is the most likely vent area for the next eruption at Taupo, especially if eruptive sites are weighted by their volume.

Taupo is one of the best examples of an 'inverse volcano' (Walker 1984), where the build-up of eruption products around the vent has been insufficient to counterbalance the effects of subsidence due to magma withdrawal and/or regional extension. The combined volumes of the post-Oruanui eruptions are not less than 73 $km^3$ and (depending largely on the volumes attributed to S and Y) may be as high as 145 $km^3$. Piled in a heap with average 15° slopes, like many andesite composite volcanoes, this would form a cone roughly 13 km (16 km) across and 1.7 km (2.0 km) high, depending on whether the 73 (or 145) $km^3$ volume is taken. Instead of forming a cone though, the land surface (i.e. the floor of Lake Taupo) around Horomatangi Reefs is at its lowest point for over 40 km in any direction (figure 1).

Several authors, notably Cole and co-workers (e.g. Cole 1990 and references therein) have divided the Taupo Volcanic Zone up into an eastern andesite-dacite arc and a western back-arc or marginal basin where rifting is occurring. In the Taupo area, the supposed arc is represented by Tauhara (a pre-Oruanui dacite dome complex) and the marginal basin by an ill-defined 'Taupo Centre' situated over N Lake Taupo. This distinction is not supported by the evidence in this paper, as Tauhara and other andesite-dacite centres further to the NE are on the same lineament as that controlling most of the late Quaternary rhyolitic vents described here (Wilson *et al.* 1984; figure 56).

### (*g*) *Taupo volcano*

#### (i) *Lake Taupo*

The modern Lake Taupo covers 606 $km^2$ and has a volume of *ca.* 60 $km^3$. Several lines of evidence suggest that the lake fills a complex caldera and volcanotectonic collapse structure largely created in conjunction with the Oruanui eruption.

(i) The bulk volume of extra-caldera Oruanui eruptives (not less than 800 $km^3$) alone would suggest a collapse area of some hundreds of square kilometres ac-

companied this event (cf. Smith 1979), and all vents for the Oruanui eruption were situated beneath the modern lake (Self 1983).

(ii) The presence of coarse lithic-rich lag breccias in the Oruanui ignimbrite at several localities around the N, W and E margins of the lake (Self 1983; Houghton & Wilson 1986).

(iii) The youthful appearance of the cliffs forming the N and W margins of the lake; cliff edges are sharply defined and nick points marked by waterfalls or rapids are present on most streams draining into the lake. These features are incompatible with the western margin of the lake being the caldera for the 330 000 years BP Whakamaru-group ignimbrites, the immediately previous caldera-forming eruption in this area.

Following on from this, other evidence suggests that after an immediate post-Oruanui high stand of the lake represented by a fossil cliff line and associated shoreline sediments at 495 m above sea level (asl ) at several localities W of the lake (e.g. 7536 2792), the lake has not risen by more than 33 m above its modern level of 357 m asl during the past *ca.* 20 000 years.

1. The delta of the Tongariro River at the south end of the lake is graded to roughly the modern level, yet much of the fan surface is pre-1800 years BP in age from the covering tephra stratigraphy.

2. Lacustrine sediments only occur below 390 m asl , and parts of the pyroclastic sequence described here rest on palaeosols at localities within 10 m of the modern lake level (see below). Furthermore, sparker seismic surveys (Northey 1983) show features such as alluvial fans graded to lower levels and notches in the lake floor topography to suggest that some significantly lower lake levels also occurred in the time period considered here.

The lake outlet is cut into Oruanui ignimbrite, and graded to a resistant horizon of silicified, indurated volcaniclastic sediments and (?)primary ignimbrite at Huka Falls, 6 km downstream. High lake stands at 495 m and 390 m reflect filling of the lake after the major Oruanui and Y eruptions to the levels where pyroclastic barriers were overtopped then destroyed. Any stands lower than the 357 m asl modern level require that either major differential warping has affected the relative level of the lake outlet, or that lower lake levels represented transient features.

At 7774 2676 a section exposes Units V, X and the base of Y about 6–10 m above modern lake level. V rests, with only localized penecontemporaneous reworking, directly on lacustrine sediments derived (from the abundance of streaky pumices) from S, suggesting that this site was on a beach. The top of V was slightly water-reworked (i.e. a renewed lake?) but good palaeosols then separate V from X, and X from Y. This sequence implies that lake levels fluctuated only slightly (reflecting choking of the outlet?), and were less than 10 m higher than the modern level, from 3550 to 1770 years BP (calibrated timescale).

(ii) *Comparison with Okataina volcano*

Okataina, some 120 km NNE of Taupo (figure 1) shows a distinctly different pattern of activity. During the past *ca.* 21 000 $^{14}$C years Okataina has produced nine rhyolitic and two basaltic eruptions (Nairn 1981, 1989), with repose periods between 600 and 3300 $^{14}$C years (Froggatt & Lowe 1990). The erupted volumes at Okataina are more uniform (though pyroclastic volumes may be overestimated, for the reasons given in § 3*b*, above), varying from 4 to 18 km$^3$ magma (Nairn

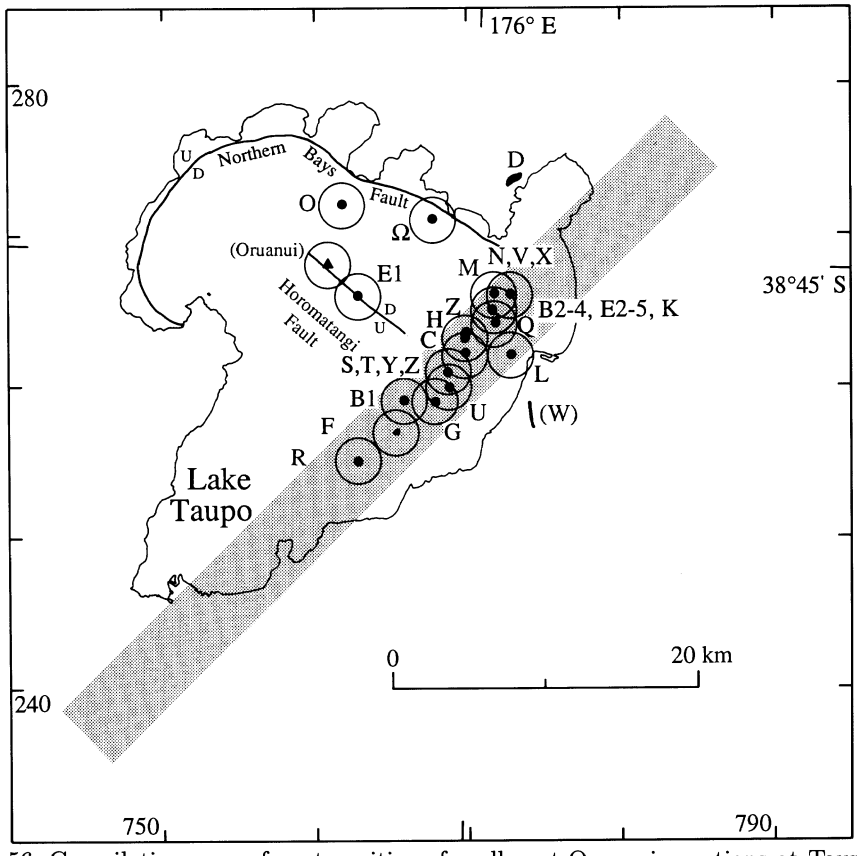


Figure 56. Compilation map of vent positions for all post-Oruanui eruptions at Taupo except those of Units Ψ, A, I, J, and P where the vent cannot be located. The stippled NNE–SSW band is the zone proposed by Wilson *et al.* (1984) as a deep-seated lineament controlling vent positions along the eastern side of Lake Taupo. The vent site marked Oruanui is that for the earliest fall deposits of that eruption, from Self (1983) and my unpublished data. Faults are from Wilson *et al.* (1984), after Northey (1983).

1981, 1989). Thus although the long-term eruption rates at both centres are broadly comparable, and both have their young vent locations controlled by large-scale linear structures, Taupo shows orders of magnitude greater variability in repose periods and eruption volumes.

(iii) *Current state*

Taupo is an area of frequent earthquakes and ground deformation accompanying regional extension (Grindley & Hull 1986). Use of the lake as a giant tiltmeter has enabled deformation around the lake shore (in essence the caldera rim) to be monitored (Otway 1986, 1989) and vertical movements of mm/month are common. However, the relationships between deformational patterns and regional tectonic activity versus the possible movement of magma are obscure. No large, high-level magma body is thought to exist beneath Taupo at present (in contrast to Okataina; Robinson *et al.* 1981; Rogan 1982), but this conclusion may not be soundly based, for three reasons.

1. No gravity data are available over Lake Taupo.

2. The great inferred thicknesses of pyroclastic material associated with and post-dating the Oruanui eruption would obscure any magnetic anomaly resulting from a magma body.

3. The resolution of the investigations means that magma bodies of modest dimensions (up to tens of cubic kilometres) could escape notice because of the ease with which seismic signals could be refracted around them.

The mapping of any magma bodies beneath Taupo is a pre-requisite for assessing the eruption potential of the volcano, and the current lack of data is a problem. If a high-level body is already in place, then the warning time before any future eruption may be short (days to months?), while if an eruption has to be preceded by the rise of a new magma batch from depth then precursor signals may occur for years to decades in advance. Another major problem is that the rise of magma to high levels is not necessarily an inevitable prelude to an eruption (cf. Mckee *et al.* 1989; Mori *et al.* 1989).

(iv) *Hazards and prediction*

The nature and extent of hazards and problems of eruption prediction at Taupo have been considered previously by Dibble *et al.* (1985) and Latter (1985, 1986). The new data in this paper modify many of these authors' conclusions. From this work and Wilson & Houghton (1993) there are three main conclusions.

1. There is a wide spectrum of eruptive volumes and repose intervals, and the size of any future eruption cannot be easily predicted.

2. The change in magma chemistry and form of the volcano after the Oruanui eruption means that only the post-Oruanui activity is strictly relevant to assessing future activity on a timescale which is of economic or social interest (i.e. the next 100 years).

3. Many eruptions in the past *ca.* 20 000 years would have caused relatively minor damage, but perceptions of the capability of the volcano are controlled by the unusually large and violent Y eruption.

## 4. Conclusions

Taupo volcano has erupted at least 28 times in the past *ca.* 25 000 years; more eruptions may have occurred (especially before 12 000 calibrated years BP) which are not documented, either because they were entirely effusive (cf. eruption Z) or their pyroclastic products were eroded during the glacial period. The volumes and repose periods vary by more than three and more than two orders of magnitude, respectively (if the Oruanui is included, volumes vary by four to five orders of magnitude, from 0.01 to 800 $km^3$).

Repose intervals and volumes considered separately follow consistent self-similar behaviour, yet there is an apparently random relationship between them. The repose period before or after any eruption is unrelated to the erupted volume, and the *ca.* 1740 year time break since the latest eruption cannot be used as a guide to when, or how large (or small), the inevitable next eruption at Taupo will be. The numbers of eruptions are inadequate to decide if this relationship could simply be the result of coupling between simple controls with different characteristic spatial and temporal scales, for example: (i) tectonic activity coupled to widening of this portion of the TVZ, (ii) viable lifetimes of high-level magma bodies, (iii) varying

proportions of the magma chamber which are ejected, or (iii) episodic supply of magma from a deeper source zone, or whether other, hidden controls are present.

The *ca.* 1740 year period since the latest eruption suggests that any new activity will involve a new body of magma. However, it is not known whether this body could already be present at high levels, or if it will have to first rise from deeper levels. If the first case applies, a new eruption could occur with little warning, whereas if the batch has to arise from its source zone it should be attended by significant seismic and tectonic precursors. In parallel with their wide variations in volume, the Taupo deposits display inter-linked spectra of characteristics which reflect wide variations in the degree and timing of: (i) vesiculation, (ii) interaction with the water of the penecontemporaneous Lake Taupo, and (iii) open- versus closed-vent activity. These variations mean that predicting the style and dynamics of the next eruption may be possible, but only if its volume can be predicted.

In terms of time and erupted volumes, the post-Oruanui record at Taupo may be considered as eruptive 'noise' superimposed on the more-regular longer-term (1.6 Ma) signal for the TVZ as a whole, where magma output is mostly expressed as greater than 100 $km^3$ eruptions (like the Oruanui) spaced at intervals of 40–60 000 years. However, volcanic 'noise' as spectacular and devastating as the Y eruption commands respect, and the problems of forecasting the scope and timing of the next eruption present formidable challenges.

I thank the Royal Society for continuing financial support, and the NERC for field support under grant GR3/7034. I am grateful for advice, comments and reviews from S. Blake, W. Hildreth, A. Hynes, C. P. M. A. Jaupart, D. M. Pyle, K. J. Wilson, and especially B. F. Houghton and R. S. J. Sparks.

## Appendix A. Type and reference sections for post-Oruanui deposits

This summarizes the type and reference localities for each deposit. Grid references are to the nearest 100 m in the New Zealand metric map grid. (TL, type locality; RL, reference locality.)

| | | |
|---|---|---|
| Unit Ψ | TL: 7704 2741 | Cutting, S side of Mapara Road, on bend (figure 2) |
| | RL: 7817 2750 | W wall of excavation for Taupo rubbish tip |
| Unit Ω | TL: 7708 2741 | Cutting, S side of Mapara Road, on gentle bend (figure 4) |
| Unit A | TL: 7798 2796 | Cutting at car park for upper lookout, Huka Falls (figure 6) |
| Unit B | TL: 7789 2729 | Cutting, S side of Highway 5, 400 m E of junction with Highway 1 (figure 7, loc. 2394) |
| | RL: 7767 2533 | Cutting, access road to Hinemaiaia C power house (figure 7, loc. 2425) |
| Unit C | TL: 7767 2533 | Cutting, access road to Hinemaiaia C power house (figure 9, loc. 2425) |
| | RL: 7649 2462 | Cutting, SE side of forestry road, 30 m NW of bridge over Tauranga-Taupo River |
| | RL: 7789 2729 | Same as TL for Unit B (figure 9, loc. 2394; figure 11) |
| Unit D | TL: 7789 2729 | Same as TL for Unit B (figure 9, loc. 2394; figure 11) |
| Unit E | TL: 7798 2729 | Cutting, S side of Highway 5, 1 km W of junction with Crown Road, opposite Terraces Hotel (figure 13, loc. 39) (also TL for Opepe Tephra (Vucetich & Pullar 1973)) |
| | RL: 7943 2584 | SE wall of gully 50 m NE of Highway 5 near Iwitahi village site (best locality for Units E3 and E4; figure 13, loc. 2309) |
| | RL: 7714 2479 | Cutting, crest of hill on Mission Bay Road (figure 13, loc. 733) |
| Unit F | TL: 7657 2506 | Cutting, Mission Bay Road, 1.2 km from junction with Highway 1 (figure 15) |
| Unit G | TL: 7739 2518 | NE side of cutting, Te Heu Heu Road, 400 m NW of junction with |

| | | |
|---|---|---|
| | | Opawa Road (figure 18, loc. 2379) |
| Unit H | TL: 7837 2556 | Cutting, disused logging track at W end of ridge, 150 m N of Southern Boundary Road (figure 20, loc. 2396) |
| Unit I | TL: 7798 2729 | As for TL of Unit E |
| Unit J | TL: 7742 2529 | Cutting, Opawa Road, 1.5 km N of junction with Te Heu Heu Road (figures 17*b*, 25, loc. 2380) |
| Unit K | TL: 7742 2529 | As for Unit J |
| Unit L | TL: 7742 2529 | As for Unit J (figures 17*b*, 27) |
| Unit M | TL: 7765 2786 | Cutting, W side of Poihipi Road, opposite large parking area (figure 29) |
| Unit N | TL: 7713 2737 | Cutting, N side Mapara Road, opposite entrance to house 'Tawelfa' (figure 31, loc. 2355) |
| Unit O | TL: 7713 2737 | As for Unit N |
| Unit P | TL: 7713 2737 | As for Unit N |
| Unit Q | TL: 7742 2529 | As for Unit J (figures 17*b*, 32) |
| Unit R | TL: 7642 2482 | SW wall, logging skid on NW side of Whataroa Road, 100 m from junction with Hingapo Road (figure 37) |
| Unit S | TL: 7899 2574 | Cut on High Level Road, proposed as new type locality by Froggatt & Lowe (1990) (no details given) |
| | RL: 7900 2580 | Prominent cutting on High Level Road, used as reference section by Walker (1981*a*) and Blake *et al.* (1992) |
| Unit T | TL: 7827 2600 | Cutting, N side of Rotoakui Road, 300 m E of junction with Straight Line Road (figures 39, 41, loc. 2397) |
| Unit U | TL: 7717 2551 | Cutting, S side of Te Heu Heu Road, on bend 900 m from junction with Highway 1 (figure 41, loc. 2378) |
| Unit V | TL: 7798 2729 | As for TL of Unit E (figure 43, loc. 39) (also TL for Whakaipo Tephra (Vucetich & Pullar 1973)) |
| | RL: 7774 2676 | Pumice pit cut into fossil shoreline cliff, 100 m E of Highway 1 (figure 43, loc. 2345) |
| Unit W | TL: 7739 2565 | Cutting, S side of Highway 1 (figures 45 and 46) |
| Unit X | TL: 7798 2729 | As for TL of Unit E (figure 48, loc. 39) (also TL for Mapara Tephra (Vucetich & Pullar 1973)) |
| | RL: 7774 2676 | As for reference locality of Unit V (figure 48, loc. 2345) |
| Unit Y | TL: 7773 2623 | Prominent cutting on Highway 1, *ca.* 1 km S of Waitahanui village |
| Y1 | RL: 7717 2551 | As for TL of Unit U (thickest known section of this subunit) |
| Y2 | RL: 7772 2547 | Cutting, Hinemaiaia Access Road, 600 m NW of junction with Maungatera Road |
| Y3 | RL: 7888 2572 | Cutting, High Level Road |
| Y4 | RL: 7773 2623 | As for TL; thickest known section of this subunit |
| Y5 | RL: 7916 2714 | Cutting, SW side of Luthridge Road (aka Off Highway 1); thickest known section of this subunit |
| Y6 | RL: 7773 2623 | As for TL; thickest known section of proximal early flow units |
| Y7 | RLs: various | See Wilson (1985) for localities showing facies of this subunit |
| Eruption Z | TL: 7674 2535 | Cutting, State Highway 1, between Bulli Point and Motutere Bay motor camp, where best example of floated giant pumice exposed (Wilson & Walker 1985, fig. 8) |

## Appendix B. New $^{14}$C age determinations from Taupo volcano

Twenty samples of charcoal from tephras or palaeosols in the post-Oruanui sequence have had age determinations made at the Radiocarbon Dating Laboratory at The University of Waikato, Hamilton, New Zealand. Of these age determinations, five gave anomalous values when compared with existing data and are discussed in the body of the paper. Preparation techniques used by the laboratory are given in Hogg *et al.* (1987); all samples had their activity determined on a Quantalus counter. Parameters are given as follows in order:

**Sample no.** Grid ref. Lab. no. $D^{14}C$ $\delta^{13}C$ Conv. age±error (yrs BP)

The sample number refers to the locality, whose grid reference is given. The $^{14}C$ depletion ($D^{14}C$ ) is expressed in per mille with respect to 95% NBS oxalic acid. The isotopic fractionation correction ($\delta^{13}C$) is expressed in per mille with respect to PDB. The conventional age is calculated using the Libby half-life of 5568 years, with isotopic fractionation correction, 95% NBS Oxalic acid as 'modern' with AD 1950 as the reference year, and with the assumption of constancy in atmospheric radiocarbon levels. Quoted errors are ± 1 s.d., based on counting statistics only.

**20** 7595 2469 1832 −412.0±4.5 −24.6 4270±70
Charcoal fragments in palaeosol above Unit J, about 5–7 cm below base of Unit R. Provides a maximum age for Unit R.

**719** 7727 2730 1833 −415.9±4.9 −26.7 4320±70
Charcoal fragments from zone of weathering between Units O and P. This age is considered to be somewhat old on the basis of other determinations and the palaeosol development.

**2352** 7790 2796 1834 −292.2±5.5 −27.3 2780±70
Charcoal fragments from palaeosol between Units V and X. Age suggests this is material killed by eruption V which has been bioturbated into the post-V soil.

**2355** 7713 2737 1835 −438.0±13.8 −25.5 4630±200
Charcoal fragments from ashy palaeosol immediately below Unit K. Provides a maximum age for Unit K (see also 2379, below).

**2379** 7739 2518 1837 −456.2±3.5 −25.3 4890±60
Charcoal fragments from palaeosol overlying Unit H and relicts of Unit I, and below Unit J (see figure 7*a*). Gives minimum age of Unit I and maximum age of Unit J.

**2380/C1** 7742 2529 1838 −529.4±4.0 −26.1 6050±70
Charcoal fragments from palaeosol between Units F and G; provides a minimum age for the former, maximum for the latter.

**2380/C2** 7742 2529 1839 −402.0±5.0 −26.3 4130±70
Charcoal fragments from palaeosol between Units N and Q (figure 17*b*); provides a minimum age for N and a maximum for Q.

**2380/C3** 7742 2529 1840 −340.3±3.7 −24.5 3340±50
Charcoal from the outermost 5–10 growth rings from a carbonized log incorporated in the S3 ignimbrite.

**2394** 7789 2729 1841 −336.0±3.6 −26.1 3290±50
Charcoal from the outermost 5–10 growth rings from a carbonized log incorporated in the S3 ignimbrite.

**2396** 7837 2556 1842 −499.9±7.3 −26.0 5570±120
Charcoal fragments from palaeosol between Units G and H; gives a maximum age for H and a minimum for G.

**2404** 7795 2566 1843 −335.2±8.4 −27.7 3280±110
Charcoal fragments from palaeosol overlying reworked material above Unit T and below Unit U. Age suggests this is remobilized charcoal killed at the time of eruption S (cf. 2454, below).

**2405** 7796 2565 1844 −546.7±3.0 −30.2 6360±60
Charcoal from a carbonized branch in the post-E palaeosol,

about 5 cm below the basal contact of Unit F.
Provides a maximum age for F.

**2407/C1** 7663 2461 1845 −405.3±6.4 −26.4 4180±90
Charcoal fragments in fossil gully fill in palaeosol between Units G and R, *ca.* 5 cm below basal contact of R.
Provides a maximum age for Unit R.

**2407/C2** 7663 2461 1846 −718.1±4.4 −23.4 10 150±130
Charcoal fragments along the contact between Unit B and the andesitic Te Rato Lapilli (Topping 1973). Interpreted to be material killed by eruption B and buried by the andesitic tephra, so providing an age estimate for Unit B.

**2413** 7657 2506 1847 −604.3±6.5 −24.9 7450±140
Charcoal fragments in post-E soil *ca.* 5 cm below the basal contact of Unit F; provides a maximum age for F.

**2444** 7837 2817 1848 −417.0±4.2 −25.4 4330±60
Charcoal fragments in ashy palaeosol developed on Unit M, 1–3 cm below basal contact of Unit N. Gives a minimum age for M and a maximum for N.

**2445** 7788 2529 1849 −302.0±4.8 −25.9 2890±60
Charcoal fragments in palaeosol between Units S and U (Unit T is missing); provides a maximum age for Unit U.

**2446** 7796 2525 1850 −406.3±3.5 −26.7 4190±50
Charcoal from a carbonized branch enclosed in Unit N; provides a direct age estimate for his eruption.

**2454** 7836 2567 1851 −305.8±5.3 −23.3 2930±70
Charcoal fragments from weak palaeosol developed on Unit T, below Unit U. Provides a minimum age for T and a maximum for U.

**2460** 7929 2819 1853 −329.7±4.7 −29.2 3210±60
Charcoal fragments dispersed through Unit U; other age data (2445 and 2454, above) implies this is anomalously old.

## References

Bacon, C. R. 1982 Time-predictable bimodal volcanism in the Coso Range, California. *Geology* **10**, 65–69.

Bard, E., Hamelin, B., Fairbanks, R. G. & Zindler, A. 1990 Calibration of the $^{14}C$ timescale over the past 30,000 years using mass spectrometric U–Th ages from Barbados corals. *Nature, Lond.* **345**, 405–410.

Baumgart, I. L. 1954 Some ash showers of the central North Island. *N.Z. Jl Sci. Technol.* B**35**, 456–467.

Becker, B., Kromer, B. & Trimborn, P. 1991 A stable isotope tree-ring timescale of the Late Glacial/Holocene boundary. *Nature, Lond.* **353**, 647–649.

Blake, S., Wilson, C. J. N., Smith, I. E. M. & Walker, G. P. L. 1992 Petrology and dynamics of the Waimihia mixed magma eruption, Taupo Volcano, New Zealand. *J. geol. Soc. Lond.* **149**, 193–207.

Carey, S. N. & Sigurdsson, H. 1989 The intensity of plinian eruptions. *Bull. Volcanol.* **51**, 28–40.

Carey, S. N. & Sparks, R. S. J. 1986 Quantitative models of the fallout and dispersal of tephra from volcanic eruption columns. *Bull. Volcanol.* **48**, 109–125.

Chernet, T. 1987 Lithic inclusions in the Taupo Pumice Formation. M.Sc. thesis, Victoria University of Wellington, New Zealand.

Cole, J. W. 1990 Structural control and origin of volcanism in the Taupo Volcanic Zone, New Zealand. *Bull. Volcanol.* **52**, 445–459.

Conrad W. K., Nicholls, I. A. & Wall, V. J. 1988 Water-saturated and -undersaturated melting of metaluminous and peraluminous crustal compositions at 10kb: evidence for the origin of silicic magmas in the Taupo Volcanic Zone, New Zealand, and other occurrences. *J. Petrol.* **29**, 765–803.

Corlett, G., Chappell, B. W., McCulloch, M. T. & Woodhead, J. D. 1990 The origin of rhyolite in the Taupo Volcanic Zone, New Zealand; a strontium, neodymium, lead and oxygen isotope study. Abstracts, Seventh International Conference on Geochronology, Cosmochronology and Isotope Geology, Geological Society of Australia Abstracts 27, 22.

Crisp, J. A. 1984 Rates of magma emplacement and volcanic output. *J. Volcanol. geotherm. Res.* **20**, 177–211.

Dibble, R. R., Nairn, I. A. & Neall, V. E. 1985 Volcanic hazards of North Island, New Zealand—overview. *J. Geodynamics* **3**, 369–396.

Dubois. J. & Cheminée, J.-L. 1988 Application d'une analyse fractale a l'étude des cycles eruptifs du Piton de la Fournaise (La Réunion): modele d'une poussiere de Cantor. *C.r. Acad. Sci. Paris, Serie II,* **307**, 1723–1729.

Dubois. J. & Cheminée, J.-L. 1991 Fractal analysis of eruptive activity of some basaltic volcanoes. *J. Volcanol. geotherm. Res.* **45**, 197–208.

Dunbar, N. W. 1985 Investigation of volatiles in rhyolitic magma chambers. M.S. thesis, New Mexico Institute of Mining and Technology, Socorro, New Mexico.

Dunbar, N. W., Hervig, R. L. & Kyle, P. R. 1989*b* Determination of pre-eruptive $H_2O$, F and Cl contents of silicic magmas using melt inclusions: examples from Taupo volcanic center, New Zealand. *Bull. Volcanol.* **51**, 177–184.

Dunbar, N. W., Kyle, P. R. & Wilson, C. J. N. 1989*a* Evidence for limited zonation in silicic magma systems, Taupo Volcanic Zone, New Zealand. *Geology* **17**, 234–236.

Eichelberger, J. C., Carrigan, C. R., Westrich, H. R. & Price, R. H. 1986 Non-explosive silicic volcanism. *Nature, Lond.* **323**, 598–602.

Ewart, A. 1963 Petrology and petrogenesis of the Quaternary pumice ash in the Taupo area, New Zealand. *J. Petrol.* **4**, 392–431.

Fierstein, J. & Hildreth, W. 1992 The plinian eruptions of 1912 at Novarupta, Katmai National Park, Alaska. *Bull. Volcanol.* **54**, 646–684.

Froggatt, P. C. 1981*a*. Karapiti Tephra Formation: a 10 000 years BP rhyolitic tephra from Taupo. *N.Z. Jl Geol. Geophys.* **24**, 95–98.

Froggatt, P. C. 1981*b* Review of Holocene eruptions from Taupo. In *Proceedings of tephra workshop* (ed. R. Howorth *et al.*), pp. 21–28. Geology Department Victoria University of Wellington Publication 20.

Froggatt, P. C. 1981*c* Motutere Tephra Formation and redefinition of Hinemaiaia Tephra Formation, Taupo Volcanic Centre, New Zealand. *N.Z. Jl Geol. Geophys.* **24**, 99–105.

Froggatt, P. C. 1981*d* Stratigraphy and nature of Taupo Pumice Formation. *N.Z. Jl Geol. Geophys.* **24**, 231–248.

Froggatt, P. C. 1981*e* Did Taupo's eruption enhance European sunsets? *Nature, Lond.* **293**, 491.

Froggatt, P. C. 1982 Review of methods of estimating rhyolitic tephra volumes: applications to the Taupo Volcanic Zone, New Zealand. *J. Volcanol. geotherm. Res.* **14**, 301–318.

Froggatt, P. C. & Lowe, D. J. 1990 A review of late Quaternary silicic and some other tephra formations from New Zealand: their stratigraphy, nomenclature, distribution, volume, and age. *N.Z. Jl Geol. Geophys.* **33**, 89–109.

Froggatt, P. C., Wilson, C. J. N. & Walker G. P. L. 1981 Orientation of logs in the Taupo ignimbrite as an indicator of flow direction and vent position. *Geology* **9**, 109–111.

Grindley, G. W. & Hull, A. G. 1986 Historical Taupo earthquakes and earth deformation. *R. Soc. N.Z. Bull.* **24**, 173–186.

Healy, J. 1964 Stratigraphy and chronology of late Quaternary volcanic ash in Taupo, Rotorua, and Gisborne districts. Part 1. Dating of the younger volcanic eruptions of the Taupo region.

*N.Z. Geol. Surv. Bull.* **73**, 7–42.

Heiken, G. & Wohletz, K. 1987 Tephra deposits associated with silicic domes and lava flows. *Geol. Soc. Am. Spec. Pap.* no. 212, 55–76.

Henley, R. W. & Hedenquist, J. W. 1986 Introduction to the geochemistry of active and fossil geothermal systems. *Monograph series on mineral deposits*, vol. 26, pp. 1–22. Berlin and Stuttgart: Gebrüder Borntraeger.

Hildreth, W. 1981 Gradients in silicic magma chambers: implications for lithospheric magmatism. *J. geophys. Res.* **86**, 10153–10192.

Hogg, A. G., Lowe, D. J. & Hendy, C. H. 1987 University of Waikato radiocarbon dates 1. *Radiocarbon* **29**, 263–301.

Houghton, B. F. & Wilson, C. J. N. 1986 A1: explosive rhyolitic volcanism: the case studies of Mayor Island and Taupo volcanoes. Excursion Guides, International Volcanological Congress, New Zealand, 1986 (ed. B. F. Houghton & S. D. Weaver). *N.Z. Geol. Surv. Record* **12**, 33–100.

Houghton, B. F. & Wilson, C. J. N. 1989 A vesicularity index for pyroclastic deposits. *Bull. Volcanol.* **51**, 451–462.

ISG (International Study Group) 1982 An interlaboratory comparison of radiocarbon measurements in tree rings. *Nature, Lond.* **298**, 619–623.

Kohn. B. P., Neall, V. E. & Stewart, R. B. 1981 Holocene tephrostratigraphy revisited at Tiniroto, North Island, New Zealand. In *Proc. of Tephra Workshop* (ed. R. Howorth *et al.*), pp. 60–66. Geology Department Victoria University of Wellington Publication 20.

Latter, J. H. 1985 Frequency of eruptions at New Zealand volcanoes. *Bull. N.Z. Soc. Earthquake Engng* **18**, 55–110.

Latter, J. H. 1986 Volcanic risk and surveillance in New Zealand. In *Volcanic hazards assessment in New Zealand* (ed. J. G. Gregory & W. A. Watters). *N.Z. Geol. Surv. Record* **10**, 5–22.

Lowe, D. J. 1986 Revision of the age and stratigraphic relationships of Hinemaiaia Tephra and Whakatane Ash, North Island, New Zealand, using distal occurrences in organic deposits. *N.Z. Jl Geol. Geophys.* **29**, 61–73.

Lowe, D. J. 1988 Stratigraphy, age, composition, and correlation of late Quaternary tephras interbedded with organic sediments in Waikato lakes, North Island, New Zealand. *N.Z. Jl Geol. Geophys.* **31**, 125–165.

Lowe, D. J. & Hogg, A. G. 1986 Tephrostratigraphy and chronology of the Kaipo Lagoon, an 11,500 year–old montane peat bog in Urewera National Park, New Zealand. *Jl R. Soc. N.Z.* **16**, 25–41.

Mandelbrot, B. B. 1982 *The fractal geometry of nature.* (468 pages.) San Francisco, California: W. H. Freeman.

McKee, C., Mori, J. & Talai, B. 1989 Microgravity changes and ground deformation at Rabaul caldera, 1973–1985. In *Volcanic hazards, assessment and monitoring* (ed. J. H. Latter), pp. 399–428. Berlin and Heidelberg: Springer-Verlag.

Mori, J., McKee, C., Itakarai, I., Lowenstein, P., de Saint Ours, P. & Talai, B. 1989 Earthquakes of the Rabaul seismo-deformational crisis September 1983 to July 1985: seismicity on a caldera ring fault. In *Volcanic hazards, assessment and monitoring* (ed. J. H. Latter), pp. 429–462. Berlin and Heidelberg: Springer-Verlag.

Nairn, I. A. 1981 Some studies of the geology, volcanic history, and geothermal resources of the Okataina Volcanic Centre, Taupo Volcanic Zone, New Zealand. Ph.D. thesis, Victoria University of Wellington, New Zealand.

Nairn, I. A. 1989 Sheet V16 AC – Mount Tarawera. Geological Map of New Zealand 1:50,000. Wellington, New Zealand: Dept of Scientific and Industrial Research.

Nairn, I. A. 1992 The Te Rere and Okareka eruptive episodes – Okataina Volcanic Centre, Taupo Volcanic Zone, New Zealand. *N.Z. Jl Geol. Geophys.* **35**, 93–108.

Northey, D. J. 1983 Seismic studies of the structure beneath Lake Taupo. Ph.D. thesis, Victoria University of Wellington, New Zealand.

Otway, P. M. 1986 Vertical deformation associated with the Taupo earthquake swarm, June 1983. *R. Soc. N.Z. Bull.* **24**, 187–200.

Otway, P. M. 1989 Vertical deformation monitoring by periodic water level observations, Lake Taupo, New Zealand. In *Volcanic hazards, assessment and monitoring* (ed. J. H. Latter), pp. 561–574. Berlin and Heidelberg: Springer-Verlag.

Palmer, J. G., Ogden, J. & Patel, R. N. 1988 A 426-year floating tree-ring chronology from *Phyllocladus trichomanoides* buried by the Taupo eruption at Pureora, central North Island, New Zealand. *Jl R. Soc. N.Z.* **18**, 407–415.

Pearson, G. W. & Stuiver, M. 1986 High-precision calibration of the radiocarbon timescale, 500–2500 BC. *Radiocarbon* **28**, 839–862.

Pearson, G. W., Pilcher, J. R., Baillie, M. G. L., Corbett, D. M. & Qua, F. 1986 High-precision $^{14}C$ measurement of Irish oaks to show the natural $^{14}C$ variations from AD 1840 to 5210 BC. *Radiocarbon* **28**, 911–934.

Pringle, M. S., McWilliams, M., Houghton, B. F., Lanphere, M. A. & Wilson, C. J. N. 1992 $^{40}Ar/^{39}Ar$ dating of Quaternary feldspar: examples from the Taupo Volcanic Zone, New Zealand. *Geology.* **20**, 531–534.

Pullar, W. A. & Birrell, K. S. 1973 Age and distribution of late Quaternary pyroclastic and associated cover deposits of the Rotorua and Taupo area, North Island, New Zealand. *N.Z. Soil Surv.* Rep. 1.

Pyle, D. M. 1989 The thickness, volume and grainsize of tephra fall deposits. *Bull. Volcanol.* **51**, 1–15.

Robinson, R., Smith E. G. C. & Latter, J. H. 1981 Seismic studies of the crust under the hydrothermal areas of the Taupo Volcanic Zone, New Zealand. *J. Volcanol. geotherm. Res.* **9**, 253–267.

Rogan, A. M. 1982 A geophysical study of the Taupo Volcanic Zone, New Zealand. *J. geophys. Res.* **87**, 4073–4088.

Scott, E. M., Baxter, M. S. & Aitchison, T. C. 1983 An assessment of variability in radiocarbon dating. In *Methods of low level counting and spectrometry,* pp. 371–392. Berlin: International Atomic Energy Agency.

Self, S. 1983 Large-scale phreatomagmatic silicic volcanism: a case study from New Zealand. *J. Volcanol. geotherm. Res.* **17**, 433–469.

Self, S. & Sparks, R. S. J. 1978 Characteristics of widespread pyroclastic deposits formed by the interaction of silicic magma and water. *Bull. Volcanol.* **41**, 196–212.

Smith, R. L. 1979 Ash-flow magmatism. *Geol. Soc. Am. Spec. Pap.* no. 180, pp. 5–27.

Sornette, A., Dubois, J., Cheminée, J.-L. & Sornette, D. 1991 Are sequences of volcanic eruptions deterministically chaotic? *J. geophys. Res.* **96**, 11931–11945.

Stothers R. B. & Rampino, M. R. 1983 Volcanic eruptions in the Mediterranean before AD 630 from written and archeological sources. *J. geophys. Res.* **88**, 6357–6371.

Stuiver, M. & Pearson, G. W. 1986 High-precision calibration of the radiocarbon timescale, AD 1950–500 BC. *Radiocarbon* **28**, 805–838.

Talbot, J. P. 1988 Grain morphology and origins of fine ash deposits from the 180 AD Taupo eruption, central North Island, New Zealand. M.S. thesis, University of Texas, Arlington, Texas.

Topping, W. W. 1973. Tephrostratigraphy and chronology of late Quaternary eruptives from the Tongariro Volcanic Centre, New Zealand. *N.Z. Jl Geol. Geophys.* **16**, 397–424.

Topping W. W. & Kohn, B. P. 1973 Rhyolitic tephra marker beds in the Tongariro area, North Island, New Zealand. *N.Z. Jl Geol. Geophys.* **16**, 375–395.

Vucetich, C. G. & Howorth, R. 1976*a* Late Pleistocene tephrostratigraphy in the Taupo district, New Zealand. *N.Z. Jl Geol. Geophys.* **19**, 51–69.

Vucetich, C. G. & Howorth, R. 1976*b* Proposed definition of the Kawakawa Tephra, the c. 20 000 yrs B.P. marker horizon in the New Zealand region. *N.Z. Jl Geol. Geophys.* **19**, 43–50.

Vucetich, C. G. & Pullar, W. A. 1964 Stratigraphy and chronology of late Quaternary volcanic ash in Taupo, Rotorua, and Gisborne districts. Part 2. Stratigraphy of Holocene ash in the Rotorua and Gisborne districts. *N.Z. Geol. Surv. Bull.* **73**, 43–81.

Vucetich, C. G. & Pullar, W. A. 1969 Stratigraphy and chronology of late Pleistocene volcanic ash beds in central North Island, New Zealand. *N.Z. Jl Geol. Geophys.* **12**, 784–837.

Vucetich, C. G. & Pullar, W. A. 1973 Holocene tephra formations erupted in the Taupo area and interbedded tephras from other volcanic sources. *N.Z. Jl Geol. Geophys.* **16**, 745–780.

Walker, G. P. L. 1973 Explosive volcanic eruptions: a new classification scheme. *Geol. Rundsch.* **62**, 431–446.

Walker, G. P. L. 1980 The Taupo Pumice: product of the most powerful known (ultraplinian) eruption? *J. Volcanol. geotherm. Res.* **8**, 69–94.

Walker, G. P. L. 1981*a* The Waimihia and Hatepe plinian deposits from the rhyolitic Taupo Volcanic Centre. *N.Z. Jl Geol. Geophys.* **24**, 305–324.

Walker, G. P. L. 1981*b* Characteristics of two phreatoplinian ashes and their water-flushed origin. *J. Volcanol. geotherm. Res.* **9**, 395–407.

Walker, G. P. L. 1984 Downsag calderas, ring faults, caldera sizes, and incremental caldera growth. *J. geophys. Res.* **89**, 8407–8416.

Walker, G. P. L. & Wilson, C. J. N. 1983 Lateral variations in the Taupo ignimbrite. *J. Volcanol. geotherm. Res.* **18**, 117–133.

Walker, G. P. L., Heming, R. F. & Wilson C. J. N. 1980*b* Low-aspect ratio ignimbrites. *Nature, Lond.* **283**, 286–287.

Walker, G. P. L., Wilson, C. J. N. & Froggatt, P. C. 1980*a* Fines-depleted ignimbrite in New Zealand: product of a turbulent pyroclastic flow? *Geology* **8**, 245–249.

Walker, G. P. L., Self, S. & Froggatt, P. C. 1981*a* The ground layer of the Taupo ignimbrite: a striking example of sedimentation from a pyroclastic flow. *J. Volcanol. geotherm. Res.* **10**, 1–11.

Walker, G. P. L., Wilson, C. J. N. & Froggatt, P. C. 1981*b* An ignimbrite veneer deposit: the trail marker of a pyroclastic flow. *J. Volcanol. geotherm. Res.* **9**, 409–421.

Wan, T. & Hedenquist, J. W. 1981 A reassessment of the structural control of the Broadlands geothermal field, New Zealand. *Proc. N.Z. Geotherm. Workshop 1981*, pp. 195–202. Auckland, New Zealand: Geothermal Institute, University of Auckland.

Wickmann, F. E. 1966 Repose period patterns of volcanoes I–V. *Arkiv Miner. Geol.* **4**, 291–367.

Wilson, C. J. N. 1985 The Taupo eruption, New Zealand. II. The Taupo ignimbrite. *Phil. Trans. R. Soc. Lond.* A**314**, 229–310.

Wilson, C. J. N. 1991 Ignimbrite morphology and the effects of erosion: a New Zealand case study. *Bull. Volcanol.* **53**, 635–644.

Wilson C. J. N. & Walker, G. P. L. 1981 Violence in pyroclastic flow eruptions. In *Tephra studies* (ed. S. Self & R. S. J. Sparks), pp. 441–448. Dordrecht: D. Reidel.

Wilson, C. J. N. & Walker, G. P. L. 1982 Ignimbrite depositional facies: the anatomy of a pyroclastic flow. *J. geol. Soc. Lond.* **139**, 581–592.

Wilson, C. J. N. & Walker, G. P. L. 1985 The Taupo eruption, New Zealand. I. General aspects. *Phil. Trans. R. Soc. Lond.* A**314**, 199–228.

Wilson, C. J. N., Ambraseys, N. N., Bradley, J. & Walker, G. P. L. 1980 A new date for the Taupo eruption, New Zealand. *Nature, Lond.* **288**, 252–253.

Wilson, C. J. N., Rogan, A. M., Smith, I. E. M., Northey, D. J., Nairn, I. A. & Houghton, B. F. 1984 Caldera volcanoes of the Taupo Volcanic Zone, New Zealand. *J. geophys. Res.* **89**, 8463–8484.

Wilson, C. J. N., Houghton, B. F. & Lloyd, E. F. 1986 Volcanic history and evolution of the Maroa-Taupo area, central North Island. *R. Soc. N.Z. Bull.* **23**, 194–223.

Wilson, C. J. N., Switsur, R. V. & Ward, A. P. 1988 A new $^{14}C$ age for the Oruanui (Wairakei) eruption, New Zealand. *Geol. Mag.* **125**, 297–300.

Wilson, C. J. N., Houghton, B. F., Lanphere, M. A. & Weaver, S. D. 1992 A new radiometric age estimate for the Rotoehu Ash from Mayor Island volcano, New Zealand. *N.Z. Jl Geol. Geophys.* **35**, 371–374.

*Received 12 December 1991; accepted 6 August 1992*

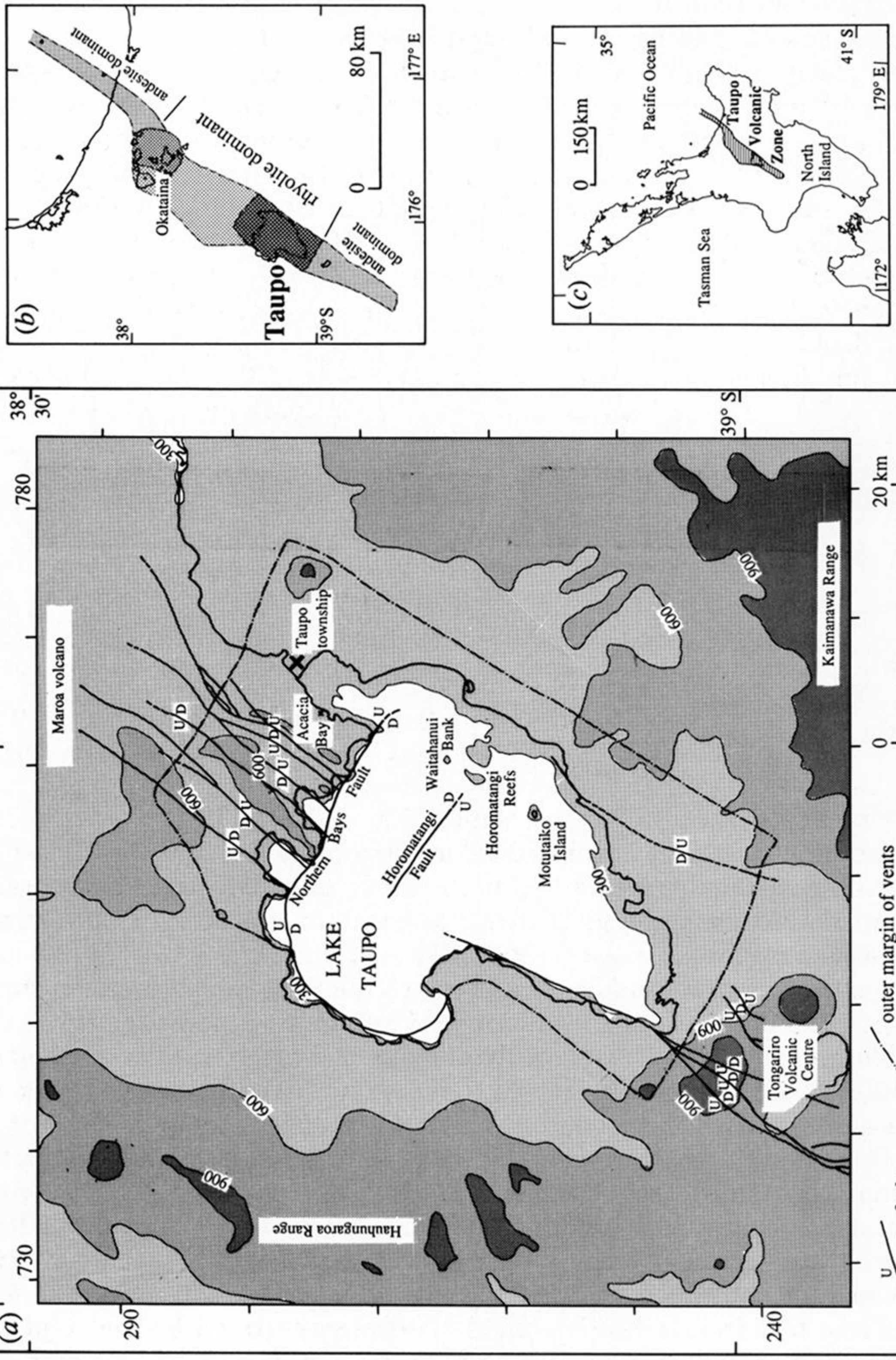


Figure 1. Location and index maps. (*a*) Topographic map of Taupo volcano, showing its inverse nature. Contours are at 300 m intervals. Major faults, and localities mentioned in the text are shown. In this and all other maps, the marginal ticks and numbers represent 10 km grid squares in the New Zealand metric map grid. From Wilson & Walker (1985). (*b*) Index map showing the position of Taupo and Okataina volcanoes within the central rhyolite-dominated Taupo Volcanic Zone (TVZ). The TVZ boundary is that defined in Wilson *et al.* (1984) as the envelope enclosing vents active after the Whakamaru-group ignimbrites, i.e. younger than 330 000 years. (*c*) Index map showing the position of the TVZ within the central North Island of New Zealand.

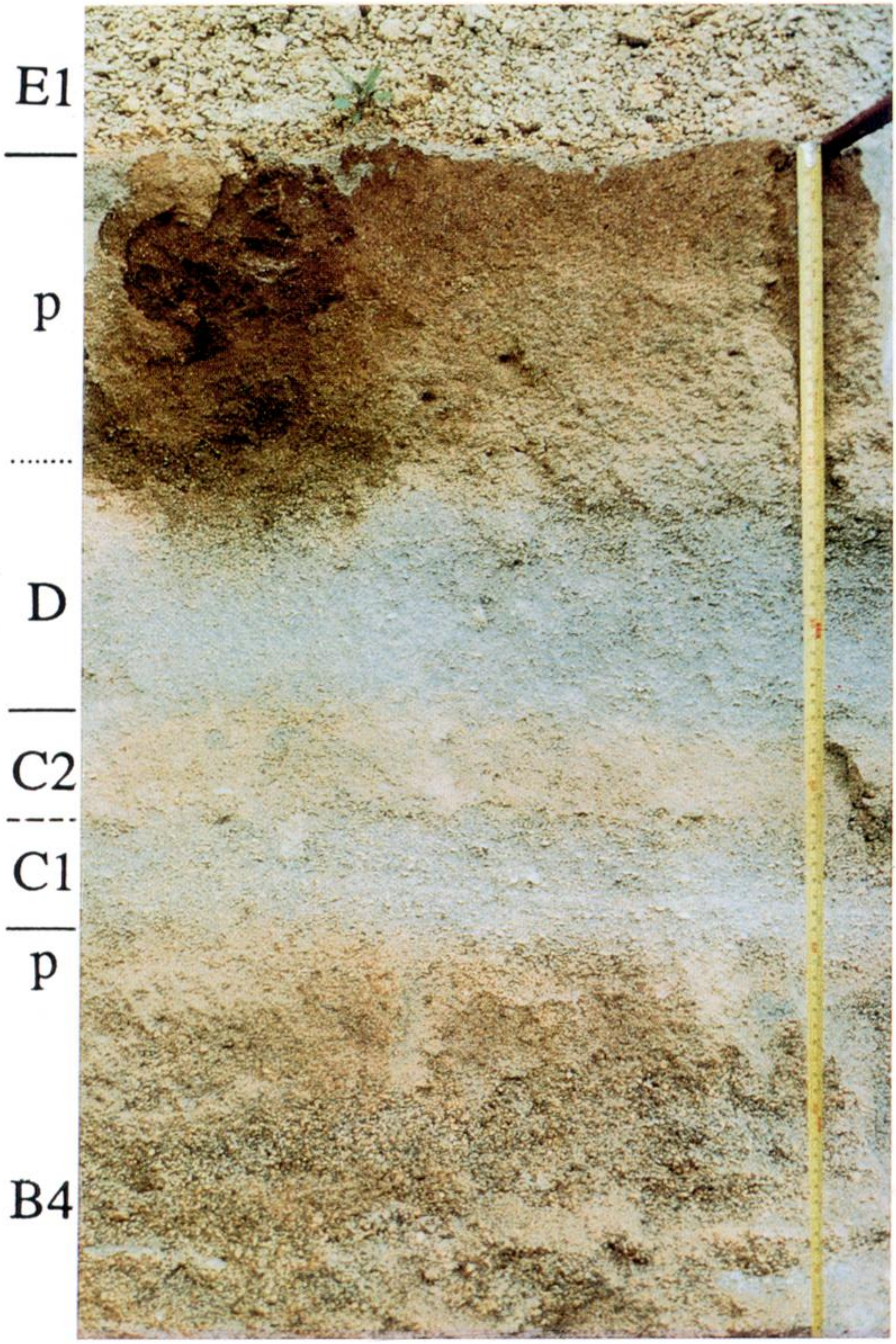


Figure 11. Photograph of Units C and D at the type locality for D (figure 9, locality 2394) at 7789 2729, to show the development of a weathered horizon (incipient palaeosol) between them. Fall deposits are designated by their letter, and p = palaeosol.


Figure 17. (*a*) Photograph of part of the section at 7739 2518 (figure 22, locality 2379) to show relationships between Units G and H, and units in the 'Hinemaiaia Tephra'. Eruption units are labelled in capitals, tr = trace, $p_1$ = pre-G palaeosol with traces of Unit F, $p_2$ = palaeosol separating G from H (see text), and $^{14}C$ = palaeosol where a $^{14}C$ age was obtained (Appendix B, sample 2379) (other palaeosols not labelled).

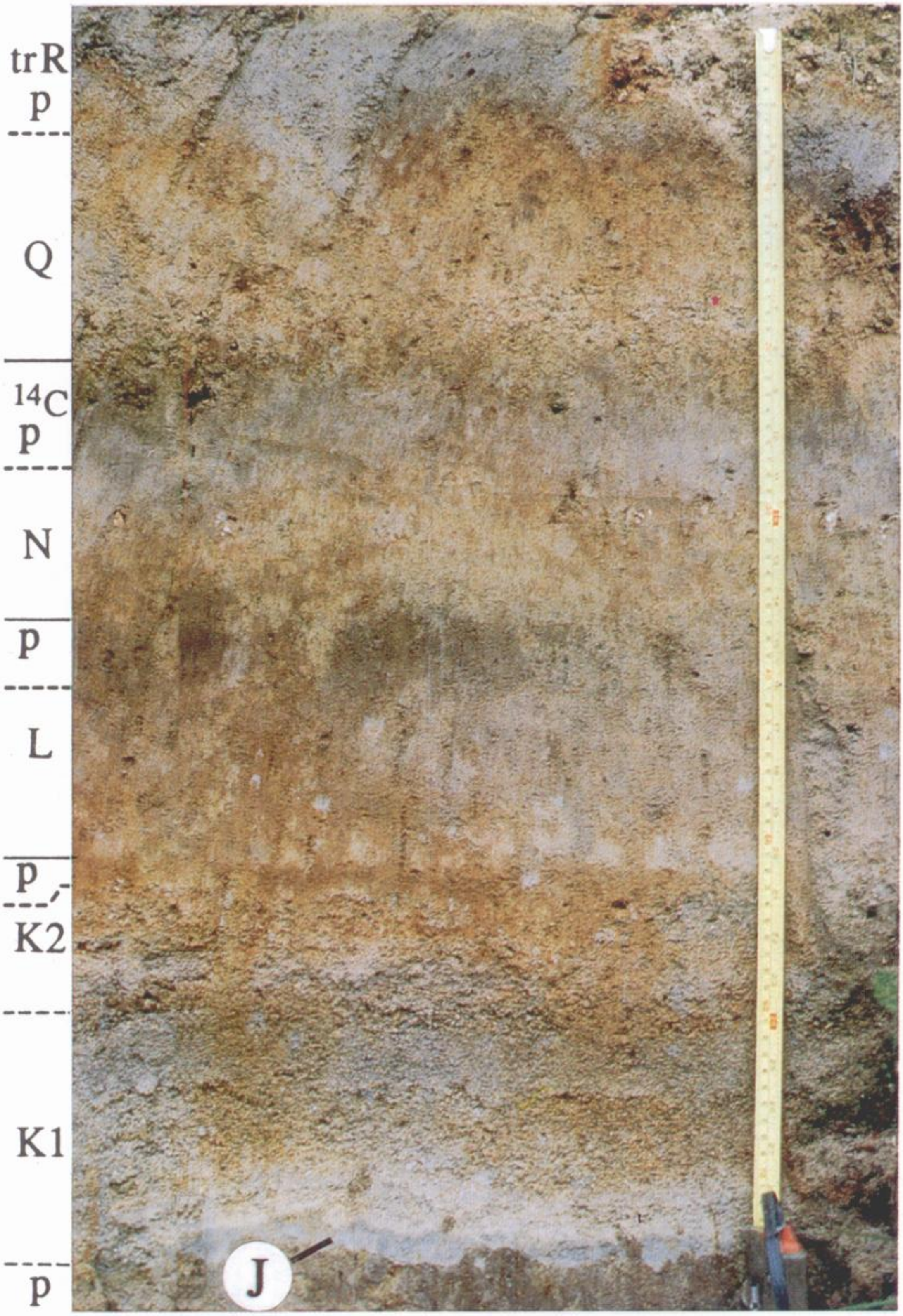


Figure 17. (*b*) Photograph of 'Hinemaiaia Tephra' at 7742 2529 (figure 22, locality 2380) to show units interpreted to be present. Lettering as in (*a*); the $^{14}C$ sample is 2380/C2 (Appendix B).

V

p

U

p

T

p

Figure 39. Photograph of Units T and U at 7827 2600, the type locality for T (Appendix A; figure 41, locality 2397), to show their relationships to each other, and to V and the post-S palaeosol. Palaeosols denoted by p.


Figure 45. Photograph of the type locality of Unit W at 7739 2565 (Appendix A; figure 46). W rests on weathered (brown) U and V material which in turn overlie a palaeosol on reworked S material. W is separated from X by a clear palaeosol (p). Scale bar is 50 cm.